EESTI MAAÜLIKOOL
ESTONIAN UNIVERSITY OF LIFE SCIENCES

Eesti Maaülikool
Estonian University of Life Sciences

CONDITION AND RESIDUAL BEARING CAPACITY OF EXISTING REINFORCED CONCRETE STRUCTURES

OLEMASOLEVATE RAUDBETOONTARINDITE SEISUND JA JÄÄKKANDEVÕIME

MIHKEL KIVISTE

A Thesis
for applying for the degree of Doctor of Philosophy
in Rural Building

Väitekiri
filosoofiadoktori kraadi taotlemiseks maaehituse erialal

Tartu 2011

Institute of Forestry and Rural Engineering,
Estonian University of Life Sciences

According to verdict No. 15 of 10.12, 2010, the Doctoral Committee of the Engineering Sciences of the Estonian University of Life Sciences has accepted the thesis for the defence of the degree of Doctor of Philosophy in Rural Building.

Opponents: Dr. John Cairns, PhD
Civil Engineering in the School of the Built Environment
Heriot-Watt University, Edinburgh, UK

Prof. Ralf Lindberg, Dr. Tech
Institute of Structural Engineering
Tampere University of Technology, Tampere, Finland

Supervisor: Prof. Jaan Miljan, Cand Sc
Institute of Forestry and Rural Engineering
Estonian University of Life Sciences

Language editor: Stewart Johnson

Defence of the thesis:
Estonian University of Life Sciences, room 1C2 , Kreutzwaldi 5, Tartu on 21 January, 2011, at 12.00.

Publication of this thesis is supported by the Estonian University of Life Sciences

ISBN 978-9949-426-95-9

CONTENTS

LIST OF ORIGINAL PUBLICATIONS

This thesis is based on the following publications, which are referred to in the text by their Roman numerals. The publications are reproduced with the permission of the publishers.

I Miljan, J., **Kiviste, M**. 2010. Influence of visual condition on the residual flexural capacity of existing pre-cast concrete panels. 9th International Scientific Conference, Engineering for Rural Development, Jelgava: 260-266.

II **Kiviste, M.**, Miljan, J. 2010. Evaluation of residual flexural capacity of existing pre-cast pre-stressed concrete panels-A case study. Engineering Structures 32(10): 3377-3383.

III Miljan, J., Keskküla, T., Miljan, R., **Kiviste, M.**, Laiakask, E., Tomann, H. 2004. Service life prediction of reinforced concrete structures damaged by reinforcement corrosion. CIB World Building Congress 2004. Building for the Future, Toronto: 155-165.

IV **Kiviste, M.**, Miljan, J., Miljan, R., Kiprušenkov, M.† 2009**.** Condition of structures and properties of concrete of an existing oil shale chemical plant. Oil Shale 26(4): 513–529.

V Kiprušenkov, M†., Miljan, J., **Kiviste, M.**, Miljan. R. 2007. Condition assessment of concrete structures in chemical plant's gas generator building. 5th International Conference on Concrete under Severe Conditions of Environment and Loading (CONSEC), Tours: 223-230.

THE AUTHOR'S CONTRIBUTION TO THE ORIGINAL PUBLICATIONS

I Mihkel Kiviste (co-author) co-tested eight precast prestressed concrete ribbed slabs (ribbed panels) and supervised master students, who tested five ribbed panels. Tests with 46 ribbed panels are discussed in this publication. Mihkel Kiviste collected and analysed test results. He interpreted the results and compared them with literature. He also wrote the manuscript and is responsible for its revision.

II Mihkel Kiviste (co-author) co-tested eight ribbed panels and supervised master students, who tested ten ribbed panels. Test with 28 ribbed panels are discussed in this publication. Mihkel Kiviste analysed, interpreted and compared the results with literature. He also wrote the manuscript and is responsible for its revision.

III Mihkel Kiviste (co-author) co-tested eight of 12 ribbed panels, the results of which are also discussed in this publication. He wrote an experimental part of the results, a discussion and is responsible for the revision of manuscript.

IV Mihkel Kiviste (co-author) participated in acquisition, measuring and testing of concrete samples (excluding chemical analysis). He analysed, interpreted and compared the results with literature. He also wrote the manuscript and is responsible for its revision.

V Mihkel Kiviste (co-author) performed the rebound hammer test and interpreted its results. He co-operated in writing of the manuscript and is also responsible for its revision.

INTRODUCTION

Reinforced concrete is a versatile, economical and successful construction material. The combination of the high compressive strength of concrete and high tensile strength of reinforcing steel gives a composite material that offers, compared to other materials, a wide range of applications in structural engineering. Reinforced concrete is usually durable and strong, performing well throughout its service life. However, sometimes it does not perform adequately as a result of poor design, poor construction, inadequate selection of materials, a more severe environment than expected or a combination of these factors.

During the last decades the expense of repair and rehabilitation of existing structures has increased. Within Europe it has been estimated that the value of structures and infrastructure represents approximately 50% of the national wealth of most countries. Furthermore, it is estimated that approximately 50% of the expenditure in the construction industry is spent on repair, rehabilitation and maintenance of existing reinforced concrete structures (Long 2001). For example, in the United States the cost of corrosion damage to reinforced concrete bridges due to the use of de-icing salts alone is estimated to be between $325 million and $1 billion/year (Transportation Research Board 1991). There are similar statistical results from Australia and the Middle East. It is evident, therefore, that the deterioration of reinforced concrete structures is a major problem in almost all parts of the world.

According to Torres-Acosta *et al.* (2007) the durability of a reinforced concrete structure consists of three stages: corrosion initiation, corrosion propagation and residual life stage. Although research on steel corrosion in concrete has been both extensive and intensive for the past three decades; it has focused largely on the initiation of corrosion and, to a lesser extent, its propagation, rather than on its effect on structural performance (Li *et al.* 2008). From those investigations dealing with corrosion propagation and residual life periods, quite a few have dealt with the concept of the residual bearing capacity of reinforced concrete members due to corrosion of the embedded steel (Torres-Acosta *et al.* 2007).

Most of the studies on the structural tests of corroded reinforced concrete structures have been conducted under laboratory conditions in a controlled environment. Structures are cast with chlorides to initiate pitting corrosion and/or an external impressed current is applied (galvanostatic method) to accelerate the corrosion rate of reinforcing steel. However, accelerated corrosion processes for simulating on site structure corrosion degradation are quite complicated and do not always give comparable results (Torres-Acosta *et al.* 2007). The surface characteristics of a corroded steel bar, however, are found to be different when the corrosion is induced by the galvanostatic method or by the natural environment (Yuan *et al.* 2007).

Unfortunately, tests with existing reinforced concrete structures exposed in natural conditions are scarce in literature, but those are valuable for substantiating the findings from the laboratory study on accelerated corrosion. Consequently, the main objective of the current thesis is to complement the research results of the condition and residual bearing capacity of existing reinforced concrete structures.

The first part of the research consists of structural and materials tests of 46 existing precast concrete ribbed panels. In Estonia, the bearing structures of many agricultural and industrial buildings constitute a precast concrete skeletal frame. Intensive construction, based on industrially manufactured members, started in the 1960s when standardised design solutions and reinforced concrete structure designs were employed. After a relatively short period of service, the initial signs of corrosion of steel reinforcement became evident in agricultural buildings. In Estonia today, there are about 4000 agricultural buildings with an average floor space of 1800 m^2. Many of their precast concrete bearing members (columns, beams and ribbed panels) have reached an undefined state. The ribbed panels studied in this part of the research are common in Estonian agricultural buildings. There is an increasing demand for informed decisions about the structures' capability to serve their intended function or, otherwise, the need for repair or demolition.

The second part of the research is a case study for investigating the condition of reinforced concrete structures and properties of concrete under the aggressive indoor environment of an existing oil shale chemical plant. The condition of reinforced concrete structures in the

plant (constructed in 1951) was assessed visually. On the basis of visual assessment structures with most severe deteriorations were located for subsequent investigation. The compressive strength of cores, carbonation depth, cover, water absorption as well as sulphate, chloride and nitrate content in concrete were determined. According to the results the suggestions were proposed to repair deteriorated reinforced concrete structures in the plant.

The present doctoral thesis is an extension of the bachelor (Kiviste and Tomann 2002) and master (Kiviste 2004) thesis.

1. REVIEW OF THE LITERATURE

1.1. Previous research at the Estonian University of Life Sciences

The Department of Rural Building at the Estonian University of Life Sciences (EMU) has gathered data describing the condition of reinforced concrete structures in agricultural buildings from 1974 to the present. An external (non-destructive) visual six-point assessment scale ranging from grades 5 to 0 (**Table 1.1**; Miljan and Keskküla 1975; **I; III; IV; V**) and an internal (destructive) twenty-one-point assessment scale from grades 20 to 0 (**Table 1.2**; Miljan 1977; **III**) were developed.

The critical indicators of the structures observed by both scales are:

- Grade 1—evidence of the occurrence of over 0.3 mm wide cracks in the cover, and
- Grade 0—indicated by spalling of the cover.

Table 1.1. External assessment grades for classification of deterioration states of reinforced concrete structures (Miljan and Keskküla, 1975; **I; III; IV; V**)

Grade	Description of state
5	No corrosion detected
4	Less than 20% of stirrups are corroded (cracks or spalled concrete cover)
3	More than 20% of stirrups are corroded
2	Micro-cracks (width 0–0.3 mm) in the concrete cover of main reinforcement
1	Cracks (width >0.3 mm) in the concrete cover of main reinforcement
0	Concrete cover of the main reinforcement has spalled

Reinforced concrete precast members of various ages ranging from 1 to 34 years were visually assessed in 258 agricultural buildings from 1974 to 1997. External assessment grades were assigned to 1198 columns, 2601 beams and 23,336 ribbed ceiling panels (i.e. about 3.5% of the total number of ribbed panels in the agricultural buildings of Estonia).

Table 1.2. Internal assessment grades for classification of deterioration states in reinforced concrete structures (**III)**

Internal grade (Miljan 1977)	Carbo-nation	Steel grades (Oit & Ojamaa 1974)	Description of state	Corrosion stages (Tuutti 1982)
20	10	10	Cover is not carbonised	Initiation
19	9	10	Cover is 10% carbonised	
18	8	10	Cover is 20% carbonised	
17	7	10	Cover is 30% carbonised	
16	6	10	Cover is 40% carbonised	
15	5	10	Cover is 50% carbonised	
14	4	10	Cover is 60% carbonised	
13	3	10	Cover is 70% carbonised	
12	2	10	Cover is 80% carbonised	
11	1	10	Cover is 90% carbonised	
10	0	10	Cover is 100% carbonised, no corrosion	Depassivation
9	0	9	<20% dots of corrosion, < 3 mm	Propagation
8	0	8	>20% dots of corrosion;	
7	0	7	<20% stains of corrosion, > 5 mm	
6	0	6	>20% stains of corrosion;	
5	0	5	>80% corrosion;	
4	0	4	Full corrosion;	
3	0	3	Full corrosion, signs of the growing volume of corrosion products;	
2	0	2	Full corrosion, the corrosion products press into concrete;	
1	0	1	Cracks in the cover as a result of growing volume of corrosion products;	
0	0	0	Cover spalling as a result of reinforcement corrosion.	

Reinforced concrete members of various ages ranging from 1 to 32 years were assessed internally from 1974 to 1996. The internal condition was assessed in 585 columns, 592 beams as well as in the 624 longitudinal and 620 transversal ribs of ribbed panels.

Analyses of variance and regression were applied (Miljan R 2005) on both data sets. The average age of a member (column, beam and ribbed panel) at the time of cover spalling (noted as an asterisk in **Fig. 1.1)** was found. Also the residual bearing capacity of the structure with spalled cover (grade 0) was calculated (also noted as an asterisk in **Fig. 1.1)**. After cover spalling a corrosion rate of 125 μm (Ostrovsky 1984) was assumed in the bearing capacity calculations of a reinforced concrete structure. Based on these results a model (**Fig. 1.1**; Laiakask and Miljan 2002; **III**) describing the reduction of the bearing capacity of common precast concrete structures in the agricultural buildings of Estonia was developed.

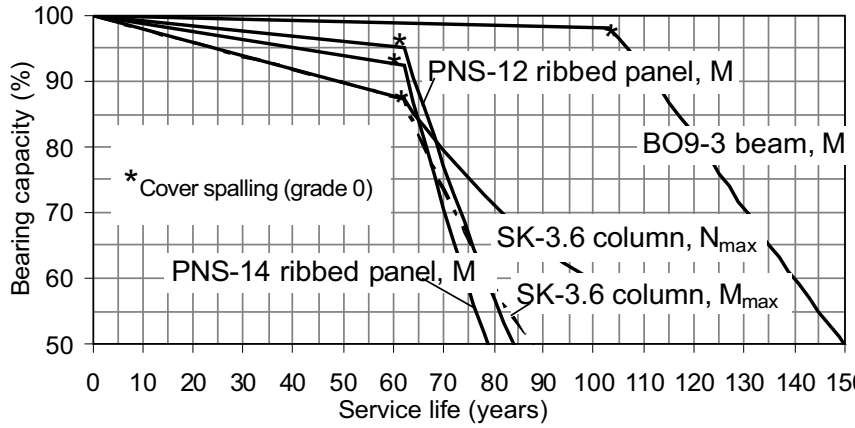

Fig. 1.1. A hypothetical model describing the decrease of the bearing capacity of common precast concrete structures in agricultural buildings (Laiakask and Miljan 2002, **III**). After cover spalling a corrosion rate of 125 μm per year is assumed (Ostrovsky 1984).

1.2. Service life estimation regarding reinforcement corrosion

The most well-known service life model for reinforcement corrosion in concrete is published by Tuutti (1982; **Fig. 1.2**). From his work it is understood that the service life of a reinforced concrete structure may be divided into following two stages: an initiation period and propagation period. The initiation period comprises the time taken by an aggressive (chlorides or carbonation) to reach and depassivate reinforcing steel. The propagation stage is reached when steel starts to corrode and corrosion products cause cracking and spalling. Eventually a situation is reached,

defined as the end of service life, when either repair or demolition must take place. Alekseyev and Rozental (1976) have indicated a depassivation period that exists between the initiation and propagation phases. Broomfield (1997) likewise has included an additional period but refers to it as an 'activation' stage.

Grades from 20 to 11 in the internal assessment scale (**Table 1.2)** are comprised in the initiation period, as shown in **Fig. 1.2**. Grade 10 equals to the depassivation period and grades 9 to 0 are a part of the propagation period. Further investigations are required to specify the length of period 'r' (**Fig. 1.2**) from grade 0 to the end of the service life.

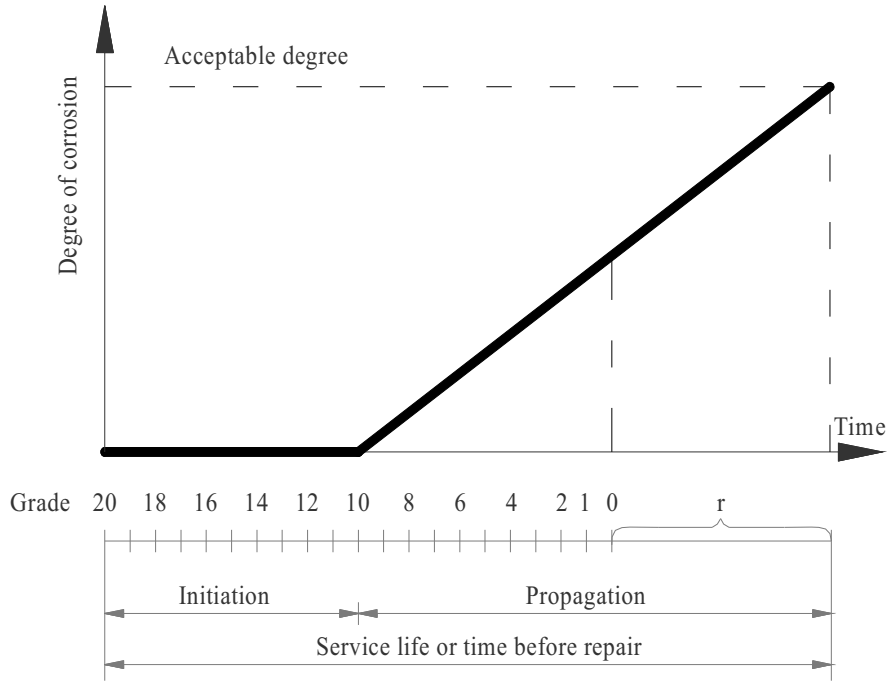

Fig. 1.2. Service life model for reinforcement corrosion (Tuutti 1982; Miljan 1977; Oit and Ojamaa 1974; **III**).

There has been extensive research on steel corrosion in concrete in the past decades (ACI Committee 365 2000; Andrade *et al.* 1993; Castel *et al.* 2000; Hong and Hooton 1999; Melchers and Li 2006; Pantazopoulou and Papoulia 2001; Roberts *et al.* 2000; Weyers *et al.* 1994); and it is now possible to provide a reasonable estimation of the whole process of corrosion in reinforced concrete infrastructure. Despite of these

significant advances, there are still fields of considerable uncertainty in the various models and in the data available.

Recently, Melchers and Li (2006) developed a phenomenological model for the corrosion of reinforcing steel bars in concrete as a function of time (**Fig. 1.3**). The model has a number of features in common with earlier models (Tuutti 1982; Weyers *et al.* 1994; Bentur *et al.* 1997; Francois and Arliguie 1999) but differs from them in important ways. In principle, the model applies to the steel bar at a generic cross section of a reinforced concrete member. The model divides the corrosion process into two stages with six detailed phases. The two stages of corrosion initiation and propagation are similar to those of Tuutti (1982), but the detailed phases comprising them are derived from the dynamics of corrosion (Melchers 2003).

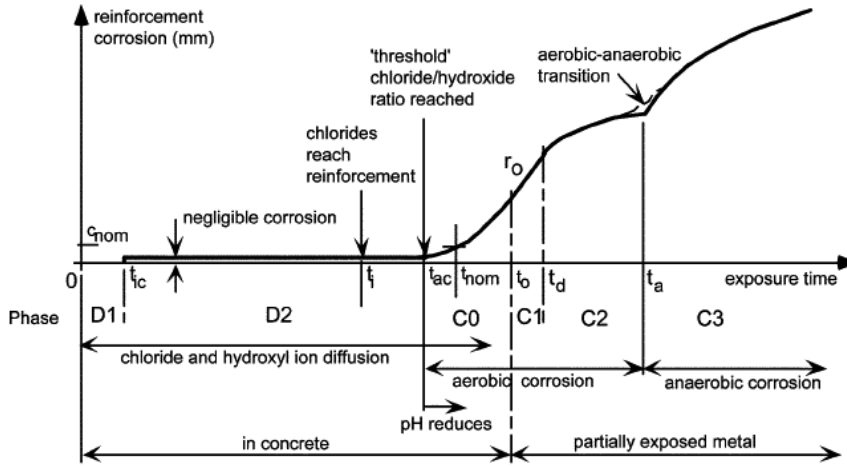

Fig. 1.3. Phenomenological model for chloride-induced steel corrosion in concrete (Li *et al.* 2008). *Diameter loss in mm.*

As shown in **Fig. 1.3**, Phase D1 is the diffusion of chlorides into the concrete and the commencement of hydroxyl ions leaching out of the concrete. When there are cracks present in the member (for example, flexural members), the local time to initiation t_{ic} is governed by the time of occurrence of the local crack(s) (Li 2002). When no cracks occur in the member, t_{ic} tends to be the initiation time t_i, which is governed by the rate of diffusion and therefore the permeability of the concrete (Melchers and Li 2006). At t_i, the chlorides have reached the steel but the balance

between the concentrations of the Cl^- and $(OH)^-$ ions and the pH may not be such that active corrosion will commence (which is denoted as t_{ac}). During phase C0, the rate of corrosion tends to increase because the pH will typically reduce due to the hydroxyl ions leaching out of the concrete. In phase C1, the propagation of corrosion is governed by the rate of oxygen and water supplies and the conditions on the steel corroding surface. Because of micro-cracking (for example, caused by stress) and the resulting loss of influence from Cl^- and $(OH)^-$ ions and the greater permeability, the environment external to the concrete will increasingly control the corrosion rate. As corrosion progresses, there will be an increasing build-up of corrosion products and associated increased radial stresses, causing longitudinal cracking and, eventually, concrete cover spalling. Moreover, the increasing build-up of corrosion products on the corroding surfaces will contribute to an increasing resistance to oxygen diffusion (that is, the rate of oxygen supply to the corroding surfaces). Phase C2 denotes the period when this controls the rate of corrosion. Eventually, the rate of oxygen diffusion to the corroding bars through the rust layer will become so low that anaerobic corrosion activity will set in (Melchers 2003). This is shown as phase C3 in **Fig. 1.3**.

1.3. Service life estimation regarding structural bearing capacity

A hypothetical model describing the reduction of the bearing capacity of common precast concrete structures in the agricultural buildings of Estonia was presented in **Fig. 1.1.** A common model for a reinforced concrete structure exposed to a corrosive environment was proposed by Torres-Acosta *et al.* (2007) in **Fig. 1.4.** The durability of a reinforced concrete structure is considered to be a three-phase process. The lifetime, T, of the structure, is defined as:

$$T = T_1 + T_2 + T_{RL} \tag{1.1}$$

where T_1 is the corrosion initiation stage from the time of construction to the time of corrosion initiation;
T_2 is the corrosion propagation stage during which the steel corrodes until an unacceptable level of corrosion is reached and;
T_{RL} is the residual life stage from serviceability to ultimate limit state.

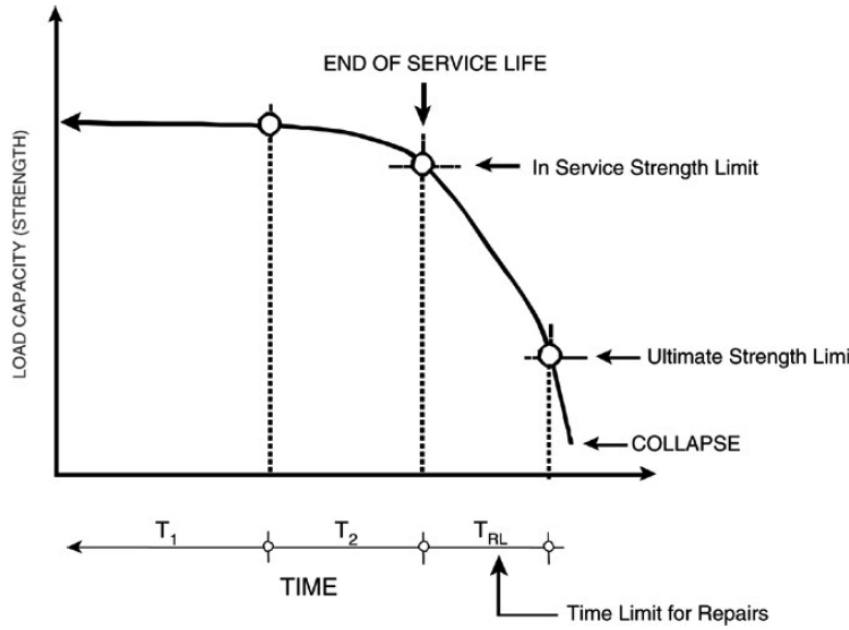

Fig. 1.4. Durability model of a reinforced concrete structure exposed to a corrosive environment (Torres-Acosta *et al.* 2007).

Investigations have been conducted during the last three decades regarding chloride or CO_2 penetration and prediction of corrosion initiation (T_1 length). But few investigations have dealt with corrosion propagation, T_2, and even less with residual life, T_{RL}, predictions, which are also needed for durability forecasting. From those investigations dealing with T_2 and T_{RL} periods, quite a few have dealt with the concept of the residual bearing capacity of concrete members due to corrosion of the embedded steel (Torres-Acosta *et al.* 2007). The whole process of corrosion in reinforced concrete infrastructure and, in particular, its effects on structural deterioration over time have been accorded little attention (Val and Melchers 1997; Iwanami *et al.* 2002, Li *et al.* 2008).

Fig. 1.5 presents a summary of the results of such investigations (Tachibana *et al.* 1990; Almusallam *et al.* 1996; Rodriguez *et al.* 1996; Almusallam *et al.* 1997; Huang and Yang 1997; Rodriguez *et al.* 1997; Mangat and Elgarf 1999a; Mangat and Elgarf 1999b); where different structural members (beams, columns, slabs) were corroded and tested up to failure. The horizontal axis in **Fig. 1.5** represents the corrosion-induced rebar radius loss, which is presented as a ratio between the average

corrosion penetration (x_{AVER}), and the initial radius of the rebar (r_0). The experimental load-bearing capacity values from these investigations were used to estimate the Load Capacity ratio, LC_{COR}, regardless of the type of loading (flexure for beams and slabs, compression for columns). The LC_{COR} values were calculated by dividing the bearing capacity for corroded members by the bearing capacity for the non-corroded (control) members. The load-bearing capacity pattern observed in **Fig. 1.5** follows what was established in the durability model presented in **Fig. 1.4**.

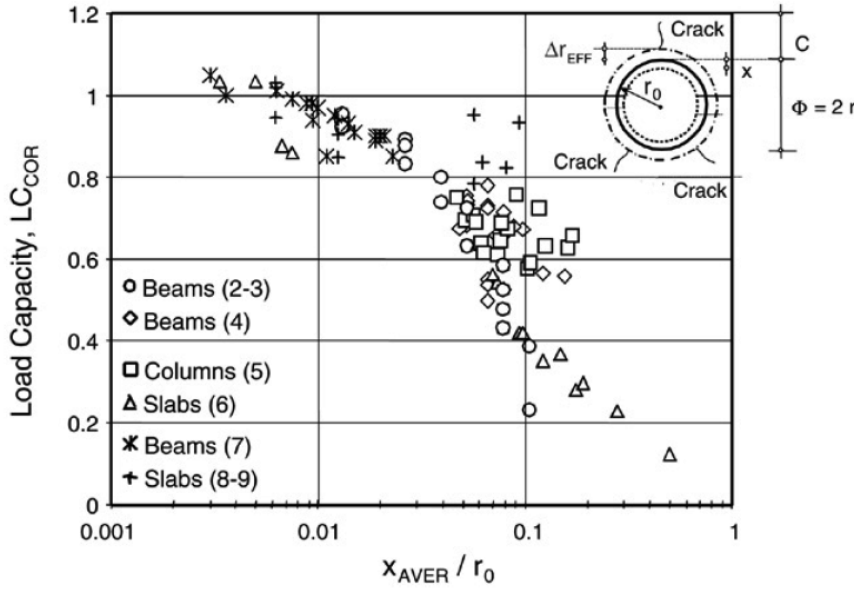

Fig. 1.5. LC_{COR} vs. x_{AVER}/r_0 experimental results (Torres-Acosta *et al.* 2007). Based on the results of: 2—Mangat and Elgarf (1999a); 3—Mangat and Elgarf (1999b); 4—Rodriguez *et al.* (1997); 5—Rodriguez *et al.* (1996); 6—Almusallam *et al.* (1997); 7—Almusallam *et al.* (1996); 8—Huang and Yang (1997); 9—Tachibana *et al.* (1990).

Most of the studies (including the studies in **Fig. 1.5**) reporting structural tests on corroded reinforced concrete members have been conducted under laboratory conditions. Valuable data is available from flexural bearing capacity tests of reinforced concrete beams, where the steel corrosion rate is enhanced by applying an external impressed current (Azad *et al.* 2007; Du *et al.* 2007; Mangat and Elgarf 1999a; Huang and Yang 1997). In addition to electric current, reinforced concrete beams are cast with chlorides to initiate pitting corrosion (Torres-Acosta *et al.* 2007; Rodriguez *et al.* 1997). The combined effect of corrosion

and various sustained loads on the structural performance of reinforced concrete beams has also been investigated (El Maaddawy *et al.* 2005; He *et al.* 2005; Yoon *et al.* 2000). Also, full-scale structural tests with bridge deck panels (Dowell and Smith 2006) and deck girders (Higgins *et al.* 2007) have been performed.

However, laboratory studies cannot fully represent all the aspects of the on-site behaviour of reinforced concrete structures. Accelerated corrosion processes to simulate on site structure corrosion degradation are quite complicated and do not always give comparable results (Torres-Acosta *et al.* 2007). Commonly, the galvanostatic method is used for accelerating steel bar corrosion in concrete. The surface characteristics of the corroded steel bar, however, are found to be different when the corrosion is induced by the galvanostatic method or by the natural environment (Yuan *et al.* 2007).

Although field studies can help us to account for the reduction in strength and serviceability of reinforced concrete structures over time, investigations on the condition and residual bearing capacity of the existing reinforced concrete structures, after long-term exposure to the on-site environment, are scarce in the literature. Some of these studies are presented as follows.

Flexural bearing capacity tests have been performed with beams in harbour docks (Jin *et al.* 2004) that had been in an aggressive environment for more than 10 years (Fan *et al.* 2004). Wipf *et al.* (2006) conducted an extensive field-testing of precast channel bridges as well as laboratory testing of their precast panels. An experimental study was conducted on two 28-year-old reinforced concrete bridge arch ribs to explore the residual load-bearing capacity and failure pattern (Zhang *et al.* 2006). In the study by Shdid *et al.* (2006) 40-year old precast prestressed concrete bridge piles were rated visually and tested on bending. Durham *et al.* (2007) and Heymsfield *et al.* (2007) had tested 33 existing precast non-prestressed channel beams, which were used in short multi-span bridges in Arkansas in the 1950s through the early 1970s. The beams, constructed without shear reinforcement, were categorised as 'good', 'average' or 'poor' as a function of percentage and location of exposed longitudinal reinforcing steel (**Table 1.3**).

Table 1.3. Beam classification criteria (Heymsfield *et al.* 2007)

	Exposed reinf. length, L_{reinf}, m	Min. anchorage length, L_{end}, m
Poor	$L_{reinf} > 1.68$	1.07
Average	$1.68 > L_{reinf} > 0.30$	$1.98 > L_{end} > 1.07$
Good	$0.30 > L_{reinf}$	$L_{end} > 1.98$

2. SIGNIFICANCE AND AIMS OF THE RESEARCH

Research on steel corrosion in concrete has been both extensive and intensive for the past three decades. However, it has focused largely on the initiation of corrosion and, to a lesser extent, its propagation, rather than on its effect on structural performance (Li *et al.* 2008; Torres-Acosta *et al.* 2007). Quite a few researchers have dealt with the concept of the residual bearing capacity of reinforced concrete members due to corrosion of the embedded steel (Torres-Acosta *et al.* 2007). The effects on structural deterioration over time have been accorded little attention (Val and Melchers 1997; Iwanami *et al.* 2002; Li *et al.* 2008).

Most structural tests, however, are performed under laboratory conditions in a controlled environment. Often, laboratory tests are short-term with accelerated corrosion. Accelerated corrosion results do not always give comparable results with structures exposed to the on site environment Relying mainly on accelerated corrosion studies of reinforced concrete structures is a compromise. Tests with existing reinforced concrete structures are scarce and, hence, valuable to substantiate the findings from laboratory tests with accelerated corrosion. Consequently, the main aim of the research is to complement research results of the condition and residual bearing capacity of existing reinforced concrete structures.

A) The novelty of this research consists in tests with existing reinforced concrete members (ribbed panels), which have been exposed in a natural on-site environment for at least ten (**I**) years. 46 existing precast concrete ribbed panels (14 reinforced concrete ribbed panels PKZH-2 and 32 prestressed concrete ribbed panels PNS-3, PNS-12 and PNS-14) are studied experimentally. The aims of this part of the research are presented as follows.

1. To study the residual flexural bearing capacity, behaviour and failure mode of ribbed panels (**I; II; III**).
2. To study the influence of visually discernible corrosion deteriorations (visual grades) on the residual flexural bearing capacity of ribbed panels (**I; III**).
3. To evaluate the conformity of existing ribbed panels to the bearing capacity and rigidity (PNS-12 and PNS-14) requirements of factory-issued (new) ribbed panels (**II**).

4. To compare the residual flexural behaviour of ribbed panels PNS-12 with factory-issued ribbed panels (**II**).
5. To find the causes of different bearing capacities of ribbed panels PNS-12 and PNS-14 through material tests (**II**).

B) Several studies have dealt with condition and reliability assessments of reinforced concrete structures in nuclear power plants (Ellingwood and Mori 1997; Braverman *et al.* 2004; Naus *et al.* 1999) or bridges (Sasmal and Ramanjaneyulu 2008; Stewart 2001; Enright and Frangopol 1999). However, no attention has been given to the effects of the gases and phenols that arise from oil shale retorting to the load-bearing structures of a chemical plant. The aggressive environment inside the plants that manufacture oil shale could adversely affect the material properties and structural bearing capacity inside the building. The aims of this part of the research are presented as follows.

1. To quantify and locate reinforced concrete structures with the most severe deterioration in the plant with visual assessment (**IV; V**).
2. To compare the strength of concrete cores with concrete strength from design drawings to verify if the studied structures were cast in accordance with the drawings (**IV**).
3. To find the most probable cause of deterioration of reinforced concrete structures in the studied plant (**IV**).
4. According to results to propose measures to rehabilitate deteriorated reinforced concrete structures in the studied plant (**IV**).

3. MATERIALS AND METHODS

3.1. Research objects

A) In the first part of the research, structural and material tests with 46 existing reinforced and prestressed concrete ribbed panels are reported. Fourteen reinforced concrete ribbed panels PKZH-2 and 32 prestressed concrete ribbed panels PNS-3, PNS-12 and PNS-14 were tested. The summary of test series is presented in **Table 3.1**. Letter(s) in the first column is(are) associated with the location of ribbed panels. Reinforced concrete (RC) ribbed panels are marked with a hyphen between the letter and number, while prestressed concrete (PC) ribbed panels are marked without a hyphen. M. Kiviste supervised the students in the structural tests of ribbed panels V1–V12 in 2005.

B) In the second part of the research the condition of structures and properties of concrete of the generator building of an existing oil shale chemical plant is studied. The studied generator building is located in North-eastern Estonia. The 7-storey building of 64 by 15 m has been almost constantly in service since its construction in 1951. The generator processes 1.4 million tons of oil shale every year. Oil shale is processed in the generators of the plant to produce shale oils, fuel oils and resins. There are 12 generators in the plant. The object was investigated by M. Kiprušenkov, M. Kiviste, J. Miljan and R. Miljan from February to December 2006. Additional samples were taken and tested in April 2009.

Table 3.1. Test series of reinforced and prestressed concrete ribbed panels

Ribbed panels (amount)	Type	Object and purpose	Test location	Loading, location	Test year	Age of ribbed panels	Test performer
K-1–K-7 (7)	PKZH-2	Kärstna pigsty	Kärstna field tests	Sand uniformly, soil	1973	12	J. Miljan
K-8–K-10 (3)	PKZH-2	Kärstna pigsty	Tallinn, test hall	Cast iron loads uniformly, RC floor	1974	13	J. Miljan
P11–P13 (3)	PNS-3	Pandivere pigsty	Tallinn, test hall	Cast iron loads uniformly, RC floor	1974	10	J. Miljan
VA14–VA19 (6)	PNS-3	Vao pigsty	Vao field tests	RC foundation blocks uniformly, soil	1975	11	J. Miljan
T-20–T-23 (4)	PKZH-2	Torma cowshed	Torma field tests	RC curbstones uniformly, soil	1978	15	J. Miljan
L1–L10 (10)	PNS-12, PNS-14	Luha cowshed	Tartu, EMU lab.	Hydrocylinder, 4-point bending, RC force floor	2000-2001	26	E. Laiakask
R1–R8 (8)	PNS-12	Raadi garage	Tartu, EMU lab.	Hydrocylinder, 4-point bending, RC force floor	2002	Un-known	M. Kiviste, H. Tomann, M. Tarto
V1–V6 (5)*	PNS-14	Vara pigsty	Tartu, EMU lab.	Hydrocylinder, 4-point bending, RC force floor	2005	32	R. Patrael J. Hinto-Kivimaa J. Toper
V8–V12 (5)	PNS-12, PNS-14	Corridor of Vara pigsty	Tartu, EMU lab.	Hydrocylinder, 4-point bending, RC force floor	2005	32	R. Halgma, L. Linnus, T. Salu

**–Test results of ribbed panel V3 are omitted since the test was ended before the determination of ultimate residual bearing capacity.*

3.2. Visual assessment

Structures of the generator building of an existing oil shale chemical plant were assessed visually on a 6-grade scale (**Table 1.1**). The scale was adapted (**Table 3.2**; **I; II; III)** for the visual assessment of ceiling ribbed panels. Ribbed panels were assessed visually prior to structural tests.

Table 3.2. Classification of deterioration states of the ceiling ribbed panels

Grade	Description of state
5	No corrosion detected
4	1) Less than 20% of the concrete cover of a slab has spalled; 2) Noticeable longitudinal cracks (0.3–1.0 mm) in transverse ribs.
3	1) More than 20% of the concrete cover of slab reinforcement has spalled; 2) Less than 20% of the concrete cover of stirrups in the longitudinal ribs has spalled; 3) In transverse ribs wide (>1.0 mm) cracks have occurred; 4) Less than 20% of the concrete cover in transverse ribs has spalled.
2	1) More than 20% of the concrete cover of stirrups in longitudinal ribs has spalled; 2) More than 20% of the concrete cover of reinforcement in transverse ribs has spalled; 3) Longitudinal micro cracks (0–0.3 mm) due to corrosion in longitudinal ribs.
1	Longitudinal cracks (> 0.3 mm) in longitudinal ribs;
0	Concrete cover of the reinforcement in longitudinal ribs has spalled.

3.3. Structural tests

3.3.1. Ribbed panels

The residual flexural bearing capacity of existing reinforced concrete ribbed panels PKZH-2 and 32 prestressed concrete ribbed panels PNS-3, PNS-12 and PNS-14 were studied experimentally. Precast ribbed panels

of aforementioned types are common in the industrial and agricultural buildings of Estonia (but also in other former Soviet Union countries) built from the 1950s to 1990s. All tested roof and ceiling ribbed panels had a length of 5970 mm and width of 1490 mm (**Fig. 3.1**).

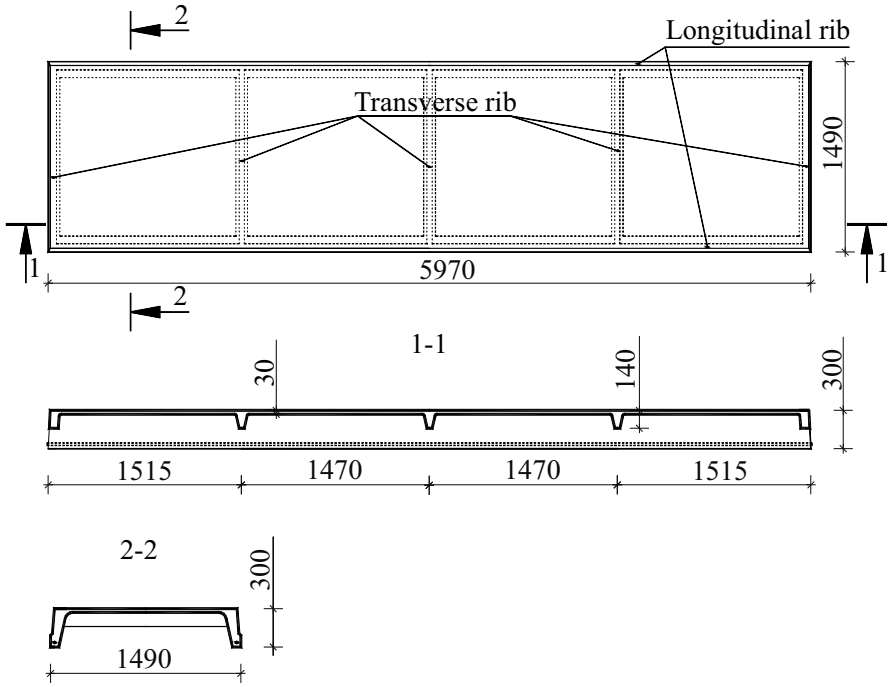

Fig. 3.1. Top view, longitudinal and transverse sections of a ribbed panel (PK-01-111 1961). *Dimensions are in mm.*

The types of ribbed panels reflect the former Soviet Union standard GOST. Reinforced concrete ribbed panels PKZH were manufactured (in accordance with GOST 7740-55) from the 1950s until 1964–1965. Prestressed concrete ribbed panels PNS were manufactured from 1964–1965 until at least 1990. Ribbed panels PNS-3 were manufactured in the relatively short period of transition from PKZH to PNS. Manufacture of ribbed panels PNS-12 (a further development of PNS-3) and PNS-14 started in the mid-1960-ies (in accordance with PK-01-111 1961).

Generally, the type of a ribbed panel was painted in a factory after curing. In the absence of a painted type, the diameter of the longitudinal working rebar was measured to determine the type of a ribbed panel. Structural and materials tests with prestressed PNS-12 and PNS-14 ribbed panels are discussed in more detail in **II**.

Prestressed concrete ribbed panels PNS-10–14 employed two hot-rolled low-alloyed prestressing bars 35 GS (C = 0.3–0.37%, Mn = 0.8–1.2%, Si = 0.6–0.9%, Cr = 0.3%, Ni = 0.3, Cu = 0.3; GOST 5058-65). The diameter (and prestress) of prestressing bars of ribbed panels PNS-12 and PNS-14 were 16 mm (343 N/mm^2) and 20 mm (481 N/mm^2), respectively (GOST 5058-65). The ultimate strength of prestressing steel (of both PNS-12 and PNS-14) should be at least 5500 kgf/cm^2 (539 N/mm^2) to correspond to its type (PK-01-111 1961). Prestressing bars are welded to the details at the support ends of a ribbed panel (PK-01-111 1961). Reinforcing and anchorage of ribbed panels PNS-12 and PNS-14 are shown in **Fig. 3.2**.

The strength of concrete of ribbed panels PNS-12 and PNS-14 should correspond to concrete strength mark M200 = 200 kgf/cm^2 and M300 = 300 kgf/cm^2, respectively (PK-01-111 1961). Hence, the concrete strength of ribbed panels PNS-12 and PNS-14 should be at least 19.6 N/mm^2 and 29.4 N/mm^2, respectively.

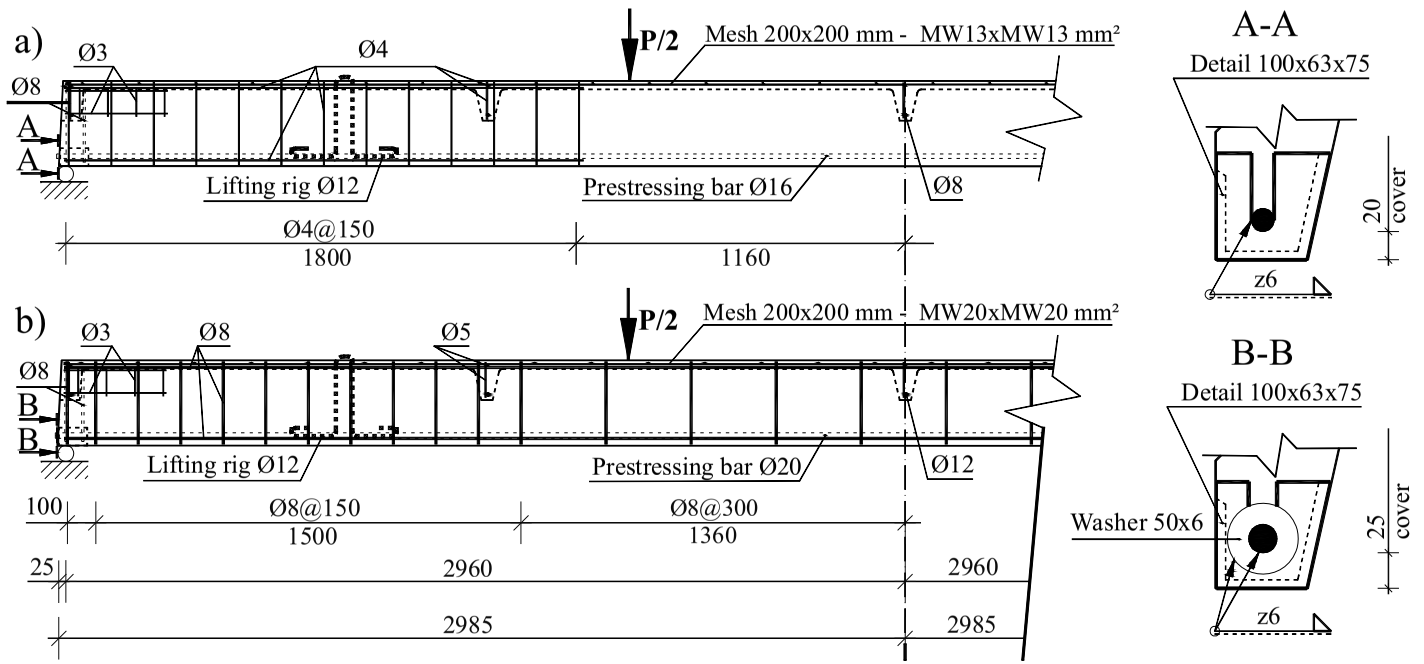

Fig. 3.2. Reinforcement and anchorage of the ribbed panels a) PNS-12 and b)PNS-14 (PK-01-111 1961)**.**
Dimensions are in mm.

3.3.2. Requirements for ribbed panels

According to GOST 8829 (1985), a randomly chosen precast concrete member from each production batch from the factory must be tested to assess its conformity to the load-bearing capacity, rigidity and crack resistance requirements. In this study the requirements for bearing capacity (all studied ribbed panels) and rigidity (ribbed panels PNS-12 and PNS-14) were considered. Due to corrosion deteriorations (cracked or spalled cover) most of the studied ribbed panels could not meet crack resistance requirements prior to loading.

The control load (GOST 8829-85) (q_c) was set to check the bearing capacity requirements of a ribbed panel. A ribbed panel meets the bearing capacity requirements of its type if the ultimate load of the tested ribbed panel exceeds the control load. Repetition tests were made if the ultimate load of a ribbed panel was less than the control load but not less than 85% of the control load. A ribbed panel does not meet the bearing capacity requirements if a single ultimate load in primary or repetition tests is less than 85% of the control load (PK-01-111 1961).

The control load (q_c) was calculated with the following formula (PK-01-111 1961):

$$q_c \geq \frac{s}{t} \cdot (q_d + q_{dead}) - q_{dead} \ , \tag{3.1}$$

where
s is the coefficient of overload, 1.4;
t is the coefficient of working conditions, 1.0;
q_d is the design load, kN/m^2;
q_{dead} is the dead load of a ribbed panel, kN/m^2.

The value of design load (q_d) could be found from catalogues (ZHI-EST-69) and the design drawings (PK-01-111 1961) of precast concrete members. The design load was implemented by the structural engineering design of a building.

A ribbed panel, including initial deflection, should be rigid enough not to exceed a deflection of 20 mm under a load of 3.73 kN/m^2 and 7.75 kN/m^2 for ribbed panels PNS-12 and PNS-14, respectively (PK-01-111 1961).

3.3.3. Test setup and loading

As shown in **Table 3.1**, all tested ribbed panels had been in service for at least 10 years. Ribbed panels were demounted and individually loaded. Ribbed panels were tested in a laboratory (K-8–K-10, P11–P13, L1–L10, R1–R8, V8–V12) as well as on site (K-1–K-7, VA14–VA19, T-20–T-23). Uniformly distributed load was imitated on a flexural test of ribbed panels PKZH-2 and PNS-3 in the 1970-ies (**Table 3.1**).

For the flexural test of ribbed panels PNS-12 and PNS-14, a four-point bending test arrangement (**Fig. 3.3**) was applied as follows. Two loads, acting as an equivalent for the uniformly distributed load, were applied to the middle third of the ribbed panel. The loads were applied by means of a hydraulic cylinder of a nominal maximum force of 250 kN. A steel main distribution beam divided the total applied load from the cylinder into two loads. The distributing beams further divided it across the width of the ribbed panel, resulting in a total of four concentrated loads on the ribbed panel. The main and distributing beams acted as a simple beam with a pin and roller support. The application of load was controlled by a manually activated hydraulic pump. Ribbed panels were simply supported with a pin and roller support (GOST 8829-85).

Before loading, a stressed wire was held on the supports to measure the initial deflection of each longitudinal rib in the mid-span of the ribbed panel. The initial deflection was measured by means of a ruler with a precision of 1 mm. A mean initial deflection of both ribs was calculated as an initial mid-span deflection of a ribbed panel (Δ_{in}) (GOST 8829-85). As a general rule, a negative initial deflection of a ribbed panel had been provided by prestressing it in the factory. The initial deflection was found on ribbed panels PNS-12 and PNS-14.

Ribbed panels were loaded stepwise of 10% of the control load (q_c), which was kept constant for at least 10 min. at each stage (GOST 8829-85). Ribbed panels were tested to failure or limit state whereby deflections of a ribbed panel increased without adding further load (GOST 8829-85). The maximum load a ribbed panel could carry was recorded as the ultimate load (q_u).

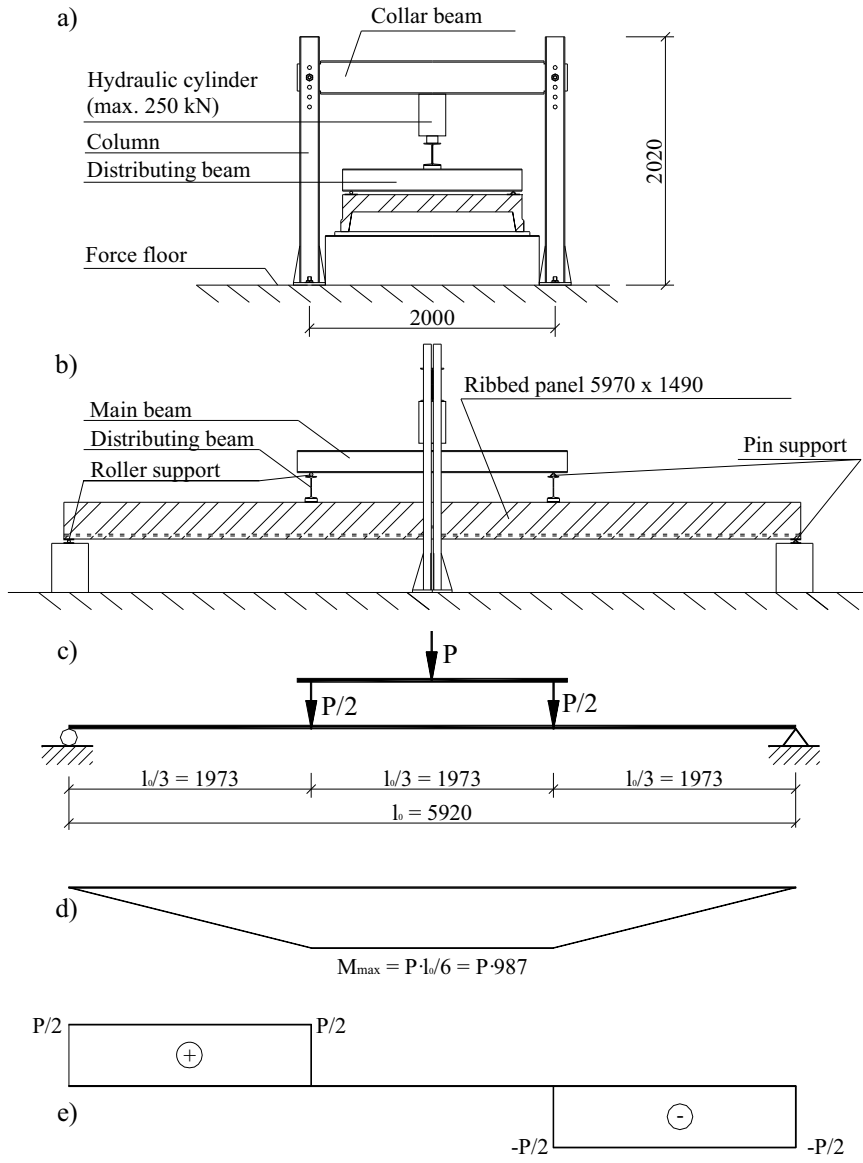

Fig. 3.3. a) End and b) side view of the test device with c) load, d) bending moment and e) shear diagram. *Dimensions are in mm.*

Existing cracks and cracks developing during the test were carefully recorded with a marker on the surface of a ribbed panel. Vertical displacements were measured at the four corners (on supports) and on both longitudinal ribs at the mid-span of each ribbed panel. Dial gauges with a precision of 0.01 mm were applied at the corners and compliant

measuring gauges with a precision of 0.1 mm and 0.01 mm at the mid-span of a rib. The mid-span deflection of a ribbed panel was calculated as the difference of the mean mid-span deflection of both longitudinal ribs and of the mean displacement at the supports of the ribbed panel (GOST 8829-85).

3.4. Material tests

3.4.1. Concrete cores

A) Ten cores with a diameter of 54 mm were drilled at the longitudinal rib of each ribbed panel (**II**).

B) 55 cores with a diameter of 75 mm were drilled from the columns and beams of the generator building. 36 cores were acquired from the 1st floor (columns) or the 2nd floor (beams) where the highest structural loads and most deteriorated structures were present (**IV**).

The concrete core test was based on Estonian National Standard EVS-EN 12504-1:2003. A cover meter was applied to locate the reinforcement in the structure before drilling. This generally enabled extraction of cores from a location where they contained no reinforcement. Cores were cut by means of a rotary cutting drill with diamond bits. The ends of the cores were ground or capped with rapid hardening cement. Each core was measured in accordance with EVS-EN 12504-1:2003. The mean cross-sectional area was calculated from five diameter measurements and the mean height of the cores was calculated from five height measurements. The estimated cube strength ($f_{est.cube}$) was calculated by applying the following equation (3.2) in BS 6089:1981:

$$f_{est.cube} = \frac{D}{1.5 + \mathbf{1/\lambda}} \cdot f_{\mathbf{core}}, \qquad (3.2)$$

where D = 2.5 for cores drilled horizontally (perpendicular to the cast direction), or D = 2.3 for cores drilled vertically (parallel to the cast direction),
λ is the height/diameter ratio, and
f_{core} is found by dividing the maximum load sustained by the core to its average cross-sectional area.

Cores with a height/diameter ratio of 1 were tested, because cylinders with this ratio have very nearly the same strength as standard cubes (EVS-EN 12504-1:2003; EVS-EN 13791:2007). The estimated cube strength was compared to the concrete strength mark from design drawings to verify if the structures were cast in accordance with the drawings. The concrete strength mark (operative until 1984) was calculated as a mean compressive strength of standard cube specimens of sides 150 mm in kgf/cm^2 (e.g. concrete of mark M200; SNiP II-21-75).

3.4.2. Carbonation depth and cover of concrete

Carbonation depth was measured by the conventional phenolphthalein test based on EVS-EN 14630:2006. Carbonation depth measurements should be taken only on the hardened cement paste (not in a location of a large piece of aggregate).

A) Phenolphthalein solution was applied to a freshly opened surface of the non-cracked concrete cover of the longitudinal rib of a ribbed panel after the flexural test. Carbonation depth was measured with a ruler at ten different locations (at least five readings for each location) on the longitudinal rib of a ribbed panel. The mean value of carbonation depth ($D_{carb,m}$) of a ribbed panel was calculated. A cover was also measured by means of a ruler at the same location where the carbonation test was performed (at least five readings at each location). The mean value of the cover (c_m) of prestressing bars of a ribbed panel was calculated.

B) Phenolphthalein solution was applied to a drilled surface of concrete cores on site. Carbonation depth was measured by means of a ruler at ten locations of the core. Concrete cover was also measured by means of a ruler at ten locations in the core hole. In most cases the core hole had to be widened to find the nearest reinforcement.

3.4.3. Chemical analysis of concrete

B) In order to have an overview of the deleterious salts in the concrete of an oil shale chemical plant a chemical analysis was performed. After a compression test three cores extracted from the beams carrying the generator (on the 2nd floor) were sent to the Remmers chemical laboratory (in Germany) by the company REV Special OÜ. From these

cores samples were obtained for quantitative analysis of water-soluble salts. With respect to durability sulphate, chloride and nitrate content were determined as a percentage of the mass of concrete samples. The analysis was performed according to German standard DIN 51100 (1957).

A) The chloride content was determined on 20 samples taken from the concrete cover of prestressing bars of adjacent ribbed panels of R1–R8 at the Raadi research object. Chloride content was determined by applying Quantab chloride titrator stripes.

3.4.4. Water absorption of concrete

Ten samples were extracted from the columns on the 1st floor of an oil shale chemical plant to determine the water absorption of concrete. The former Soviet Union standard water absorption measuring method (GOST 12730-67) was applied since the building was constructed in 1951. Samples were immersed in 20 °C water and weighed every 24 hours until a constant value was reached. After that, samples were oven-dried until reaching a constant dry mass. Water absorption was found with the formula (3.3):

$$W = \frac{m_H - m_O}{m_O} \tag{3.3}$$

where W is the water absorption, %;
m_H is the mass of a water-saturated sample, g, and
m_0 is the mass of a dried sample, g.

3.4.5. Yield, ultimate strength and corrosion of steel

The strength properties and corrosion of steel cut from the ribbed panels were investigated. Six prestressing steel specimens of visually larger corrosion damage were cut from the longitudinal ribs of each ribbed panel. Specimens were cut to a length of 450 mm, cleaned and weighed. The percentage gravimetric mass loss of each prestressing steel sample was calculated. The mean gravimetric mass loss ($\Delta m_{gr,m}$) of six samples was found to show the mean corrosion penetration of the prestressing bars of a ribbed panel. After mass loss determination, each prestressing bar was further inspected for evidence of pitting. However, no pits were

found on the prestressing bars. At least ten calliper gauge measurements were performed and the minimal diameter of each prestressing bar was recorded. The maximum diameter loss (Δd_{max}) of six bars was calculated to represent the maximum corrosion penetration of the prestressing bars of a ribbed panel.

All prestressing steel specimens were subjected to tensile testing. An R-20 universal testing machine (maximum force 200 kN) with the software for test data recording was applied. The mean yield ($f_{y,m}$) and ultimate strength ($f_{u,m}$) of six prestressing bars were calculated from the test data.

4. RESULTS AND DISCUSSION

4.1. Reinforced and prestressed concrete ribbed panels

4.1.1. Influence of visual condition on ultimate residual bearing capacity

A) In this part of the research, the results of structural and material tests with 46 existing reinforced and prestressed concrete ribbed panels are reported and discussed. In order to compare the residual bearing capacity of ribbed panels of four different types, the ratio (q_u/q_c) of ultimate load and control load was calculated. The *one-way analysis of variance* (*ANOVA*) did not reveal a significant difference in the average ratio of ultimate load and control load by the types of a ribbed panel (PKZH-2, PNS-3, PNS-12, PNS-14) at a confidence level of $\alpha=0.05$. Also, for comparison purposes the ultimate load (q_u) of ribbed panels was divided by design load (q_d). The results of the visual assessment and flexural test of ribbed panels are presented in **Table 4.1**.

Table 4.1. Results of visual assessment and flexural test of ribbed panels

Ribbed panel	Type	Grade	q_u, kN/m^2	q_u/q_c	q_u/q_d	Failure
K-1	PKZH-2	0	4.52	1.19	1.71	TR
K-2	PKZH-2	1	5.18	1.36	1.96	FD
K-3	PKZH-2	0	3.97	1.05	1.50	FD
K-4	PKZH-2	1	4.79	1.26	1.81	FD
K-5	PKZH-2	1	5.16	1.36	1.95	FD
K-6	PKZH-2	0	4.31	1.14	1.63	LR
K-7	PKZH-2	1	4.54	1.20	1.71	TR
K-8	PKZH-2	0	4.10	1.08	1.55	FD
K-9	PKZH-2	0	2.67	0.70	1.01	FD
K-10	PKZH-2	0	2.67	0.70	1.01	SU
P11	PNS-3	2	11.01	1.50	2.44	FD
P12	PNS-3	1	8.07	1.10	1.79	FD
P13	PNS-3	2	9.56	1.30	2.12	FD
VA14	PNS-3	1	8.79	1.19	1.95	FD
VA15	PNS-3	1	8.79	1.19	1.95	FD
VA16	PNS-3	2	9.90	1.35	2.20	FD
VA17	PNS-3	2	9.90	1.35	2.20	FD
VA18	PNS-3	2	9.90	1.35	2.20	FD

VA19	PNS-3	2	9.90	1.35	2.20	FD
T-20	PKZ-2	1	5.64	1.49	2.13	FD
T-21	PKZ-2	2	5.94	1.57	2.24	FD
T-22	PKZ-2	1	5.64	1.49	2.13	FD
T-23	PKZ-2	1	5.43	1.43	2.05	FD
L1	PNS-12	0	9.00	1.22	2.00	FD
L2	PNS-12	4	9.20	1.25	2.04	FD
L3	PNS-12	1	9.25	1.26	2.05	FD
L4	PNS-12	3	9.70	1.32	2.15	FD
L5	PNS-12	1	9.75	1.33	2.16	FD
L9	PNS-12	3	9.04	1.23	2.00	FD
L6	PNS-14	5	16.95	1.20	1.82	FD
L7	PNS-14	0	13.56	0.96	1.46	WR
L8	PNS-14	0	10.17	0.72	1.09	WR
L10	PNS-14	0	15.82	1.12	1.70	SH
R1	PNS-12	0	8.35	1.14	1.85	FD
R2	PNS-12	0	7.26	0.99	1.61	FD
R3	PNS-12	1	9.12	1.24	2.02	FD
R4	PNS-12	1	9.64	1.31	2.14	FD
R5	PNS-12	1	9.86	1.34	2.19	FD
R6	PNS-12	0	8.59	1.17	1.90	FD
R7	PNS-12	1	7.91	1.08	1.75	WR
R8	PNS-12	0	8.28	1.13	1.84	FD
V8	PNS-12	0	9.00	1.22	2.00	SH
V9	PNS-12	0	10.53	1.43	2.33	FD
V10	PNS-12	1	8.80	1.20	1.95	FD
V11	PNS-12	2	9.30	1.26	2.06	FD
V12	PNS-14	1	15.28	1.08	1.64	SH

Failure: FD–flexural ductile, TR–rebar rupture in transversal rib, LR–rebar rupture in longitudinal rib, SU–failure of longitudinal rib near support, WR–weld rupture at support, SH–shear failure. The results of V1–V6 (ribbed panels PNS-14) are omitted. The reasons for omitting ribbed panels V1…V6 are explained in sub-section 4.1.4.

The control loads (after transformation from kgf/m^2 to kN/m^2) of ribbed panels PKZH-2, PNS-3 (later PNS-12) and PNS-14 are 3.80 (GOST 7740-55), 7.35 (PK-01-111 1961) and 14.12 kN/m^2 (PK-01-111 1961), respectively. The design loads of ribbed panels PKZH-2, PNS-3 (later PNS-12) and PNS-14 are 2.65 (GOST 7740-55), 4.51 (PK-01-111 1961) and 9.32 kN/m^2 (PK-01-111 1961), respectively.

The ultimate load of only five of the 46 ribbed panels (in **Table 4.1**) was less than the control load. All of these five ribbed panels received grade 0 on the visual rating scale (**Table 3.2**). Consequently, attention should be paid to ribbed panels where the concrete cover of longitudinal reinforcement has spalled (grade 0) which could be a sign of decreased bearing capacity in comparison with factory-issued (new) ribbed panels. The visual scale proposed has the potential to serve as a tool for practitioners, operators and asset managers to make decisions about the optimal timing for repairs, strengthening, and/or rehabilitation of corrosion-affected reinforced concrete structures. Scale-acquainted engineers can assess reinforced concrete structures relatively quickly and simply to locate ribbed ceiling panels (if any) of spalled concrete cover. Later on the residual bearing capacity of ribbed panels with grade 0 needs the judgment of a structural expert. All ribbed panels with a corrosion-induced crack in the longitudinal rib (grade 1) could carry the control load. Hence, these ribbed panels conform to the strength requirements of new ribbed panels even after a period of service from 10 to 32 years (**Table 3.1**).

From the point of view of a structural engineer it is important that all studied ribbed panels (irrespective of their grade) are able to carry the design load ($q_u/q_d > 1.01$; **Table 4.1**). The values of the design load could be found from the catalogues (e.g. ZHI-EST-69) of precast concrete members. These catalogues were updated every 4–6 years. Since engineers compare the calculated structural bearing capacity with the design load, the latter could be employed as an equivalent of the ultimate limit state. Hence, all studied ribbed panels corresponded to the ultimate limit state. Despite of their sufficient residual bearing capacity ribbed panels with grade 1 or 0 need repairs.

The influence of the visual condition (grade) on the bearing capacity (q_u/q_c) of 46 ribbed panels is presented in **Fig. 4.1**. The box plot in **Fig. 4.1** was generated with statistical software R. The box plot shows the distribution of the data points around the median (thick horizontal line in **Fig. 4.1**), indicating the upper and lower quartiles (horizontal edges of the box) and minimum and maximum values (ends of the vertical bar). **Fig. 4.1** shows a non-linear decreasing trend of the ratio q_u/q_c with the decreasing grade of the ribbed panel. Only a few samples of high grades exist in the current data set. Neither statistical nor substantial reasons

exist to assume a trend in the ratio q_u/q_c at grade 2 or higher. However, box plots from grade 2 to 0 demonstrate an evident decrease of the ratio q_u/q_c. The one-way *ANOVA* revealed a significant effect for grades, $F(5,40) = 5.35; p = 0.0007$. The magnitude of the grade to the ratio q_u/q_c was computed as $R^2 = 0.40$. *Tukey's HSD test for multiple comparison of means* proved the significant difference of the ratio q_u/q_c between grade 0 and higher grades.

Fig. 4.1 demonstrates that the ratio q_u/q_c varies the most in ribbed panels with spalled concrete cover (grade 0). This means that ribbed panels, which may have just reached grade 0 as well as ribbed panels in a critical state in terms of their load-bearing capacity are both rated as grade 0. Consequently, ribbed panels with a spalled concrete cover should be differentiated to specify their different residual bearing capacity. Deterioration states employed for the ribbed panel's classification in the current study (in **Table 3.2**) were developed already in 1974 and the condition corresponding to grade 0 should be updated and improved in further research.

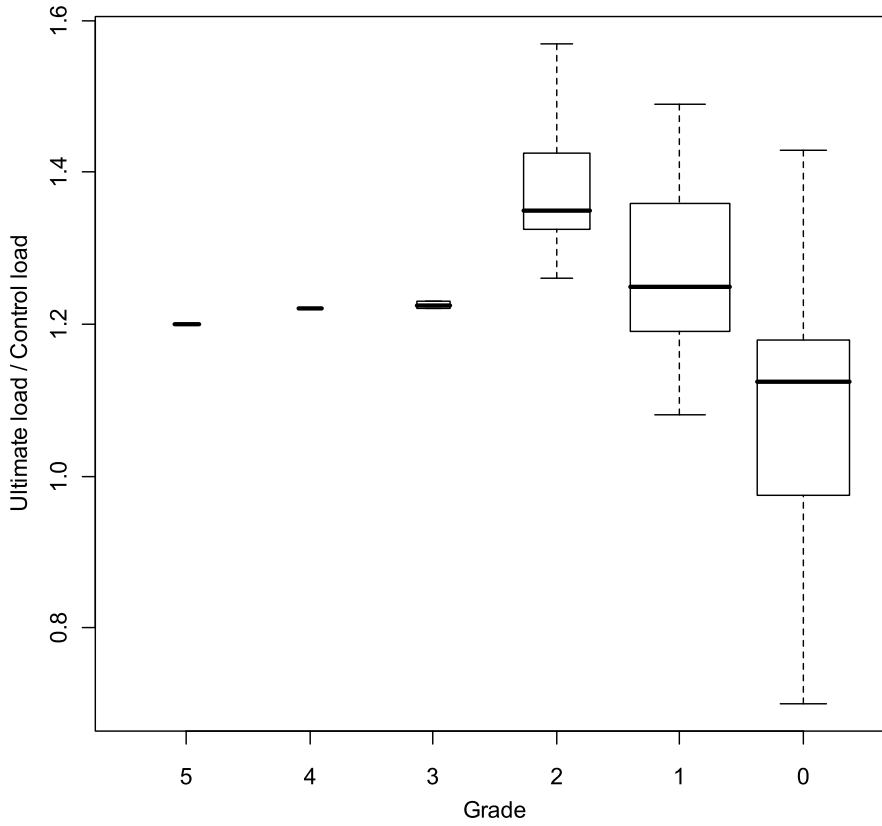

Fig. 4.1. Box plot of the ratio q_u/q_c for individually tested ribbed panels of different visual grades. *The box plots show distribution characteristics: the median (thick horizontal line), upper and lower quartiles (horizontal edges of the box) and minimum and maximum values (ends of the vertical bar) of the ratio q_u/q_c by different grades.*

As mentioned in sub-section 1.3 Durham *et al.* (2007) and Heymsfield *et al.* (2007) had tested 33 existing precast non-prestressed channel beams, which were used in short multi-span bridges in Arkansas in the 1950s through the early 1970s. Flexural members with similar length (5.79 m) and cross section (ribbed slab) were also tested on a four-point loading frame. The beams, constructed without shear reinforcement, were categorised as 'good', 'average' or 'poor' as a function of the percentage and location of the exposed longitudinal reinforcing steel (**Table 1.3**). All three of these classifications correspond to grade 0 on the visual rating scale of the current study.

Fig. 4.2 represents an illustrative load-bearing capacity model for a reinforced (or prestressed) concrete flexural member (RCM) based on Torres-Acosta *et al.* (2007) (**Fig. 1.4**) and the current study with the addition of the research results by Heymsfield *et al.* (2007) and Li *et al.* (2008). The lifetime of RCM in **Fig. 4.2** consists of three stages (also described in sub-section 1.3): T_I is the corrosion initiation stage from the time of manufacture to the time of corrosion initiation; T_P is the corrosion propagation stage during which the steel corrodes until an unacceptable level of corrosion is reached and; T_{RL} is the residual life stage from serviceability to ultimate limit state.

In this study, the unacceptable level (end of stage T_P) of corrosion is defined as a corrosion-induced crack in the longitudinal rib of a ribbed panel being more than 0.3 mm wide (grade 1). This might also be implied as the serviceability limit state of a ribbed panel. Li *et al.* (2008) stated that once the structure is considered to be unserviceable due to corrosion-induced cracking, there is considerable residual lifetime before the structure can be considered as having become unsafe. The residual life stage T_{RL} starts from the time the structure becomes unserviceable until the ultimate limit state is reached, before structural collapse.

The categorisations of 'good', 'average' and 'poor' by Heymsfield *et al.* (2007) are also included in **Fig. 4.2**. An attempt has to be made to add the six detailed phases of the phenomenological model (Li *et al.* 2008) for steel corrosion in concrete. However, the model by Li *et al.* (2008) has a different approach. The latter differentiates six phases (D1, D2, C0, C1, C2, C3) of corrosion applied to the steel bar at a generic cross section of a reinforced concrete member. In addition, the initiation period of the model by Li *et al.* (2008) was based on corrosion induced by chloride attack.

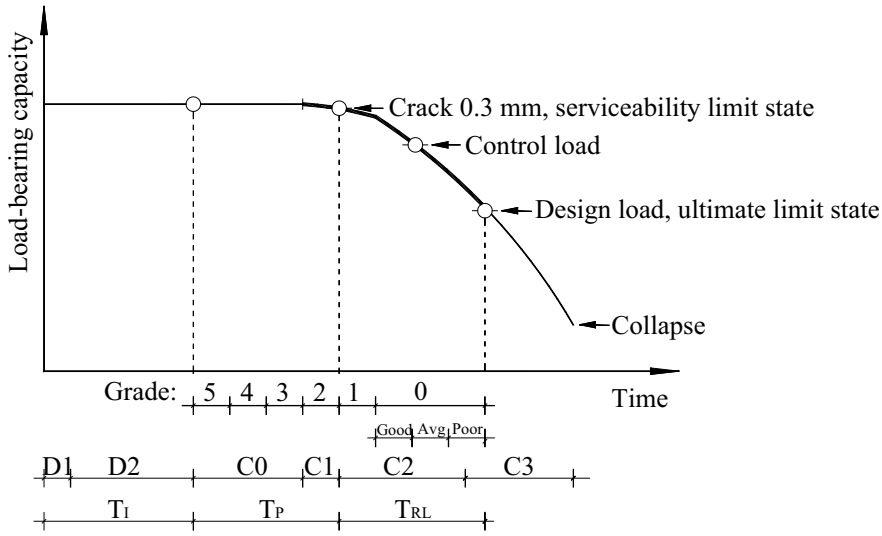

Fig. 4.2. An illustrative load-bearing capacity model for an RCM. Based on Torres-Acosta *et al.* (2007) and the current study with the addition of research results by Heymsfield *et al.* (2007); Li *et al.* (2008).

As mentioned before, all ribbed panels with a visual grade of 1 or higher overreached the control load, which explains the location of the control load on the time axis. Since the structural engineering designers based their calculations on the design load, the latter is employed as an equivalent of the ultimate limit state in **Fig. 4.2**. The thick load-bearing capacity line in **Fig. 4.2** represents the period for RCM covered by the current structural tests. As observed from **Figs. 4.1** and **4.2** the structural bearing capacity remains almost the same during the initiation and propagation stages until reaching grade 0 (in the residual life stage), where the bearing capacity decrease rate is accelerated.

4.1.2. Influence of visual condition on flexural behaviour and failure mode of ribbed panels PKZH-2 and PNS-3

The flexural behaviour of ribbed panels PKZH-2 and PNS-3 (in terms of their load-deflection curves) are presented in **Figs. 4.3** and **4.4,** respectively. The curves of a ribbed panel with grade 2 or higher (no visual deterioration or micro-cracks in the longitudinal ribs) is shown as a solid line. A dashed line with long dashes or short dashes describes the load-deflection curve of ribbed panels, which received grade 1 or 0,

respectively. Ribbed panels from the same test series have identical curve markers (if any). Generally, curve markers denote different load steps except of **Fig. 4.4**, where data describing different load steps (of ribbed panels PNS-3) has not been extant.

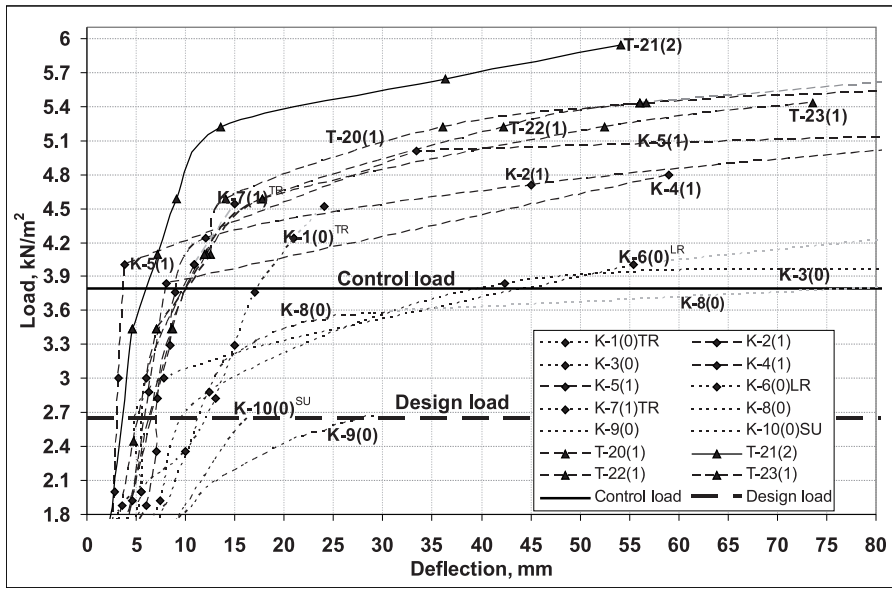

Fig. 4.3. Load-deflection curves of 14 reinforced concrete ribbed panels PKZH-2. *Failure: TR–rebar rupture in transversal rib, LR–rebar rupture in longitudinal rib, SU–failure of longitudinal rib near support.*

Fig. 4.3 shows that ribbed panels with a lower visual grade tend to have larger deflections at the same load. For example, at control load ribbed panel with grade 2 has deflected 6 mm, while ribbed panels with grades 1 (except of K-5) and 0 have deflected 8–10 mm and at least 17 mm, respectively. Ribbed panels K-3, K-6 and K-8 (with grade 0) deflected at least 40 mm at control load. This trend conforms to Azad *et al.* (2007), who found that the corroded beams had higher deflection than the corresponding control beams at the same load due to degrading stiffness. However, Azad *et al.* (2007) applied sodium chloride and a direct current to initiate and accelerate corrosion, respectively, which complicates the comparison with the current study. It should be noted that only a limited amount of ribbed panels of different grades are presented in **Figs. 4.3** and **4.4**. However, the statement that lower grade ribbed panels have larger deflections is not clear with ribbed panels PNS-3 in **Fig. 4.4**.

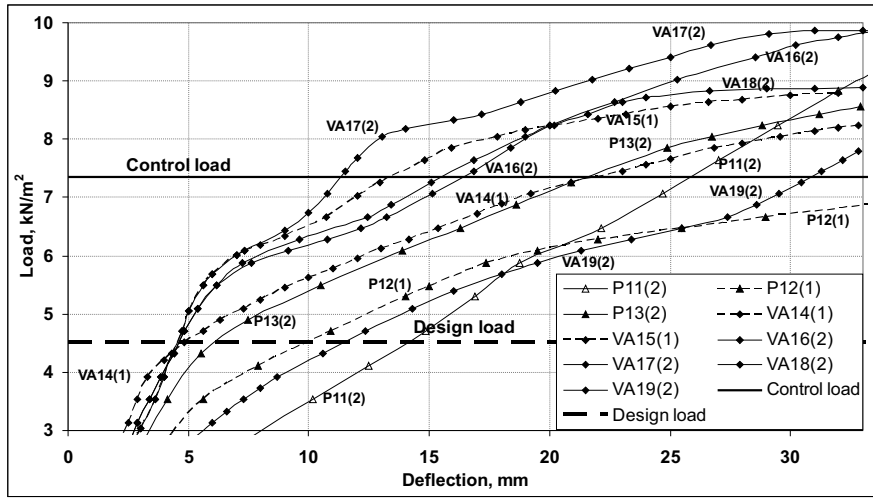

Fig. 4.4. Load-deflection curves of 9 prestressed concrete ribbed panels PNS-3.

Although not measured in all tested ribbed panels, a significant initial deflection might appear in existing ribbed panels after long-term service. The load-deflection curves of ribbed panels PNS-12 and PNS-14 including their initial deflection is presented in **Figs. 4.8** (sub-section 4.1.3) and **4.12** (4.1.4), respectively.

Of the 46 ribbed panels flexural ductile mode of failure was noticed in 36 ribbed panels in **Table 4.1**. These 36 ribbed panels reached a yield level, where deflections increased rapidly without considerable load addition. The unconventional failure mode of the other 10 ribbed panels is marked in superscript on the label of a ribbed panel in **Figs. 4.3, 4.4, 4.7, 4.8, 4.11** and **4.12**. All 10 of those ribbed panels had serious visual corrosion deterioration to receive either grade 0 (7 ribbed panels) or grade 1 (3 ribbed panels). However, 16 ribbed panels with visual grade 0 and 18 ribbed panels with grade 1 were tested. The one-way *ANOVA* did not reveal significant effect of failure mode on the average grade of ribbed panel, $F(5,44) = 1.59$; $p = 0.18$.

Fig. 4.3 shows that ribbed panels K-1, K-7 and K-10 exhibited no yielding. Ribbed panels K-1 and K-7 failed due to rebar fracture in the transversal rib. Accumulation of sand (which was applied as a load; **Table 3.1**) in the middle of the transversal rib might have caused that mode of failure. The longitudinal rib of ribbed panel K-10 failed near

support. Concrete in the failure place had crumbled prior to the loading tests probably because of poor manufacturing quality. The longitudinal rib of ribbed panel K-6 failed in the mid-span region due to a rebar fracture although the ribbed panel overcome yielding (in **Fig. 4.3**) before the fracture. The longitudinal rebar fracture occurred at a ribbed panel K-6. Corrosion-caused severe reduction of the cross-section in the longitudinal rebar of ribbed panel K-6 was detected on visual inspection. Du *et al.* (2007) mentioned that corrosion could alter the failure mode and affect the ductile behaviour of reinforced concrete bending members substantially. Corrosion reduces the area of tension bars and therefore makes concrete members less reinforced and, in general, more ductile. In case of very under-reinforced beams, however, the reduced bar area can be so small that failure occurs by bar fracture rather than bar yield. As a result, there can be a reduction of bar ductility (Du *et al.* 2007). Unfortunately no rebar tensile test was performed in test series K-1–K-7 to verify the ultimate strength or ductility of the longitudinal rebar from ribbed panel K-6.

The failure mode of all nine ribbed panels PNS-3 was flexural ductile, which could also be deduced from the load-deflection plots in **Fig. 4.4**. The almost linear curve of a ribbed panel P11 should be pointed out. The other ribbed panels PNS-3 demonstrated yielding. The results and discussion of the flexural and material tests of prestressed concrete ribbed panels PNS-12 and PNS-14 are presented in the following sub-sections 4.1.3 and 4.1.4, respectively.

4.1.3. Flexural and material tests of ribbed panels PNS-12

The results of the flexural and material tests of 18 prestressed concrete ribbed panels PNS-12 are presented in **Table 4.2**. **Table 4.2** shows that ribbed panel R2, with the largest initial mid-span deflection (Δ_{in}) of 53 mm, also had the lowest flexural bearing capacity. Thus, the visually detectable initial mid-span deflections of a ribbed panel could be a sign of decreasing flexural bearing capacity. The mean yield strength of prestressing steel specimens of ribbed panel R2 was at least 53 MPa lower than that of other ribbed panels PNS-12. This could also have reduced the flexural bearing capacity of R2, because most of the ribbed panels (including R2) were tested until deflections increased without further load, meaning that the prestressing steel of a ribbed panel had begun to yield.

Prestressing steel specimen no. 3, cut from the mid-span of ribbed panel R1, was significantly more corroded (m_{red} = 19.6 %, $d_{red,\ max}$ = 10.3 %) and weaker (f_y = 458 MPa, f_u = 531 MPa) than any other specimen cut from ribbed panels PNS-12 (**Table 4.2**). The ultimate strength of the prestressing steel of PNS-12 should be at least 539 MPa to correspond to its strength (PK-01-111 1961). Except for specimen no. 3 from R1, the ultimate strength of all prestressing steel specimens from ribbed panels PNS-12 considerably exceeded their corresponding strength. However, the characteristics of that sample have not significantly reduced the flexural bearing capacity (q_u/q_c=1.14) of ribbed panel R1.

Table 4.2. Results of flexural and material tests of ribbed panels PNS-12

RP	Δ_{in} mm	q_u kN/m^2	q_u/q_c	Failure	$f_{est,cube,m}$ MPa	$D_{carb,m}$ mm	c_m mm	$f_{y,m}$ [*Min^n] MPa	$f_{u,m}$ [*Min^n] MPa	$\Delta m_{G,m}$ [*Max^n] %	Δd_{max} %
L1	NA	9.00	1.22	FD	37.6	NA	NA	605	652	8.7 [17.6[1]]	6.3
L2	-15	9.20	1.25	FD	NA	NA	NA	NA	NA	NA	NA
L3	-19	9.25	1.26	FD	32.6	NA	NA	599	658	6.6	4.8
L4	-14	9.70	1.32	FD	NA	NA	NA	NA	NA	NA	NA
L5	-12	9.75	1.33	FD	30.6	NA	NA	624	674	7.3	5.1
L9	-21.5	9.04	1.23	FD	32.5	NA	NA	591	639	9.4	5.3
R1	-4	8.36	1.14	FD	45.4	11.8	32	537 [458[3]]	646 [531[3]]	9.7 [19.6[3]]	10.3[3]
R2	53	7.24	0.98	FD	47.1	NA	31	484	663	8.4	2.0
R3	-19	9.12	1.24	FD	41.6	10.1	30	605	723	5.9	0
R4	8	9.64	1.31	FD	34.7	9.9	24	539 [418[4]]	681	8.4	2.0
R5	-10	9.86	1.34	FD	40.2	NA	33	582	702	7.1	1.0
R6	5	8.59	1.17	FD	41.7	8.8	31	547	695	5.1	0.7
R7	-1	7.91	1.08	WR	NA	NA	30	569	701	4.9	3.7
R8	34	8.28	1.13	FD	32.2	7.4	22	506	696	5.8	2.7
V8	-12	9.04	1.23	SH	18.4	24.7	24	620	699	NA	7.9[6]
V9	18	10.53	1.43	FD	56.4	8.4	25	576	649	NA	3.4
V10	0.5	8.81	1.20	FD	43.7	9.7	27	576	636	NA	5.1
V11	-11	9.26	1.26	FD	45.8	8.6	24	566	661	NA	2.3

*RP–Ribbed panel; NA–Result not available; Failure: FD–Flexural ductile, WR–Weld rupture at supports, SH–Shear failure; [*Min/Max] –shown if significantly different from mean; []^n – no. of prestressing bar.*

Sixteen ribbed panels PNS-12 had a flexural ductile failure, ribbed panel R7 had an anchorage failure and V8 had a shear failure. The prestressing bars of PNS-12 are welded to the details at the supports of a ribbed panel (section A-A in **Fig. 3.2a**; PK-01-111 1961). During the failure of ribbed panel R7 the weld ruptured and the longitudinal prestressing bar slipped inwards at the support (**Fig. 4.5.**). Ribbed panel R7 also showed a relatively low flexural bearing capacity in comparison with the other ribbed panels PNS-12. The ultimate load of R7 was registered shortly before weld rupture.

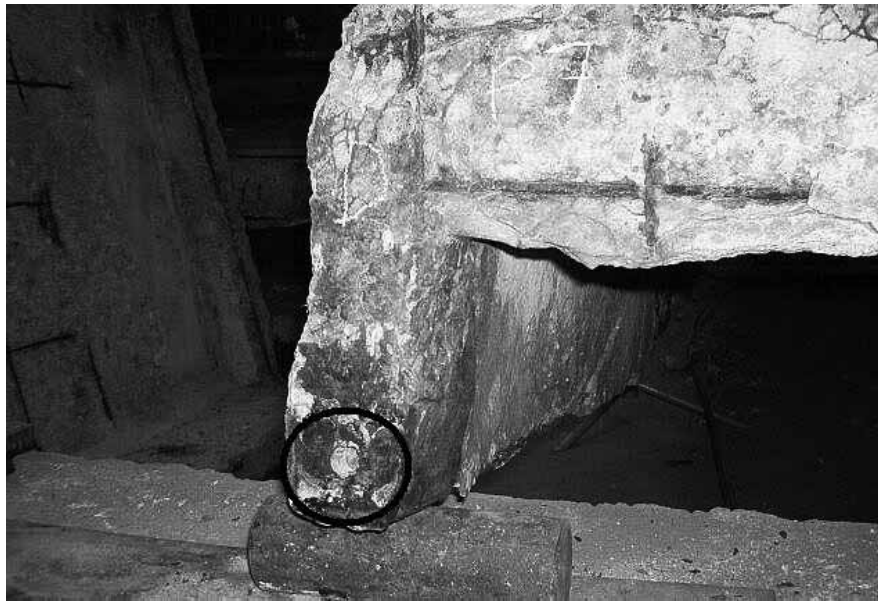

Fig. 4.5. The support of ribbed panel R7 after anchorage failure.

The critical shear crack of ribbed panel V8 started from the point of load application and ended at the lower end of the last stirrup (**Fig. 4.6**). No stirrups were in the critical shear crack, because the stirrups ended at 1800 mm, and the point of load application was 1973 mm from the support (**Fig. 3.2a** and **Fig. 4.6**). Therefore, the shear resistance of V8 in the critical section depended only on concrete strength. **Table 4.2** shows that the concrete strength of ribbed panel V8 ($f_{est,cube,\mathrm{m}}$ = 18.4 MPa) was considerably lower than that of other ribbed panels PNS-12. As mentioned earlier, the concrete strength of ribbed panels PNS-12 should be at least 19.6 MPa to be in accordance with their strength mark M200 (PK-01-111 1961). Except for ribbed panel V8, the concrete strength of all ribbed panels PNS-12 substantially exceeded its strength mark (**Table**

4.2). Low concrete strength of ribbed panel V8 also explais why the the cover of only V8 was fully carbonated ($D_{carb,m}$ = 24.7 mm > c_m = 24 mm). About one-third of the cover was carbonated on the other ribbed panels PNS-12.

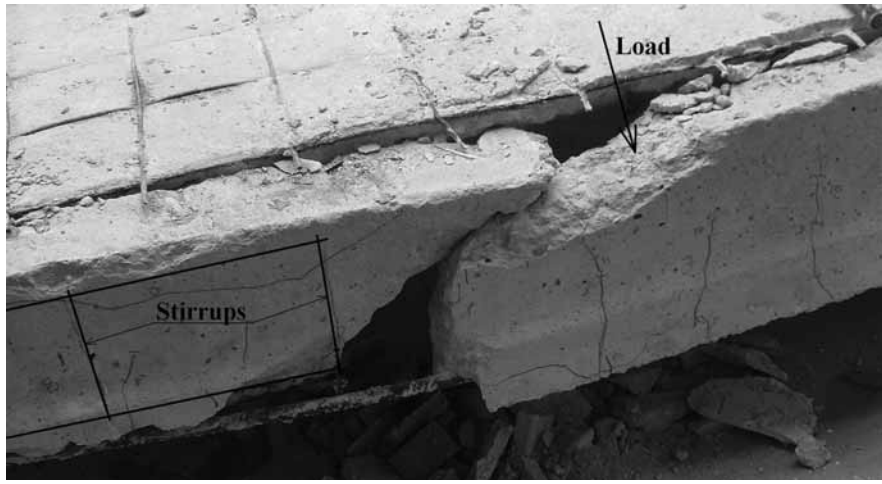

Fig. 4.6. Shear failure of ribbed panel V8.

The shear failure of V8 was caused probably by chosen four-point bending test arrangement which resulted in larger shear stresses than uniformly distributed load at the section of load application. GOST 8829-85 recommends a loading scheme of a reinforced concrete structure with a uniformly distributed load **(Fig. 4.7(a))** and its equivalent load (**Fig. 4.7(b)**). An equivalent load with four equally concentrated loads can replace the uniformly distributed load if a total uniformly distributed control load exceeds 35 kN (GOST 8829-85). The bending moment (**Fig. 4.7(b1**)) and shear (**Fig. 4.7(b2**)) of an equivalent load (GOST 8829-85) (solid line) are compared to those of the current study (dashed line). The equivalent loading arrangement would result in half the shear stresses (P/4 in **Fig. 4.7(b2**)) as those (P/2 in **Figs. 4.7(b2)** and **3.3(e))** developed with the chosen loading arrangement at the section of load application.

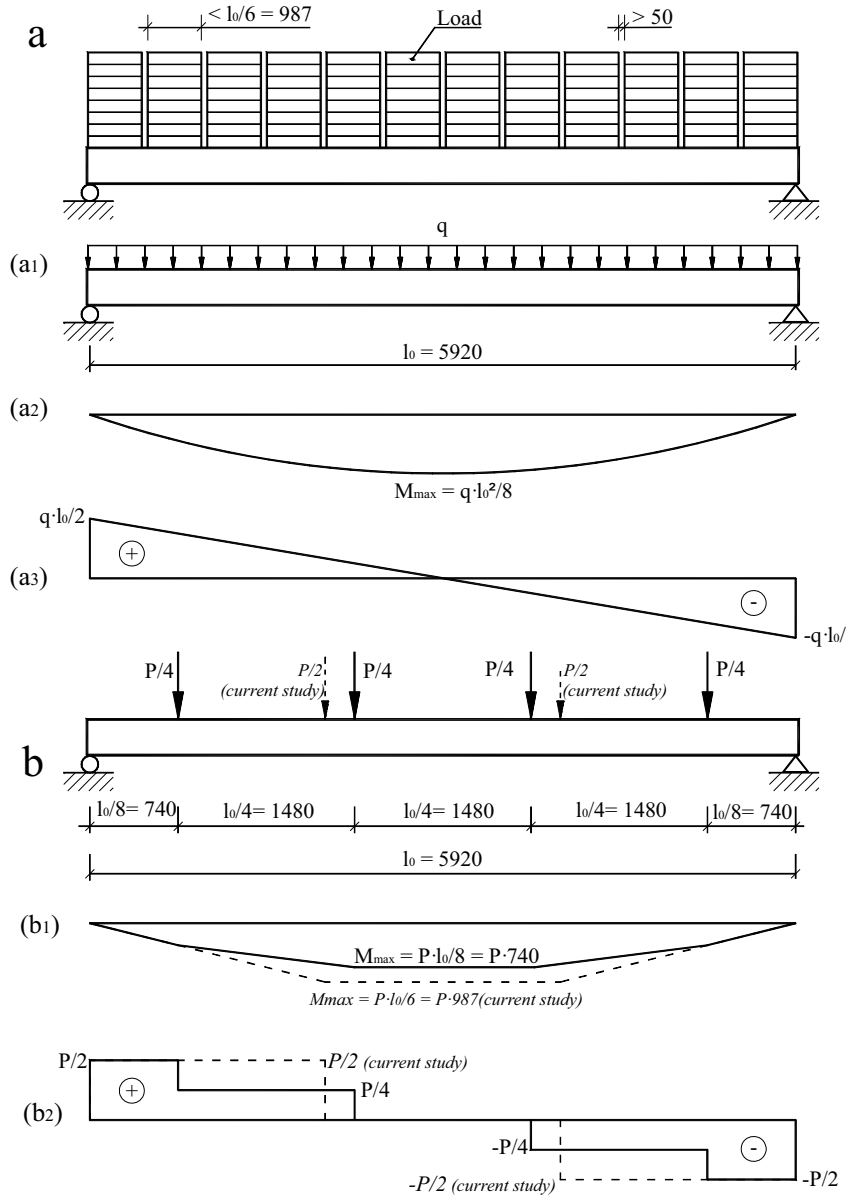

Fig. 4.7. Loading scheme of reinforced concrete structure (GOST 8829-85) with (a) uniformly distributed load and (b) equivalent load with corresponding bending and shear diagrams. *Dimensions are in mm.*

The load-deflection curves of ribbed panels PNS-12, including initial deflection, are presented in **Fig. 4.8**. Curves with dashed lines indicate ribbed panels of spalled cover in the longitudinal rib. The authors managed to acquire several test documents of new ribbed panels (tested in the 1970s) from concrete factories in Estonia. The load-deflection curves of eight new ribbed panels, which conformed to the requirements (GOST 8829-85) for PNS-12, are plotted with thick solid lines in **Fig. 4.8**. It should be noted that new ribbed panels were tested only up to the control load, i.e. until the strength requirement was met.

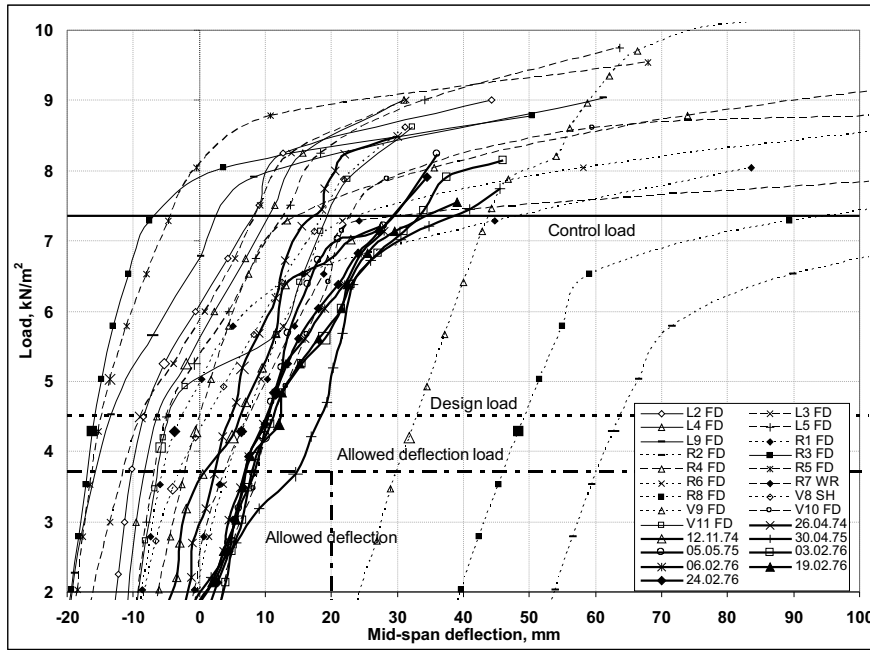

Fig. 4.8. Load-deflection curves of ribbed panels PNS-12, including initial deflection. *Thick solid curves denote new ribbed panels. Large markers indicate the load step at which the first flexural crack appeared. Failure: FD–Flexural ductile, WR–Weld rupture at supports, SH–Shear failure.*

Fig. 4.8 shows that ribbed panels R2, R8 and V9 failed to meet the rigidity requirements, caused by their initial deflection of 18 mm or more. These ribbed panels also had a spalled cover. However, other ribbed panels with a spalled cover (e.g. ribbed panels V8, R1 and R6 in **Fig. 4.8**) met both strength and rigidity requirements. **Fig. 4.8** also shows that the flexural behaviour of the analysed existing ribbed panels (which have been in service for at least 25 years) was not substantially different from the new ribbed panels PNS-12.

4.1.4. Flexural and material tests of ribbed panels PNS-14

The results of flexural and material tests of ten prestressed concrete ribbed panels PNS-14 are presented in **Table 4.3**. The ultimate load of five ribbed panels PNS-14 was less than the control load. The ultimate load of L7, V5 and V6 consisted of more than 0.85 of the control load, which would mean repetition tests for new ribbed panels issued from the factory. The strength of L8 and V4 was less than 0.85 of the control load. Hence, these ribbed panels did not meet the strength requirements for new ribbed panels.

Both the yield and ultimate strength of prestressing steel specimens from ribbed panels V1–V6 were questionably low in comparison with other samples from ribbed panels PNS-14 (**Table 4.3**). The ultimate strength of prestressing steel 35GS (applied in PNS-14) should be at least 539 MPa (PK-01-111 1961). The mean ultimate strength of prestressing bars from ribbed panels V1–V6 was at the threshold of (V1) or lower (V2, V4, V5, V6) than steel mark 35GS. The mean yield strength of prestressing bars from ribbed panels V1–V6 was 442 MPa or less. Therefore, these prestressing bars would have started to yield under the prestress of 481 N/mm^2 for ribbed panels PNS-14 (PK-01-111 1961). The visual condition of these ribbed panels was good (grade 3) and the corrosion level on the prestressing bars was insignificant ($d_{red,max} \leq 2.6$ %). The nominal diameter of prestressing bars from ribbed panels V1–V6 was about 20 mm as it should be for the ribbed panels PNS-14 (**Fig. 3.2**; PK-01-111 1961). Also, a factory-painted type–PNS-14–was observable on one of the ribbed panels (V1–V6). Therefore, prestressing steel of an inferior strength was probably applied to ribbed panels V1–V6. This also explains the poor residual flexural bearing capacity of those ribbed panels. Because of the above stated reasons ribbed panels V1–V6 are omitted from the analysis and **Table 4.1** in sub-section 4.1.1.

Table 4.3. Results of flexural and material tests of ribbed panels PNS-14

RP	Δ_{in}, mm	q_u, kN/m^2	q_u/q_c	Failure	$f_{est,cube,m}$ MPa	$D_{carb,m}$ mm	c_m, mm	$f_{y,m}$ MPa	[*Min^n],	$f_{u,m}$ MPa	[*Min^n],	$\Delta m_{gr,m}$, %	$\Delta d_{max,}$ %
L6	-18.5	16.95	1.20	FD	48.4	NA	NA	598		649		6.8	2.6
L7	0	13.56	0.96	WR	38.1	NA	NA	588		640		5.6	2.5
L8	7.5	10.17	0.72	WR	27.1	NA	NA	606		652		4.4	2.4
L10	-3	15.82	1.12	SH	35.3	NA	NA	585		642		7.2	3.6
V1	-4	15.2	1.08	FD	48.6	10.5	27	442	[302^6]	540	[369^6]	NA	1.6
V2	-5.5	14.82	1.05	FD	45.3	10.3	26	283		417		NA	1.6
V4	-3	11.36	0.80	FD	49.1	8.0	32	345	[267^1]	520	[401^1]	NA	2.1
V5	-5.5	13.80	0.98	FD	38.5	8.8	28	360		525		NA	2.6
V6	-8	12.17	0.86	FD	45.8	10.0	31	362	[255^3]	521	[427^3]	NA	0.5
V12	0	14.81	1.05	SH	42.7	11.7	20	552		616		NA	3.8

*RP–Ribbed panel; NA–Result not available; Failure: FD–Flexural ductile, WR–Weld rupture at supports, SH–Shear; [*Min/Max] –shown if significantly different from mean; []^n–no. of prestressing bar.*

Seven ribbed panels PNS-14 had a flexural ductile failure. The weld failed at the support ends of ribbed panels L7 and L8. As reported earlier, the ultimate load of both ribbed panels was less than the control load. The prestressing bar of a ribbed panel PNS-14 was welded to the washer, which itself was welded to the detail at the support (section B-B in **Fig. 3.2b**; PK-01-111 1961). Therefore, the condition of anchorage (weld) should be checked at the support ends, because it could reduce the flexural bearing capacity of a ribbed panel. The concrete strength of ribbed panels PNS-14 should be at least 29.4 MPa (mark M300; PK-01-111 1961). Except for ribbed panel L8 the concrete strength of all ribbed panels PNS-14 corresponded to (or exceeded) its strength mark (**Table 4.3)**. Even the concrete strength of L8 ($f_{est,cube,\mathrm{m}}$ = 27.1 MPa) was not considerably lower than the strength mark for ribbed panels PNS-14. The mean gravimetric mass loss ($\Delta m_{gr,\mathrm{m}} \leq 7.2\%$) and the maximum diameter loss ($\Delta d_{max} \leq 3.8\%$) of the prestressing bar samples cut from ribbed panels PNS-14 were not significant.

Ribbed panels L10 and V12 had a shear failure with a large inclined crack at the longitudinal rib starting from the point of load application (ribbed panel V12 in **Fig. 4.9**). This type of failure can be accounted for by the loading arrangement involved. The reasons were explained in previous sub-section.

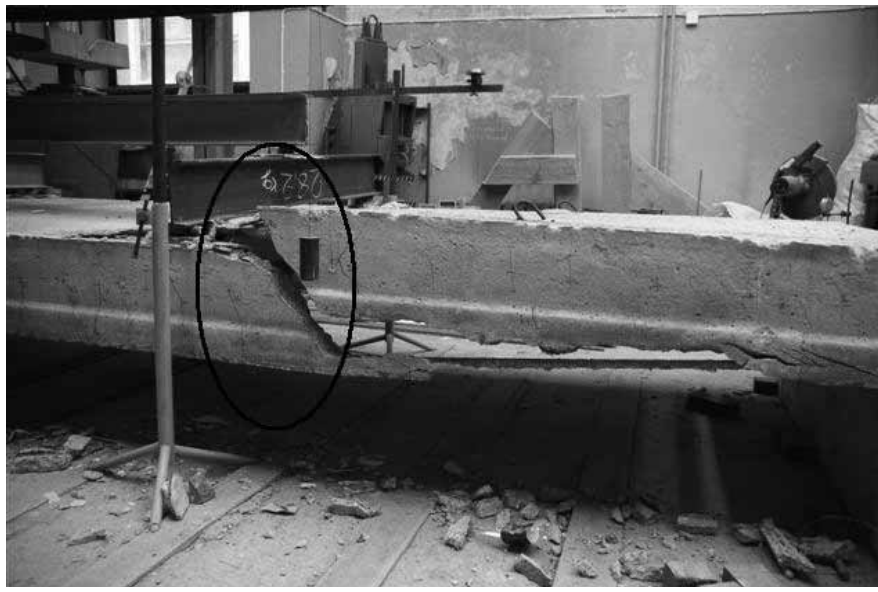

Fig. 4.9. Shear failure of ribbed panel V12.

The load-deflection curves of ribbed panels PNS-14, including initial deflection, are presented in **Fig. 4.10**. **Fig. 4.10** shows that ribbed panels L8 and L10 just failed to meet the rigidity requirements set for the new ribbed panels PNS-14 (PK-01-111 1961).

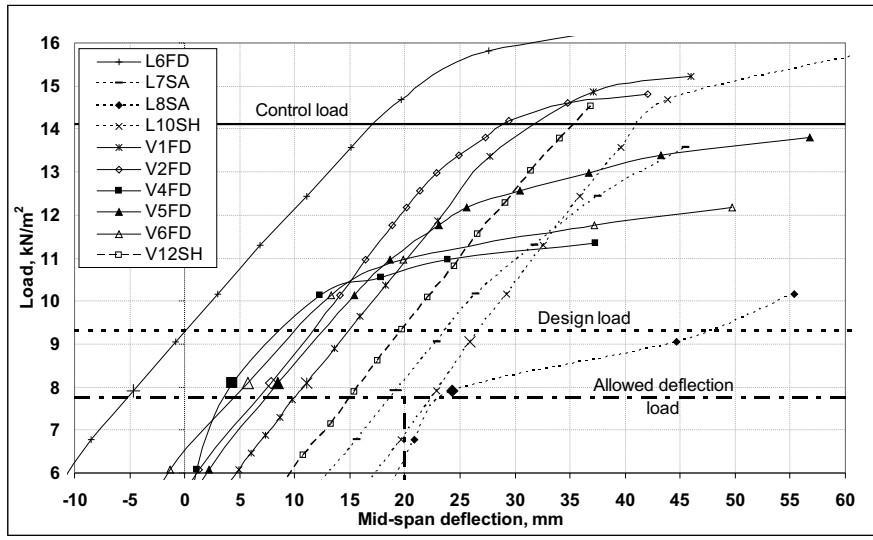

Fig. 4.10. Load-deflection curves of ribbed panels PNS-14 including initial deflection. *Large markers indicate the load step at which the first flexural crack appeared. Failure: FD–Flexural ductile, WR–Weld rupture at supports, SH–Shear failure.*

4.1.5. Carbonation and chlorides of ribbed panels PNS-12 and PNS-14

Except for ribbed panel V8, about one-third of the concrete cover of the studied ribbed panels PNS-12 and PNS-14 was carbonated (**Table 4.2** and **Table 4.3**). The cover of the prestressing bar of ribbed panel V8 was probably fully carbonated because of its low concrete strength (when compared to the other ribbed panels). Concrete of low strength is usually more porous and hence, more permeable to the CO_2.

Chloride content was determined in 20 samples taken from the adjacent ribbed panels of R1–R8 at the Raadi research object. The mean chloride content was 0.20% with a minimum and maximum values of 0.15% and 0.22% by mass of cement, respectively. Chloride-induced corrosion can only take place once the chloride content in concrete in contact with the steel surface has reached a threshold value. The morphology of a chloride

attack is typically pitting or localised corrosion. However, no signs of pitting corrosion were found visually on any of the prestressing bars of the ribbed panels studied. **Table 4.2** and **Table 4.3** also show no serious local cross-section reduction ($d_{red,max} \leq 10.3\%$) of the studied prestressing bar samples. These results show that corrosion deteriorations in the studied ribbed panels were probably neither carbonation nor chloride-induced. In further research the most probable causes of deterioration of ribbed panels should be ascertained. A combination of freezing-thawing and wetting-drying cycles as well as rainwater infiltration could be considered.

4.1.6. Conclusions

Based on the results of the experimental investigation of 46 existing precast concrete ribbed panels, the following conclusions are drawn:

1. All ribbed panels whose ultimate load was lower than the control load received grade 0 on the visual rating scale. Consequently, attention should be paid to ribbed panels where the concrete cover of the longitudinal reinforcement has spalled (grade 0), which could be a sign of decreased flexural bearing capacity in comparison with factory-issued (new) ribbed panels.

2. All studied ribbed panels with a corrosion-induced crack in the longitudinal rib (grade 1) could carry the control load. Hence, these ribbed panels conform to the strength requirements of new ribbed panels even after a relatively long period of service.

3. From the point of view of a structural engineer it is important that all studied ribbed panels (irrespective of their grade) were able to carry the design load. Since engineers compare the calculated structural bearing capacity with the design load, the latter could be employed as an equivalent of the ultimate limit state. Hence, all studied ribbed panels corresponded to the ultimate limit state. Despite of their sufficient residual bearing capacity, ribbed panels with cracked or spalled cover of the longitudinal reinforcement (grade 1 or 0, respectively) need repairs.

4. The flexural behaviour (in terms of load-deflection curves) of the studied ribbed panels PNS-12 was not significantly different from factory-issued (new) ribbed panels.

5. Of the 46 ribbed panels tested the flexural ductile mode of failure was noticed in 36 ribbed panels. Also, rupture of the rebar in transversal (2 ribbed panels) and longitudinal (1 ribbed panel) ribs, failure of a longitudinal rib (1 ribbed panel), weld (anchorage) rupture (3 ribbed panels) and shear failure (3 ribbed panels) were noticed.

6. It is likely that the corrosion deterioration of the studied ribbed panels PNS-12 and PNS-14 was neither carbonation nor chloride-induced. In further research the most probable causes of deterioration should be ascertained.

4.2. Reinforced concrete structures of the generator building of an oil shale chemical plant

4.2.1. Visual inspection

B) In this part of the research the results of a case study of the generator building of an existing oil shale chemical plant are presented and discussed. The condition of each column and beam in the plant was carefully assessed visually. The summary of the visual assessment of the beams and columns on different floors is presented in **Table 4.4**. **Table 4.4** shows that the condition of beams is somewhat worse than that of the columns—the majority of beams on floors 2–4 operate with spalled concrete cover. However, columns with spalled concrete cover are located on floors 1–3. On the upper floors of the generator building the concentration of gases is less intense and the temperature is lower. On the basis of visual assessment the reinforced concrete structures with the most severe deterioration were located for subsequent investigation.

Table 4.4. Summary of visual assessment grades of reinforced concrete members on different floors

Floor no.	Mean grade of beams	Mean grade of columns
1	-*	0
2	0	0
3	0	0
4	0	3
5	3	3
6	4	4
7	5	5

* *There are no beams on the 1st floor.*

From the structures to which grade 0 was assigned the beams carrying the generator on the 2nd floor were in the worst condition. The condition of the beams is worse because they are probably more exposed to aggressive gases and closer to the generator. Numerous visually discernible structural deteriorations occurred on those girders and joists. For example, the concrete cover of tensile (but sometimes also neutral or compressive) reinforcing bars has spalled (**Figs. 4.11** and **4.12**), many stirrups are loose or broken (**Figs. 4.11** and **4.12**), concrete is delaminated (**Fig.**

4.12) or containing incompatible aggregates such as brick pieces, etc. (**Fig. 4.11**). The reduction of the flexural and shear bearing capacities of beams carrying the generator was also calculated. A serious reduction in shear bearing capacity (max. 40 %) in a critical section (no stirrups) of a beam carrying a generator was found (**V**). Due to uniform corrosion the cross-section of the longitudinal bars was not reduced considerably. Consequently, the calculated reduction in the flexural bearing capacity of beams carrying a generator was not so critical (max. 19.5 %; **V**).

Fig. 4.11. Bottom view of a fragment of a girder carrying a generator on the 2nd floor.

Fig. 4.12. Bottom view of a fragment of a joist carrying a generator on the 2nd floor.

The columns on floors 1–3 and beams on floors 3–4 also received grade 0 i.e. operate with spalled concrete cover. Their condition was slightly better in comparison with the beams carrying a generator on the 2nd floor. In general, reinforced concrete structures with cracked or spalled cover (grade 1 and 0) need extensive repairs. Cracked or spalled concrete cover does not serve its function of providing fire and corrosion protection as well as bond to the reinforcement. Loose stirrups have to be re-attached or replaced during repairs in order to restore the initial shear bearing capacity of beams on the 2nd floor.

4.2.2. Compressive strength of concrete cores

The results of the compressive strength of 55 cores acquired from columns and beams are presented in **Figs. 4.13** and **4.14**, respectively.

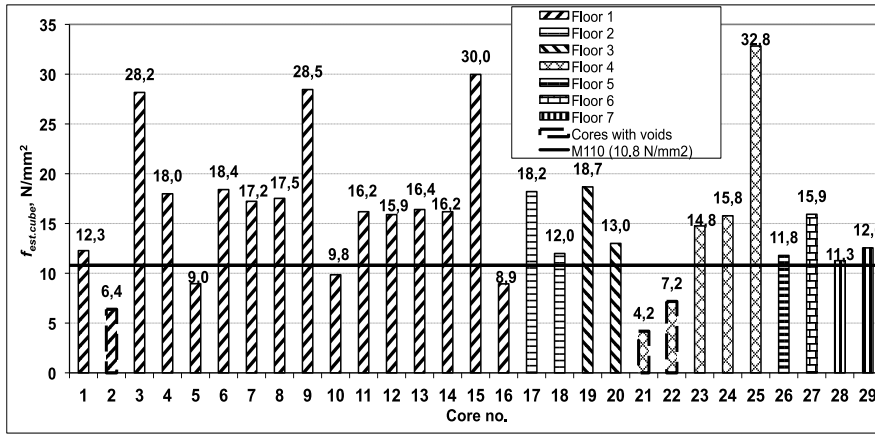

Fig. 4.13. Compressive strength of 29 cores drilled from columns.

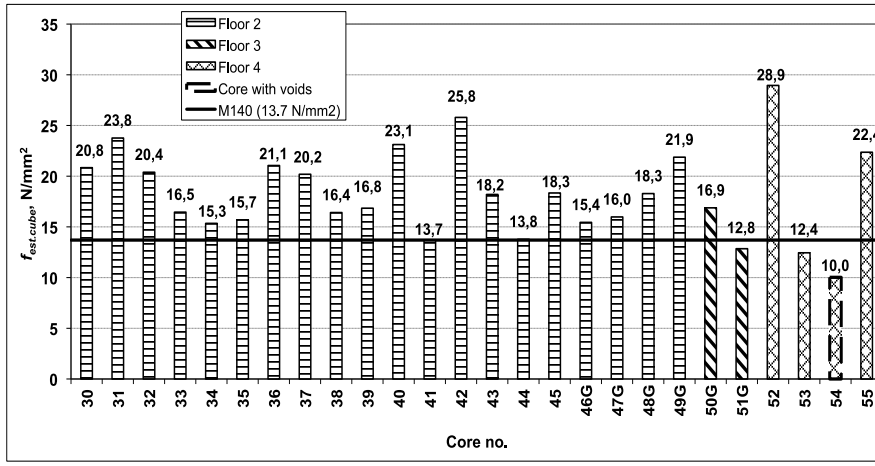

Fig. 4.14. Compressive strength of 26 cores drilled from beams. *G behind core number denotes cores drilled from beam carrying generator.*

The mean core strength (derived to mean estimated cube strength) drilled from columns (**Fig. 4.13**) was 15.8 N/mm^2 with a standard deviation of 6.9 N/mm^2. The mean core strength drilled from beams (in **Fig. 4.14**) was 18.3 N/mm^2 with a standard deviation of 4.4 N/mm^2. The mean strength of cores drilled both from columns and beams exceed

the compressive strength mark of M110 (10.8 N/mm^2) and M140 (13.7 N/mm^2), respectively. It should be mentioned that **Figs. 4.13** and **4.14** present the compressive strength of unbroken cores only. Eight cores broke during drilling as a result of cracks or large voids (e.g. core 13* in **Fig. 4.15**) and could not be repaired for the compressive test.

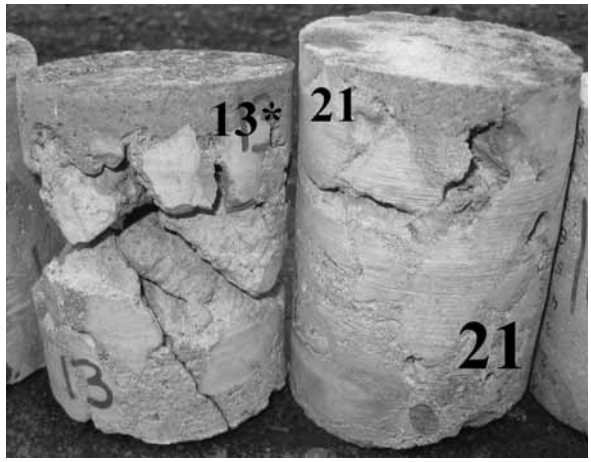

Fig. 4.15. Concrete cores 13* and 21 after drilling from columns.

Assessment of in-situ compressive strength directly from core tests constitutes the reference method described in EVS-EN 13791 (2007), which enables to compare the results to concrete strength classes applied today (EVS-EN 206-1:2007). The lower value of the estimated in-situ characteristic strength (according to Approach A in EVS-EN 13791 (2007)) of cores drilled from columns and beams was 5.6 N/mm^2 and 11.8 N/mm^2, respectively. Therefore, the strength of cores drilled from beams corresponds to the lowest strength class—C8/10. The strength of cores drilled from columns was lower than any strength class applied today. The strength of concrete should be taken into account when considering the bond between repair mixture (or concrete) and original concrete in the repairs of the reinforced concrete structures of the plant.

The compressive test revealed that some cores had questionably low compressive strength (e.g. cores 2, 21, 22 in **Fig. 4.13** and core 54 in **Fig. 4.14**). Large voids occurred on those cores. The presence of voids in concrete greatly reduces its strength: approximately 1% voidage decreases the strength by 5—8 % (Neville 1995). Voids in columns and beams could be a result of insufficient compaction or freezing of concrete during the construction of the plant in 1951.

Table 4.5. Concrete strength of columns and beams on different floors

Floor no.	$\bar{f}_{est.cube} \pm s$ from columns, N/mm^2 (no. of cores)	$\bar{f}_{est.cube} \pm s$ from beams, N/mm^2 (no. of cores)
1	16.8 ± 7.1 (16)	-[a]
2	15.1 ± 4.4 (2)	18.6 ± 3.4 (20)
3	15.8 ± 4.0 (2)	14.9 ± 2.9 (2)
4	14.9 ± 11.1 (5)	18.4 ± 8.8 (4)
5	11.8 (1)	-[b]
6	15.9 (1)	-[b]
7	11.9 ± 0.9 (7)	-[b]

[a]—*There are no beams on the 1st floor.*
[b]—*No cores were drilled from beams on floors 5-7.*

The mean estimated cube strength ($\bar{f}_{est.cube}$) as well as standard deviation of cores drilled from columns and beams on different floors are presented in **Table 4.5**. **Table 4.5** shows no trend in core strengths drilled from columns or beams on different floors. These results contrast with the results of visual inspection, where a clear trend of grades on different floors was observable. On the basis of **Tables 4.4** and **4.5**, the visual condition and the strength of the material (concrete) of the structure are not related. However, since the majority of cores were drilled from either the 1st floor (columns) or 2nd floor (beams) no detailed comparison of strength can be performed on cores drilled from different floors in **Table 4.5**.

The mean strength of six cores drilled from beams carrying a generator (i.e. cores 46G—51G in **Fig. 4.14**) was 16.9 N/mm^2 with a standard deviation of 3.0 N/mm^2. The mean strength of 20 cores drilled from other beams was 18.7 N/mm^2 with a standard deviation of 4.7 N/mm^2. The mean strength of cores drilled from beams carrying a generator was slightly lower (by 1.8 N/mm^2) than the cores drilled from other beams. However, due to a small difference in mean strength and high standard deviation no clear trend can be found in the results.

4.2.3. Carbonation depth and cover of concrete

The results of carbonation depth as well as concrete cover measurements are presented in **Fig. 4.16**. **Fig 4.16.** shows that the mean carbonation depth of cores is considerably lower than the corresponding concrete cover. Thus, in general the carbonation front has not reached the vicinity of the surface of the rebar. Only one core exists in **Fig. 4.16** where the mean carbonation depth (core 19) was nearly the same as the concrete cover. Also, a single carbonation depth measurement of core 53 could overreach the cover (shown as an overlap of standard deviations of the cover and carbonation depth of core 53). Still, according to the data sample presented in **Fig. 4.16**, the corrosion of steel reinforcement in the studied generator building was not carbonation-induced.

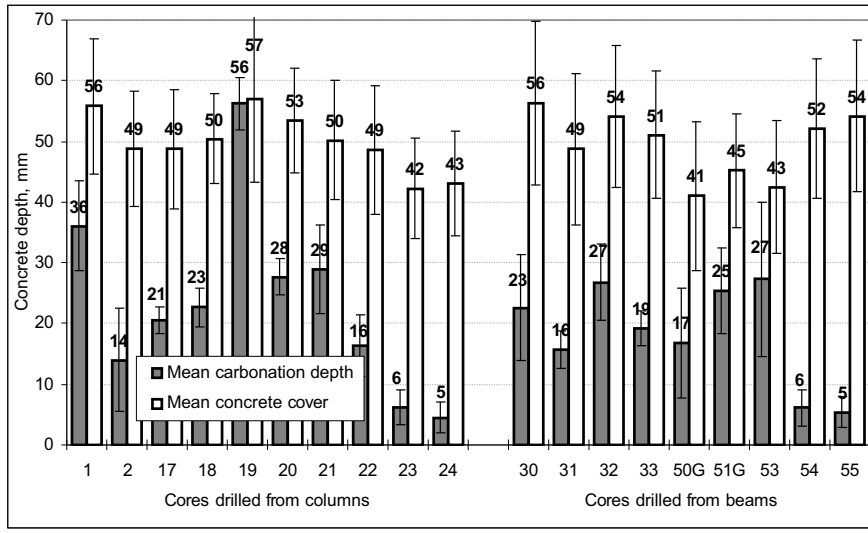

Fig. 4.16. Carbonation depth and concrete cover on cores drilled from columns and beams. *"Whiskers" on bars denote the standard deviation of the measurements. G behind the core number denotes cores drilled from a beam near the generator.*

A photograph of the most representative cores is presented in **Fig. 4.17**. Because of the presence of coarse aggregate, carbonation depth may vary considerably in the same core e.g. core 50G in **Fig. 4.17**.

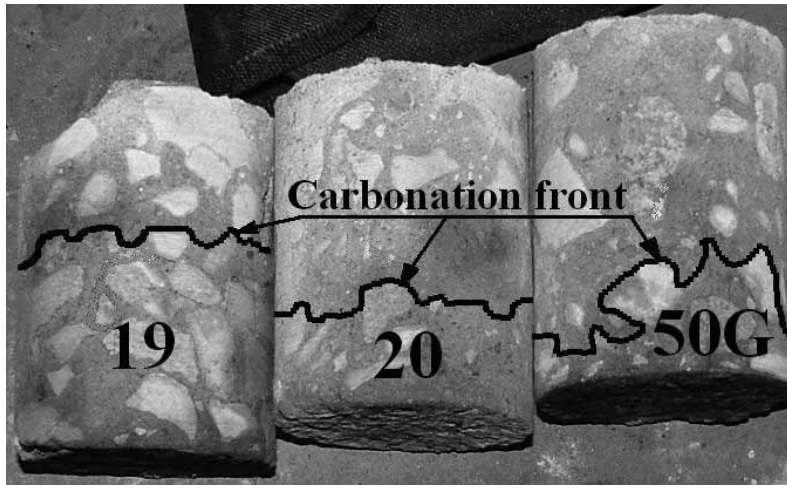

Fig. 4.17. Carbonation front estimated by the phenolphthalein method on cores 19, 20 and 50G.

It might also be noted that, if cracks are present, CO_2 can ingress through them so that the carbonation "front" advances locally from the penetrated cracks. Corrosion can take place even when the full carbonation front is still a few millimetres away from the surface of the steel if partial carbonation has taken place (Parrot and Killoch 1989). A phenolphthalein test is easy to perform and is rapid but it should be remembered that the pink colour indicates the presence of $Ca(OH)_2$ but not necessarily a total absence of carbonation. Indeed, the phenolphthalein test gives a measure of the pH but does not distinguish between a low pH caused by carbonation and by other acidic gases.

A statistically insignificant (p-value = 0.48) relationship was found between carbonation depth and the strength of cores. **Fig. 4.16** shows that carbonation depth and concrete cover do not differ substantially between the cores drilled from columns or beams. Also, carbonation depth and concrete cover were not differing on different floors.

According to the design drawings the cover for the longitudinal reinforcement of both columns and beams was 50 mm. The actual concrete cover depends on the quality of the casting of monolithic concrete. The mean cover on different columns and beams in **Fig. 4.16** varied from 41 to 57 mm. Also, a relatively high standard deviation of concrete cover was measured on the same column or beam. As an extreme

example a cover from 38 to 65 mm was measured on the same column on the 3rd floor. The variable results of cover measurements in this study characterise the quality of concrete placing in the 1950s.

4.2.4. Chemical analysis of concrete

The results of the chemical analysis of water-soluble deleterious salts in concrete cores are presented in **Table 4.6**. The content of water-soluble salts in concrete was interpreted following WTA guidelines 4-5-99/D (1999) in **Table 4.7**.

Table 4.6. Results of chemical analysis of deleterious salts in concrete

Core no.	Sample location in core	Content of water soluble salts in concrete, percentage of mass			
		Sulphate $(SO_4)^{2-}$	Chloride Cl^-	Nitrate NO_3^-	Total
46G	Surface	3.817	0.214	0.045	4.075
46G	Middle	0.173	0.654	0.012	0.839
47G	Surface	0.738	0.421	0.044	1.202
48G	Surface	0.751	0.236	0.021	1.009

G behind core number denotes cores drilled from beam near generator.

Table 4.7. Classification of the content of water-soluble salts in concrete (WTA guidelines 4-5-99/D 1999)

	Content of water-soluble salts in concrete, percentage of mass		
	Low	Middle	High
Sulphate	< 0.5	0.5—1.5	> 1.5
Chloride	< 0.2	0.2—0.5	> 0.5
Nitrate	< 0.1	0.1—0.3	> 0.3

Tables 4.6 and **4.7** show that the sulphate content near the surface of concrete beams carrying a generator on the 2nd floor was from middle (in samples 46G and 48G) to very high (in sample 46G). The sulphate content was low at the depth of a concrete beam carrying a generator on the 2nd floor. Generally, the chloride content at the surface as well as at the depth of concrete was medium. Nitrate content was found to be low in all samples presented in **Table 4.6**.

Only four samples are not enough for thorough conclusions. However, it is evident that the content of deleterious salts in concrete beams carrying generators is too high. Solid salts do not attack concrete but, when present in solution, they can react with hydrated cement paste. The effect of sulphate and chloride ions on concrete is presented as follows.

Sulphate ions can penetrate the concrete and react with components of the cement matrix to cause expansive chemical reactions. Swelling may occur that, starting from the corners of a concrete structure gives rise to cracking and disintegration. A sulphate attack can also manifest itself as a progressive loss of strength of the cement paste due to loss of cohesion between the hydration products. In this study the strength of concrete cores 46G—48G (**Fig 4.14.**) was not substantially lower than that of cores drilled from other beams. Therefore, a sulphate content ranging from middle to very high (**Table 4.7**) had not reduced the strength of cores.

Chloride contamination of concrete is a frequent cause of corrosion of reinforcing steel. Chloride-induced corrosion can only take place once the chloride content in concrete in contact with the steel surface has reached a threshold value. Chlorides lead to a local breakdown of the protective oxide film on the reinforcement in alkaline concrete, so that a subsequent localised corrosion takes place. The morphology of the attack is that typical of pitting corrosion. However, no pitting was found on the exposed reinforcement of columns and beams (**Figs. 4.11** and **4.12**) as a result of visual inspection.

At least the beams carrying a generator on the 2nd floor should be treated with steam to reduce the concentration of sulphates and chlorides in concrete. The mixture applied during repairs has to protect the steel by both physical (i.e. preventing the ingress of deleterious substances) and chemical means (providing re-passivation).

4.2.5. Water absorption of concrete

Water absorption was determined on ten concrete samples, which were extracted from the columns on the 1st floor. The mean water absorption was 5.2 % with a standard deviation of 1.1 %. It should be noted that two pitchy concrete samples also had the lowest water absorption values. Therefore, the mean water absorption could have been higher if clean concrete samples had been acquired.

The former Soviet Union Building Code (SNIP 2.03.11-85) distinguishes between three different concrete types: normal permeability (N), lowered permeability (P) and particularly low permeability (O) with water absorption values of 4.8–5.7%, 4.3–4.7%, 4.2% and under, respectively. According to the mean water absorption value concrete of normal permeability (N) was applied on the columns on the 1st floor.

As mentioned before the columns on the 1st floor should be treated with steam to reduce the concentration of pitch from concrete during repairs. Considering the aggressive indoor environment in the generator building the repair mixture has to be of low permeability.

4.2.6. Aggressive indoor environment in the plant in the 1950s

As mentioned in the introduction the studied oil plant went into service in 1951. At that time in addition to oil production these generators supplied the nearby gas plant with heating gas. The gas plant was supplying the former Leningrad (St. Petersburg) with domestic gas through a more than 200 km long gas pipeline (under the banner "Gas for Leningrad").

The middle part of the 125-tonne generator designed by Lengiprogaz was more constricted when compared to preceding generators. This caused an unequal temperature distribution in those generators. As a result uncomposed oil shale pieces gathered with semicoke in the gasification chamber at the lower part of generators. Oil shale pieces ignited with air contact and raised the temperature in the gasification chamber whereby oil shale ash melted to become slag. Slag had to be removed (by raking) from the generator since it constrained the outlet of semicoke. Slag was raked through all four hatches of the generator manually. Hot slag was broken more efficiently by spraying water into the generator. Therefore, ash dust and harmful gases in large concentrations exited through the hatches of the generator during slag removal. The addition of air into the generator was suspended during raking. Slag raking was performed in all generators more than once a day according to a schedule. Slag was removed more rarely after the reconstruction of the generators from the end of the 1950s to the start of the 1960s. Later the amount of air added to the generator was reduced. From the start of the 1980s the gasification process of the generators was discarded and hatches were opened only for repairs (Rooks 2004).

Employees of the plant had noticed exposed reinforcement, i.e. spalled concrete cover of load-bearing reinforced concrete structures near the gas generators already at the start of the 1960s. Therefore, the deterioration of reinforced concrete structures in the studied gas-generator building originates probably from the 1950s.

4.2.7. Conclusions and suggestions

A case study for investigating the condition of reinforced concrete structures and the properties of concrete of an existing oil-shale chemical plant is presented. The studied seven-storied plant, located in North-eastern Estonia, was constructed in 1951.

1. It is found that the deteriorations of reinforced concrete structures in the studied oil plant building may originate already from the 1950s. At that time, due to a different technology, slag was removed from all generators each day. The columns and beams were exposed to a large concentration of aggressive gases exiting through the hatches of the generator during slag removal. These gases were the most probable cause of the deterioration of the reinforced concrete structures.

2. The results of visual assessment show that the majority of beams on floors 2–4 operate with spalled concrete cover (grade 0). The columns with spalled concrete cover were located on floors 1–3. From the structures to which grade 0 was assigned the beams carrying a generator on the 2nd floor were in the worst condition. In general, reinforced concrete structures with cracked or spalled cover (grade 1 and 0) need extensive repairs.

3. The mean strength of cores drilled both from columns and beams exceed their corresponding compressive strength mark. However, the strength of cores drilled from beams corresponds to the lowest strength class applied today—C8/10. The strength of cores drilled from columns was lower than any strength class.

4. Based on the results of the current study the following steps of repair are suggested:

- Removal of cracked and delaminated concrete to expose the surface of the damaged steel.

- Steaming of structures to reduce the concentration of chlorides, sulphates as well as pitch from concrete.
- Treatment of the steel bars to remove rusting layers. Application of protective coating to the steel. Re-attachment or replacement of loose stirrups. Placement of additional steel bars if necessary.
- Application of bond coat on substrate concrete to provide bond with repair mortar.
- Application of cement-based and low-permeability repair mortar to replace the damaged concrete that was removed. The repair mixture has to protect the steel by both physical means (i.e. preventing the ingress of deleterious substances) and by chemical means (providing repassivation of steel).

Deteriorated reinforced concrete structures on the 1st and 2nd floors of the studied generator building were repaired quite similarly to the above steps by the company REV Special OÜ in 2006.

5. GENERAL CONCLUSIONS

1. In both studies the external condition of the existing reinforced concrete structures was assessed visually on a 6-grade scale. The results of structural tests with ribbed panels show that the residual bearing capacity of ribbed panels varies the most in ribbed panels with spalled concrete cover (grade 0). This means that ribbed panels, which may have just barely reached grade 0 as well as ribbed panels in a critical state in terms of their load-bearing capacity, are both rated as grade 0. The same trend was observable at the concrete columns and beams in the generator building of the oil shale chemical plant. On some beams only small pieces of cover of tensile reinforcing bars have spalled. However, most of the beams carrying a generator exhibited structural deteriorations (e.g. loose or broken stirrups, delaminated concrete), which probably have reduced their bearing capacity. On both cases the beams would receive grade 0 on a visual rating scale. The visual scale applied in the current studies was developed already in 1974 and the condition corresponding to grade 0 should be updated and improved in further research. However, the benefit of the visual scale consists in its simplicity of application. Scale-acquainted engineers can assess reinforced concrete structures relatively quickly and simply to locate structures of cracked (grade 1) or spalled (grade 0) concrete cover. Later on the residual bearing capacity of these structures needs the judgment of a structural expert.

2. The length of corrosion initiation, propagation and residual life period of a reinforced concrete structure may vary substantially. Once the reinforced concrete structure is considered to be unserviceable due to corrosion-induced cracking, there is considerable residual lifetime before the structure can be considered as having become unsafe. A study of an existing oil shale chemical plant has shown that the residual lifetime (or a residual life stage) of reinforced concrete structures carrying generators was exponentially greater than the corrosion initiation and corrosion propagation periods together. The studied plant was constructed in 1951. Employees of the plant had noticed exposed reinforcement, i.e. spalled concrete cover of reinforced concrete structures near gas generators at the start of the 1960s. Deteriorated reinforced concrete structures on the 1st and 2nd floors of the studied generator building were repaired in 2006.

3. The studies have shown that an insufficient quality of materials or workmanship could affect the results. Therefore, test results originating from existing reinforced concrete structures should be interpreted with caution. The following examples were found in the current thesis:

- It is probable that the prestressing steel of an inferior strength was applied at one test series of ribbed panels (V1–V6), which also resulted in rather low ultimate residual bearing capacity. However, the visual condition of these ribbed panels was good in comparison with other ribbed panels. Consequently, the results of V1–V6 were omitted from the analysis of the influence of the visual condition on the ultimate residual bearing capacity of ribbed panels.
- The longitudinal rib of ribbed panel K-10 failed near support. The concrete in the failure place had crumbled prior to loading tests probably because of poor construction quality.
- The strength of concrete cores from ribbed panel V8 was considerably lower than the strength from other ribbed panels PNS-12. Even the colour of concrete cores drilled from V8 was visually discernible from other cores.
- Eight cores broke during drilling and some cores had a questionably low compressive strength, mainly as a result of large voids in the structures of an existing oil shale chemical plant. Voids in columns and beams were a result of insufficient compaction or freezing of concrete during the construction of the plant in 1951.

4. Uniform corrosion was noticed on the reinforcing and even on the prestressing steel of ribbed panels as well as on the exposed reinforcement of the columns and beams of an oil shale chemical plant. Due to uniform corrosion general thinning takes place until failure. Fortunately, uniform corrosion is relatively easily measured and predicted making disastrous failures of reinforced concrete structures affected by uniform corrosion relatively rare. The influence of pitting corrosion as well as stress corrosion can be considered as more serious threats to the residual bearing capacity of existing reinforced concrete structures.

REFERENCES

ACI Committee 365. 2000. Service Life Prediction (365.1R-00), American Concrete Institute, Farmington Hills, MI, 44 p.

Alekseyev, S.N., and Rozental, N.K. 1976. Коррозионная стоикость железобетонных конструкций в агрессивной промышленной среде. (Corrosion durability of reinforced concrete structures in an aggressive industrial environment). Moscow, Stroiizdat, 205 p. (in Russian).

Almusallam, A.A., Al-Gahtani, A.S., Aziz A.R., and Rasheeduzzafar. 1996. Effect of reinforcement corrosion on bond strength. *Construction and Building Materials*, **10** (2), 123-129.

Almusallam, A.A., Al-Gahtani, A.S., Maslehuddin, M., Khan, M.M., and Aziz, A.R. 1997. Evaluation of repair materials for functional improvement of slabs and beams with corroded reinforcement. *Proc. of the Inst. of Civil Eng., Structures and Buildings*, **122**, 27-34.

Andrade, C., Alonso, C., and Molina, F. J. 1993. Cover cracking as a function of rebar corrosion: Part 1 - Experimental test, *Material and Structures*, **26**, 453-464.

Arioz, O., Ramyar, K., Tuncan, M., Tuncan, A., and Cil, I. 2007. Some factors influencing effect of core diameter on measured concrete compressive strength. *ACI Materials Journal*, **104** (3), 291-296.

Azad, A., K., Ahmad, S., and Azher, S.A. 2007. Residual strength of corrosion-damaged reinforced concrete beams. *ACI Materials Journal*, **104** (1), 40-47.

Bentur, A., Diamond, S., and Berke, N.S. 1997. Steel Corrosion in Concrete: Fundamentals and Civil Engineering Practice. E&FN Spon, London, UK, 201 p.

Braverman, J.I., Miller, C.A., Hofmayer, C.H., Ellingwood, B.R., Naus, D.J., and Chang, T.Y. 2004. Degradation assessment of structures and passive components at nuclear power plants. *Nuclear Engineering and Design*, **228**, 283-304.

Broomfield, J.P. 1997. Corrosion of steel in concrete: understanding, investigation and repair. E & FN Spon, London, UK, 240 p.

BS 6089:1981. Guide to assessment of concrete strength in existing structures. British Standard Institution, UK, 16 p.

Castel, A., Francois, R., and Arliguie, G. 2000. Mechanical behavior of corroded reinforced concrete beams: Part I - Experimental study of corroded beams. *Material and Structures*, **33**, 539-544.

DIN 51100. 1957. Prüfung keramischer Roh- und Werkstoffe; Bestimmung der löslichen Salze (Perkolatorverfahren) (Testing of ceramic raw materials and materials; determination of the soluble salts (percolator method)). German Institute for Standardization, Berlin, 30 p. (in German).

Dowell, R.K., and Smith, J.W. 2006. Structural tests of precast, prestressed concrete deck panels for California freeway bridges. *PCI Journal*, **51** (2), 76-87.

Du, Y., Clark, L.A., Chan, A.H.C. 2007. Impact of reinforcement corrosion on ductile behavior of reinforced concrete beams. *ACI Structural Journal*, **104** (3), 285-293.

Durham, S.A., Heymsfield, E., and Tencleve, K.D. 2007. Cracking and reinforcement corrosion in short-span precast concrete bridges. *Journal of Performance of Constructed Facilities*, **21** (5), 390-397.

El Maaddawy, T., Soudki, K., and Topper, T. 2005. Long-term performance of corrosion-damaged reinforced concrete beams. *ACI Structural Journal*, **102**, (5), 649-656.

Ellingwood, B.R., and Mori, Y. 1997. Reliability-based service life assessment of concrete structures in nuclear power plants: optimum inspection and repair. *Nuclear Engineering and Design.* **175**, 247-258.

Enright, M.P., and Frangopol, D.M. 1999. Reliability-based condition assessment of deteriorating concrete bridges considering load redistribution. *Structural Safety*. **21**, 159-195.

EVS-EN 12504-1:2009. Konstruktsiooni betooni katsetamine. Osa 1: Puursüdamikud. Võtmine, ülevaatus ja survekatse. (Testing concrete in structures. Part 1: Cored specimens. Taking, examining and testing in compression) Estonian Centre for Standardisation, Tallinn. 11 p. (in Estonian).

EVS-EN 13791:2007. Assessment of in-situ compressive strength in structures and precast concrete components. Estonian Centre for Standardisation, Tallinn, 28 p.

EVS-EN 14630:2006. Products and systems for the protection and repair of concrete structures. Test methods. Determination of carbonation depth in hardened concrete by the phenolphthalein method. Estonian Centre for Standardisation, Tallinn, 15 p.

EVS-EN 206-1:2007. Betoon Osa 1: Spetsifitseerimine, toimivus, tootmine ja vastavus. (Concrete Part 1: Specification, performance, production and conformity.) Estonian Centre for Standardisation, Tallinn, 82 p. (in Estonian).

Fan, Y.-F., Zhou, J., and Feng, X. 2004. Prediction of load carrying capacity of corroded reinforced concrete beam. *China Ocean Engineering*, **18** (1), 107-118.

Francois, R., and Arliguie, G. 1999. Effect of microcracking and cracking on the development of corrosion in reinforced concrete members. *Magazine of Concrete Research*, **51** (2), 143-150.

GOST 5058-65. Сталь низколегированная конструкционная. Марки и общие технические требования. (Low-alloyed structural steel. Marks and general technical requirements). National construction committee of ministerial council of USSR, Moscow, 10 p. (in Russian).

GOST 7740-55. Плиты крупнопанельные железобетонные с армированными полями для покрытий производственных зданий. (Reinforced concrete ribbed panels of industrial building). National construction committee of ministerial council of USSR, Moscow, 16 p. (in Russian).

GOST 882985. Конструкции и изделия бетонные и железобетонные сборные. Методы испытаний нагружением и оценка прочности, жестокости и трещиностойкости. (Concrete and reinforced concrete prefabricated structures and products. Loading test methods and assessment of strength, rigidity and crack resistance). National construction committee of ministerial council of USSR, Moscow, 24 p. (in Russian).

Halgma, R., and Linnus, L. 2007. Eelpingestatud ribipaneelide sarruse ja betooni mõningate omaduste määramine. (Determination of

some properties of concrete and reinforcement of prestressed ribbed panels). Master thesis. Estonian University of Life Sciences, Tartu, 75 p. (in Estonian).

He, S.-Q., Gong, J.-X., and Zhao, G.-F. 2005. Experimental investigation on durability of reinforced concrete beams in a simulated marine environment. *China Ocean Engineering*, **19** (1), 11-20.

Heymsfield, E., Durham, S.A. and Jones, J.X. 2007. Structural behaviour of short span precast channel beam bridges without shear reinforcement. *Journal of Bridge Engineering*, **12** (6), 794-800.

Higgins, C., Potisuk, T., Farrow, W.C., Robelo, M.J., McAuliffe, T.K., and Nicholas, B.S. 2007. Tests of RC deck girders with 1950s vintage details. *Journal of Bridge Engineering*, **12** (5), 621-631.

Hinto-Kivimaa, J., and Toper, J. 2005. Ribipaneelide betooni ja armatuuri omaduste uurimine. (The investigation of the properties of concrete and steel reinforcement in ribbed panels). Bachelor thesis. Estonian Agricultural University, Tartu, 81 p. (in Estonian).

Hong, K., and Hooton, R.D. 1999. Effects of cyclic chloride exposure on penetration of concrete cover. *Cement and Concrete Research*, **29**, 1379-1386.

Huang, R., and Yang, C., C. 1997. Condition assessment of reinforced concrete beams relative to reinforcement corrosion. *Cement and Concrete Composites*, **19**, 131-137.

Iwanami, M., Yokota, H., and Sato, F. 2002. Quantitative evaluation of influence of rebar corrosion on structural performance of deteriorated RC beams. Proceedings of the International Conference held at the University of Dundee, 427-436.

Jin, W.-L., Chen, J., Wu, J.-H., Zhang, Y.-Z., Tao, Y.-L., and Wang, H.-W. 2004. Experimental study on flexural capacity of reinforced concrete beams in marine environment, *Journal Of Zhejiang University (Engineering Science)*, **38** (5), 603-609.

Keskküla T, Miljan J. 1982. Несущая способность плит покрытия животноводческих зданий после эксплуатации. (Bearing capacity of roofing slabs in cattle farm buildings after the end of service life). *Concrete and reinforced concrete*, **2**, 24-25 (in Russian).

Kiprushenkov, M., Miljan, J., Kiviste, M., Miljan R. 2007. Condition assessment of concrete structures in chemical plants gas generator building. Proceeding of 5th International Conference: Concrete Under Severe Conditions of Environment and Loading, LCPC, Tours, France, 223-230.

Kiviste, M. 2004. Armatuurterase korrosioon ja selle mõju ribipaneelide kandevõimele. (The influence of corrosion of steel reinforcement on the bearing capacity of ribbed reinforced concrete panels). MSc thesis. Estonian Agricultural University, Tartu, 95p. (in Estonian).

Kiviste, M., Miljan, J. 2007. Structural concrete compressive strength determination with rebound hammer. *Vagos*, Lithuanian Agricultural University, **74**(**27**) (1), 15 - 20.

Kiviste, M., Tomann, H. 2002. Betooni karboniseerumise ja armatuurterase korrosiooni mõju ribipaneelide kandevõimele. (The influence of concrete carbonation and corrosion of steel reinforcement on the bearing capacity of ribbed reinforced concrete panels). Bachelor thesis. Estonian Agricultural University, Tartu, 89 p. (in Estonian).

Laiakask E, Miljan J. 2002. Influence of steel reinforcement corrosion on the agricultural building reinforced concrete structure bearing capacity. In: Concrete for Sustainable Agriculture: Agro-, Aqua- and Community Applications, Ghent, 157-164.

Li, C.Q. 2002. Initiation of chloride induced reinforcement corrosion in concrete structural members—prediction, *ACI Structural Journal*, **99** (2), 133-141.

Li, C-Q., Yang, Y. and Melchers, R.E. 2008. Prediction of reinforcement corrosion in concrete and its effects on concrete cracking and strength reduction. *ACI Materials Journal*, **105** (1), 3-10.

Long, A.E., Henderson, G.D., Montgomery, F.R. 2001. Why assess the properties of near-surface concrete? *Construction and Building Materials*, **15** (2-3), 65-79.

Mangat, P.S. and Elgarf, M.S. 1999b. Strength and serviceability of repaired reinforced concrete beams undergoing reinforcement corrosion. *Magazine of Concrete Research*, **51** (2), 97-112.

Mangat, P.S., and Elgarf, M.S. 1999a. Flexural strength of concrete beams with corroding reinforcement. *ACI Structural Journal*, **96** (1), 149-158.

Melchers, R.E. 2003. Mathematical modelling of the diffusion controlled phase in marine immersion corrosion of mild steel. *Corrosion Science*, **45** (5), 923-940.

Melchers, R.E., and Li, C.Q. 2006. Phenomenological modelling of reinforcement corrosion in marine environments. *ACI Materials Journal*, **103** (1), 25-32.

Miljan, J. 1977. Натурное исследование состояния железобетонных конструкций в животноводческих зданиях. (Full scale examination of the condition of reinforced concrete structures in livestock buildings). Reports of Estonian Agricultural Academy No. 111, Tartu, 26-32 (in Russian).

Miljan, J., Keskküla, T. 1975. Прогнозирование долговечности железобетонных конструкций в животноводческих зданиях. (Durability prediction of reinforced concrete structures in cattle-breeding buildings). In: Questions about the Reliability of Reinforced Concrete Structures, Kuiboshev, 120-122 (in Russian).

Miljan, R. 2005. Lehmalautade uuenduse mõju piimatootjate majanduslikule suutlikkusele Eestis. (The impact of cowshed modernisation on the economic capability of milk producers in Estonia). PhD thesis. Estonian Agricultural University, Tartu, 195 p. (in Estonian).

Naus, D.J., Oland, C.B., Ellingwood, B.R., Hookham, C.J., and Graves III, H.L. 1999. Summary and conclusions of a program addressing aging of nuclear power plant concrete structures. *Nuclear Engineering and Design*, **194**, 73-96.

Neville, A.M. 1995. Properties of concrete. John Wiley & Sons Inc., London etc., 844 p.

Oit, L., and Ojamaa, E. 1974. Kas betoon kaitseb alati terast roostetamise eest? (Is steel in concrete always protected from corrosion)? *Technics and Production*, No. 7, 358-360 (in Estonian).

Ostrovsky, A.B. 1984. Коррозионная стоикость железобетонных конструкций в сельскохозяйственных зданиях. (The durability

of concrete and reinforced concrete structures in agricultural buildings). Moscow, 45 p. (in Russian).

Pantazopoulou, S.J., and Papoulia, K.D. 2001. Modeling cover-cracking due to reinforcement corrosion in RC structures. *Journal of Engineering Mechanics*, ASCE, **127** (4), 342-351.

Parrot, L.J., Killoch, D.C. 1989. Carbonation in 36 year old, in-situ concrete. *Cement and Concrete Research*, **19** (4), 649-656.

Patrael, R. 2005. Betooni ja armatuuri omaduste mõju ribipaneelide põikjõukandevõimele. (The influence of concrete and steel reinforcement properties on the shear bearing capacity of ribbed reinforced concrete panels). Bachelor thesis. Estonian Agricultural University, Tartu, 66 p. (in Estonian).

РК01111. 1961. Крупнопанельные железобетонные предварительно напряженные плиты покрытий размером 1,5х6 м. Рабочие чертежи. (Prestressed concrete ceiling ribbed panels of dimensions 1.5 by 6m. Work drawings). Moscow, Central institute of typical projects, 20 p. (in Russian).

Poupard, O., L'Hostis, V., Catinaud, S., and Petre-Lazar, I. 2006. Corrosion damage diagnosis of a reinforced concrete beam after 40 years natural exposure in marine environment. *Cement and Concrete Research*, **36**, 504-520.

Roberts, M.B., Atkins, C., Hogg, V., and Middleton, C. 2000. A proposed empirical corrosion model for reinforced concrete. *Structures and Buildings*, **140** (1), 1-11.

Rodriguez, J., Ortega, L.M., and Casal, J. 1996. Load bearing capacity of concrete columns with corroded reinforcement. In: SCI 4th international symposium on corrosion of reinforcement in concrete construction, 220-230.

Rodriguez, J., Ortega, L.M.; and Casal, J. 1997. Load carrying capacity of concrete structures with corroded reinforcement. *Construction and Building Materials*, **11** (4), 239-248.

Rooks, I. 2004. Esimesest põlevkivitööstusest Kiviterini: 1938-1998 mälestused ja faktid. (From the first oil shale industry to Kiviter: 1938-1998 memories and facts). Kohtla-Järve, 132 p. (in Estonian).

Sasmal, S., and Ramanjaneyulu, K. 2008. Condition evaluation of existing reinforced concrete bridges using fuzzy based analytic hierarchy approach. *Expert Systems with Applications*, **35**, 1430 - 1443.

Shdid, C.A., Ansley, M.H., and Hamilton III, H.R. 2006. Visual rating and strength testing of 40-year-old precast prestressed concrete bridge piling, *Transportation Research Board*, **1975**, 3-9.

SNiP 2.03.11-85. 1985. Пособие по контролю состояния строительных металлических конструкций зданий и сооружений в агрессивных средах, проведению обследований и проектированию восстановления защиты конструкций от коррозии. (Corrosion protection of building structures). National construction committee of ministerial council of USSR, Moscow, 45 p. (in Russian).

SNiP II-21-75. 1976. Бетонные и железобетонные конструкции (Concrete and reinforced concrete sructures). Design code, National construction committee of ministerial council of USSR, Moscow, 93 p. (in Russian).

Stewart, M.G. 2001. Reliability-based assessment of ageing bridges using risk ranking and life cycle cost decision analyses. *Reliability Engineering and System Safety*, **74**, 263-273.

Tachibana, Y., Maeda, K., Kajikawa, Y. and Kawuamura, M. 1990. Mechanical behaviour of RC beams damaged by corrosion of reinforcement. In Page C.L., Treadaway, K.W.J. and Bamforth, P.B. (eds.): Corrosion of reinforcement in concrete.

Torres-Acosta, A.A., Navarro-Gutierrez, S., and Teran-Guillen, J. 2007. Residual flexure capacity of corroded reinforced concrete beams. *Engineering Structures*, **29**, 1145-1152.

Transportation Research Board, 1991. Special Report 235, Highway Deicing – comparing salt and calcium magnesium acetate. Transportation Research Board, National Academy of Science, Washington, DC.

Tuutti, K. 1982. Corrosion of steel in concrete. Swedish Cement and Concrete Research Institute, CBI-research 4:82, 305 p.

Val, V.D., and Melchers, R.E. 1997. Reliability of deteriorating RC slab bridges, *Journal of Structural Engineering*, ASCE, **123** (12), 1638-1644.

Weyers, R.E., Fitch, M.G., Larsen, E.P., Al-Qadi, I.L., Chamberlin, W.P., and Hoffman, P.C. 1994. Concrete bridge protection and rehabilitation: chemical and physical techniques. Strategic Highway Research Program, SHRP-S-668, National Research Council, Washington, DC, 36 p.

Wipf, T.J., Klaiber, F.W., Ingersoll, J.S., and Wood, D.L. 2006. Field and laboratory testing of precast concrete channel bridges. *Transportation Research Record*, **1976**, 88-94.

WTA guidelines 4-5-99/D. 1999. Beurteilung von Mauerwerk - Mauerwerksdiagnostik (Evaluation of masonry). Munich: WTA Publications, 16 p. (in German).

Yoon, S., Wang, K., Weiss, W.J., and Shah, S.P. 2000. Interaction between loading, corrosion and serviceability of reinforced concrete. *ACI Structural Journal*, **97** (6), 637-644.

Yuan, Y., Ji, Y., and Shah, S.P. 2007. Comparison of two accelerated corrosion techniques for concrete structures. *ACI Structural Journal*. **104** (3), 344-347.

Zhang, J.-R., Li, C.-X., Wang, L., Xu, F.-H., and Yu, X.-M. 2006. Experiment and analysis on the ultimate strength of existing reinforced concrete arch rib, *Engineering Mechanics*, **23** (12), 136-142.

ZHI-EST-69. 1969. Eesti NSV kohalike ehitusmaterjalide, -toodete ja –konstruktsioonide hindade kataloog koos ühtsete industriaalsete betoon-, raudbetoon- ja mullbetoontoodete kataloogidega ZHI-EST-69, YAI-EST-69. (Catalogue of prices of Estonian SSR local building materials, products and structures with integrated catalogue of industrial concrete, reinforced concrete and autoclaved aerated concrete products). Estonian SSR National construction committee of ministerial council, Valgus, Tallinn, 156 p. (in Estonian and Russian).

SUMMARY

The combination of high compressive strength of concrete and high tensile properties of reinforcing steel gives a composite material that offers, compared to other materials, a wide range of applications in structural engineering. Reinforced concrete structures were constructed relatively extensively in previous century. Today, a situation exists where the same structures are ageing. Therefore, the expense of maintenance, rehabilitation and replacement of existing reinforced concrete structures has increased during the last decades. Hence, the deterioration of reinforced concrete structures is a major problem in almost all parts of the world.

According to Torres-Acosta et al. (2007) the durability of a reinforced concrete structure consists of three stages: corrosion initiation, corrosion propagation and residual life stage. Although research on steel corrosion in concrete has been both extensive and intensive for the past three decades, it has focused largely on the initiation of corrosion and, to a lesser extent, its propagation, rather than on its effect on structural performance (Li et al. 2008). From those investigations dealing with corrosion propagation and residual life periods, quite a few have dealt with the concept of residual structural bearing capacity of reinforced concrete members due to corrosion of the embedded steel (Torres-Acosta et al. 2007).

Most of the studies reporting structural tests on corroded reinforced concrete structures have been conducted under laboratory conditions of controlled environment. Structures are cast with chlorides to initiate pitting corrosion and/or an external impressed current is applied (galvanostatic method) to accelerate the corrosion rate of reinforcing steel. However, accelerated corrosion processes to simulate on-site structure corrosion degradation are quite complicated and do not always give comparable results (Torres-Acosta et al. 2007). Unfortunately, tests with existing reinforced concrete structures exposed to natural environment are scarce in literature. Consequently, the main objective of current thesis is to complement research results of the condition and residual bearing capacity of existing reinforced concrete structures.

The first part of research consists of structural and materials tests of 46 existing precast concrete ribbed panels with an aim:
1. To study the residual flexural bearing capacity, behaviour and failure mode of ribbed panels (**I, II, III**).
2. To study the influence of visually discernible corrosion deteriorations (visual grades) on the residual flexural bearing capacity of ribbed panels (**I**, **III**).

The age of ribbed panels from nine different research objects (mostly pigsties and cowsheds) varied from 10 to 32 years. Ribbed panels were tested on bending where uniformly distributed load was imitated. Prior to tests ribbed panels were assessed visually on a 6-point scale. Also material tests were performed with ribbed panels from four last test series (since the year 2000). From the longitudinal ribs of a ribbed panel ten concrete cores were drilled and tested in compression. Prestressing bars were opened in order to measure cover and carbonation depth. The chloride content was determined on 20 samples taken from the concrete cover of prestressing bars of nearby ribbed panels of R1…R8 at the research object Raadi. Six prestressing steel specimens of visually larger corrosion damage were cut from the longitudinal ribs of each ribbed panel. A mean gravimetric mass loss and maximum diameter loss was found to show the mean and maximum corrosion penetration of prestressing bars of a ribbed panel, respectively. The yield and ultimate strength of prestressing bars was calculated after tensile test.

The main results and conclusions of the first part of research are summarized below:

1. All ribbed panels, the ultimate load of which was lower than control load, received grade 0 on visual rating scale. Consequently, attention should be paid on ribbed panels where concrete cover of longitudinal reinforcement has spalled (grade 0), which could be a sign of decreased flexural bearing capacity in comparison with factory-issued (new) ribbed panels.

2. All studied ribbed panels with a corrosion-induced crack in longitudinal rib (grade 1) could carry the control load. Hence, these ribbed panels conform to the strength requirements of new ribbed panels even after a relatively long period of service.

3. All studied ribbed panels (irrespective of their grade) were able to carry the design load. Since engineers compare the calculated structural bearing capacity with design load, the latter could be employed as an equivalent of ultimate limit state. Hence, all studied ribbed panels corresponded to ultimate limit state. Despite of their sufficient residual bearing capacity, ribbed panels with cracked or spalled cover of the longitudinal reinforcement (grade 1 or 0, respectively) need repairs.

4. Of the 46 ribbed panels tested flexural ductile mode of failure were noticed at 36 ribbed panels. Also, weld (anchorage) rupture (3 ribbed panels), shear failure (3 ribbed panels), rupture of rebar in transversal (2 ribbed panels) and longitudinal (1 ribbed panel) rib and a failure of longitudinal rib (1 ribbed panel) was noticed.

The second part of research is a case study for investigating the condition of reinforced concrete structures and properties of concrete under the aggressive indoor environment of an existing oil-shale chemical plant. The studied seven-storied plant, located in North-Eastern Estonia, was constructed in 1951.

The aims of this part or research are as follows.
1. To locate and quantify reinforced concrete structures with most severe deterioration in the plant with visual assessment (**IV**, **V**).
2. To compare the strength of concrete cores with concrete strength mark from design drawings to verify if the studied structures were cast in accordance with the drawings (**IV**).
3. To find the most probable cause of deterioration of reinforced concrete structures in the studied plant (**IV**).

All reinforced concrete structures of the generator building were assessed visually on a 6-grade scale. Compressive strength of 55 cores, carbonation depth, cover, water absorption as well as sulphate, chloride and nitrate content in concrete were determined.

The main results and conclusions of the second part of research are summarized below:

1. It was found that the deteriorations of load-bearing reinforced concrete structures in the studied oil plant building may originate already from the 1950-ies.

2. The mean strength of cores drilled both from columns and beams exceed their corresponding former Soviet Union compressive strength mark. However, the strength of cores drilled from beams corresponds to the lowest strength class applied today - C8/10. The strength of cores drilled from columns was lower than any contemporary strength class.

According to the results suggestions were proposed to repair deteriorated reinforced concrete structures in the plant.

General conclusions:

1. In both studies the external condition of the existing reinforced concrete structures was assessed visually on a 6-grade scale. The results show that the residual bearing capacity of structures with spalled concrete cover (grade 0) varies the most. The visual scale applied in the current studies was developed already in 1974 and the condition corresponding to grade 0 should be updated and improved in further research.

2. The length of corrosion initiation, propagation and residual life period of a reinforced concrete structure may vary substantially. A study of an existing oil shale chemical plant has shown that the residual lifetime (or a residual life stage) of reinforced concrete structures carrying generators was exponentially greater than the corrosion initiation and corrosion propagation periods together.

3. The studies have shown that an insufficient quality of materials or workmanship could affect the results. Therefore, test results originating from existing reinforced concrete structures should be interpreted with caution.

4. Uniform corrosion was noticed on the reinforcing steel of the studied reinforced concrete structures. Fortunately, uniform corrosion is relatively easily measured and predicted. The influence of pitting corrosion as well as stress corrosion can be considered as more serious threats to the residual bearing capacity of existing reinforced concrete structures.

KOKKUVÕTE

Olemasolevate raudbetoontarindite seisund ja jääkkandevõime

Betooni kõrge survetugevus ja terase head tugevusnäitajad tõmbel teevad raudbetoonist laialdaste kasutusvõimalustega komposiitmaterjali, mida kasutati möödunud sajandil ehitustarindites küllaltki ulatuslikult. Vananemise tõttu on kulutused olemasolevate raudbetoontarindite hooldusele, remondile ja asendamisele viimastel aastakümnetel oluliselt suurenenud.

Kirjanduses jagatakse raudbetoontarindi kasutusiga mitmeks perioodiks. Torres-Acosta jt. (2007) järgi eristatakse kolme perioodi: korrosiooni alg-, levimis- ning jääkperiood. Viimasel kolmel aastakümnel on ulatuslikult ja intensiivselt uuritud korrosiooni algperioodi. Vähemal määral on uuritud korrosiooni levimist ja selle mõju raudbetoontarindi käitumisele (Li jt. 2008). Korrosiooni levimise ja jääkperioodi uuringutest on üsna vähesed pühendatud korrosioonikahjustustega raudbetoontarindi jääkkandevõimele (Torres-Acosta jt. 2007).

Enamikus sellistes katsetes on korrosioon tekitatud ja kiirendatud laboratoorsetes tingimustes, kus korrosiooni tekitamiseks paigaldatakse betoon koos kloriididega ning korrosiooni kiirendamiseks kasutatakse sundvoolu. Paraku ei anna kiirendatud korrosiooniga tehtud katsed alati võrreldavaid tulemusi loomulikus keskkonnas korrodeerunud tarindite katsetega (Torres-Acosta jt. 2007). Kahjuks leidub kirjanduses vähe andmeid katsetest vananemisel korrodeerunud raudbetoontarindite kohta. Sellest tulenevalt on käesoleva doktoritöö põhieesmärgiks täiendada katsetulemusi olemasolevate raudbetoontarindite seisundi ja jääkkandevõime kohta.

Töö esimeses osas kirjeldatakse 46 vanadest hoonetest võetud raudbetoonist ribipaneeli katsetamist eesmärgiga:

1. Uurida paneelide jääkkandevõimet, käitumist ja purunemist paindel (**I, II, III**).

2. Selgitada visuaalse hinde põhjal paneelide korrosioonikahjustuste mõju nende jääkkandevõimele paindel (**I**, **III**).

Üheksalt objektilt (peamiselt sigalad ja lehmalaudad) pärinevate paneelide vanus katsetamisel oli 10…32 aastat. Kõigi 46 paneeliga tehti paindekatse. Koormamisel imiteeriti ühtlaselt jaotatud koormust. Enne katset hinnati paneele visuaalselt 6-pallist skaalat kasutades. Katseseeriatel alates 2000. aastast (4 seeriat) tehti katseid ka paneelidest võetud materjalidega. Iga paneeli pikiribidest puuriti kümme betoonkärni, mida katsetati survele. Kümnes pragunemata kohas iga paneeli pikiribis avati pingesarrus ning mõõdeti kaitsekihi paksus ja karboniseerumissügavus. Ühe katseseeria (R1…R8) kõrvalpaneelide betoonis hinnati ka kloriidide sisaldust. Iga paneeli pikiribidest lõigati kuus nähtavate korrosioonikahjustustega eelpingestusterase katsekeha. Korrodeerumise iseloomustamiseks määrati katsekehade keskmine massikadu ja diameetri maksimaalne vähenemine. Tõmbekatsega määrati pingesarruse suhteline voolavuspiir ja tõmbetugevus.

Tulemused ja järeldused:

1. Kõik paneelid, mille purustav koormus oli väiksem kui kontrollkoormus hinnati visuaalselt hindele 0. Seega tuleks tähelepanu pöörata pikiribis sarrusest eraldunud kaitsekihiga ribipaneelidele (hinne 0), kuna nende paindekandevõime võib olla vähenenud võrreldes uute paneelidega.

2. Kõik paneelid, mille pikiribis oli korrosiooni tagajärjel tekkinud pragu (hinne 1) suutsid kanda kontrollkoormust. Seega vastavad need paneelid uute paneelide tugevustingimustele isegi peale suhteliselt pikka kasutusiga.

3. Kõik uuritud paneelid (olenemata hindest) suutsid kanda arvutuslikku koormust, st. vastasid kandepiirseisundile. Siiski, piisavast jääkkandevõimest hoolimata vajavad pragunenud või sarrusest eraldunud kaitsekihiga paneelid (vastavalt hindega 1 ja 0) remonti.

4. 46 paneelist 36 purunes paindemomendile. Lisaks esines veel paneeli pikisarruse ankurduse (keevise) purunemist (3 paneeli), põikjõupurunemist (3 paneeli), põiki- (2 paneeli) ja pikiribi sarruse purunemist (1 paneel) ning pikiribi purunemist (1 paneel).

Töö teises osas esitatakse Kohtla-Järvel 1951. aastal ehitatud põlevkivikeemiatehase generaatorihoone raudbetoonist kandetarindite seisundi ja betooni omaduste uurimise tulemused. Nende uuringute eesmärk oli:

1. Leida ja hinnata visuaalselt generaatorihoone kõige tõsisemate korrosioonikahjustustega raudbetoontarindid (**IV**, **V**).

2. Võrrelda postidest ja taladest väljapuuritud betoonkärnide survetugevust ehitusprojekti andmetega (**IV**).

3. Teha kindlaks kahjustuste kõige tõenäolisem põhjus (**IV**).

Ka kõiki generaatorihoone raudbetoonposte ja –talasid hinnati visuaalselt 6-pallist skaalat kasutades. 55 puursüdamikul määrati survetugevus ja mõõdeti karboniseerumissügavus ning puuraukudes mõõdeti betoonkaitsekihi paksus. Generaatorit kandvatest taladest puuritud neljal kärnil määrati sulfaatide, kloriidide ja nitraatide sisaldus. Lisaks võeti 1. korruse postidest kümme betoonitükki veeimavuse määramiseks.

Tulemused ja järeldused:

1. Tarindite visuaalsel hindamisel selgus, et enamiku postide (1-3. korrusel) ja talade (2-4. korrusel) kaitsekiht on korrosiooni tagajärjel sarrusest eraldunud (hinne 0). Hinde 0 saanud tarinditest olid kõige halvemas seisundis generaatorit kandvad talad 2. korrusel.

2. Nii postidest kui taladest puuritud kärnide keskmine survetugevus ületas (endises Nõukogude Liidus kasutatud) projektile vastavat betooni tugevusmarki. Taladest puuritud betoonkärnide survetugevus vastaks praegu kehtivatest betooni tugevusklassidest kõige madalamale – C8/10. Postidest puuritud betoonkärnide tugevus jääb tänapäeva tugevusklassidest madalamaks.

3. Uuritud generaatorihoone raudbetoontarindite kahjustused võivad pärineda juba 1950-ndatest. Teistsuguse tootmistehnoloogia tõttu (generaatoreid kasutati gaasi tootmiseks) eemaldati tollal generaatoritest igapäevaselt šlakki. Šlaki „roopimise" ajal olid generaatorit kandvad raudbetoontarindid kaitsmata luukide kaudu väljuvate agressiivsete gaaside eest. Nende gaaside kõrge kontsentratsioon ongi kõige tõenäolisem raudbetoontarindite kahjustuste põhjus.

Uuringu tulemustest lähtudes on antud soovitused generaatorihoone kahjustunud raudbetoontarindite remondiks.

Üldised järeldused:

1. Doktoritöö mõlemas osas hinnati raudbetoontarindeid 6-pallisel skaalal. Töö tulemused näitavad, et skaalal hinde 0 saanud tarindite kandevõime varieerus kõige enam. Töös rakendatud skaala on välja töötatud 1974. aastal ja vajab hinde 0 osas edaspidistes uuringutes täiendamist.

2. Raudbetoontarindi korrosiooni algperiood, levimisperiood ja jääkperiood võivalt oluliselt varieeruda. Põlevkivikeemiatehase uuring näitas, et generaatorit kandvate talade eluea jääkperiood osutus mitmeid kordi pikemaks kui alg- ja levimisperiood kokku.

3. Doktoritöö mõlemad uuringud näitasid, et ebapiisav materjalide või ehitustööde kvaliteet võib katsetulemusi mõjutada. Sellest tulenevalt tuleks olemasolevate raudbetoontarinditega seotud katsetulemusi interpreteerida ettevaatlikkusega.

4. Doktoritöös uuritud korrosioonikahjustustega raudbetoontarinditel esines sarrusterase ühtlane korrosioon. Ühtlast korrosiooni on suhteliselt lihtne mõõta ja selle abil raudbetoontarindi eluea jääki prognoosida. Olemasolevate raudbetoontarindite kandevõime vähenemise seisukohalt on tunduvamalt ohtlikumad punktkorrosioon ja pingekorrosioon.

I

PUBLICATIONS

Miljan, J., **Kiviste, M.** 2010.
INFLUENCE OF VISUAL CONDITION
ON RESIDUAL FLEXURAL CAPACITY OF
EXISTING PRECAST CONCRETE PANELS.

9th International Scientific Conference,
Engineering for Rural Development, Jelgava: 260-266.

INFLUENCE OF VISUAL CONDITION ON RESIDUAL FLEXURAL CAPACITY OF EXISTING PRECAST CONCRETE PANELS

Jaan Miljan, Mihkel Kiviste
Estonian University of Life Sciences, Institute of Forestry and Rural Engineering
jaan.miljan@emu.ee, mihkel.kiviste@emu.ee

Abstract. The influence of visual assessment grade on the residual flexural capacity of 46 existing precast concrete ribbed panels from different agricultural buildings was studied. Before the tests the panels were assessed on a 6-point rating scale according to visually distinguishable corrosion deterioration. All panels, the ultimate load of which was lower than the control load, received grade 0 on the visual rating scale. Consequently, attention should be paid to panels where the concrete cover of longitudinal reinforcement has spalled (grade 0) which could be a sign of decreasing load capacity. The majority of panels with grade 0 exhibited larger deflections under load than panels with higher grades. Of the 46 panels tested flexural ductile failure was noticed at 36 panels.

Key words: visual grade, residual flexural capacity, corrosion, precast ribbed panels.

Introduction

In Estonia, the bearing structures of many existing agricultural and industrial buildings constitute a precast concrete skeletal frame. Particularly intensive construction based on industrially produced (precast) elements started in the 1960s when standardized design solutions and reinforced concrete structure designs were employed. However, the initial signs of corrosion of steel reinforcement became evident in agricultural buildings already in 1970s. The Department of Rural Building of the Estonian University of Life Sciences (EMU) has gathered data describing the state of concrete load-bearing structures (columns, beams and ribbed panels) in 258 agricultural buildings from 1974 to 1997 assigning grades for 23 336 ribbed ceiling panels (i.e. about 3.5 % of the total number of panels in agricultural buildings of Estonia) [1].

There are about 4 000 agricultural buildings with an average floor space of 1 800 m^2 in Estonia today. Many of their precast concrete load-bearing members (columns, beams and ribbed panels) are in service with a cracked or spalled concrete cover. Owners of buildings are most likely concerned about the condition and residual strength of their concrete structures. There is an increasing demand for informed decisions about the capability of structure to serve its intended function or, otherwise, the need for repair or demolition.

This paper reports an experimental study of 14 precast non-prestressed concrete ribbed panels of mark PKZH-2 and 32 prestressed concrete panels of mark PNS-3, PNS-12 and PNS-14. The first objective of the research is to find the residual flexural strength of the existing precast concrete ribbed panels. The second objective is to clarify whether it is possible to estimate the load capacity of a ribbed panel according to visually discernible corrosion damage. The marks of panels reflect the former Soviet Union standard GOST. Precast ribbed panels with aforementioned marks are common in the industrial and agricultural buildings of Estonia (but also in other former Soviet Union countries) built from 1950s to 1990s. All tested ribbed ceiling and roof-ceiling panels had a length of 5 970 mm and width of 1 490 mm (Figure 1).

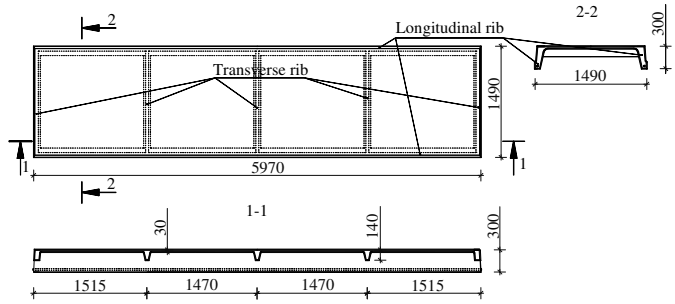

Fig. 1. **Top view, longitudinal and transversal section of a precast ribbed panel**

Non-prestressed concrete panels of mark PKZH were manufactured (in accordance with GOST 7740-55 [2]) from the 1950s until 1964…1965. Prestressed concrete panels of mark PNS were produced from 1964…1965 until at least 1990. Panels PNS-3 were produced in the relatively short period of transition from panel mark PKZH to PNS. Since the mid-1960-ies panels PNS-12 have been produced (a further development of PNS-3) and PNS-14 started [3].

Materials and methods

Before the structural tests, the panels were assessed on a scale developed at the Chair of Structural Mechanics of the former Estonian Agricultural Academy (EMU now) in 1974. The visual assessment scale distinguishes between six different states as shown in Table 1.

Table 1

Classification of deterioration states of the ribbed ceiling panels

Grade	Description of state
5	No corrosion detected
4	1) Less than 20 % of the concrete cover of a slab has spalled; 2) Noticeable longitudinal cracks (0.3-1.0 mm) in transverse ribs.
3	1) More than 20 % of the concrete cover of slab reinforcement has spalled; 2) Less than 20 % of the concrete cover of stirrups in the longitudinal ribs has spalled; 3) In transverse ribs wide (>1.0 mm) cracks have occurred; 4) Less than 20 % of the concrete cover in transverse ribs has spalled.
2	1) More than 20 % of the concrete cover of stirrups in longitudinal ribs has spalled; 2) More than 20 % of the concrete cover of reinforcement in transverse ribs has spalled; 3) Longitudinal micro cracks (0-0.3 mm) due to corrosion in longitudinal ribs.
1	Longitudinal cracks (> 0.3 mm) in longitudinal ribs;
0	Concrete cover of the reinforcement in longitudinal ribs has spalled.

The current study is based on the series of tests of ribbed panels at EMU since 1973. 14 reinforced concrete (RC) panels of mark PKZH-2 and 32 pre-stressed concrete (PC) panels of mark PNS-3, PNS-12 and PNS-14 were tested. The summary of the test series is presented in Table 2. Letter(s) in the first column is associated to the location of panels. RC panels are marked with hyphen between the letter and number, while PC panels are marked without hyphen.

Table 2

Test series of reinforced and prestressed concrete ribbed panels

Panels (amount)	Mark	Object and purpose	Test location	Loading, location	Test year	Age of panels	Test performer
K-1 ... K-7 (7)	PKZH-2	Kärstna pigsty	Kärstna field tests	Sand uniformly, soil	1973	12	J. Miljan
K-8 ... K-10 (3)	PKZH-2	Kärstna pigsty	Tallinn, test hall	Cast iron loads uniformly, RC floor	1974	13	J. Miljan
P11 ... P13 (3)	PNS-3	Pandivere pigsty	Tallinn, test hall	Cast iron loads uniformly, RC floor	1974	10	J. Miljan
VA14 … VA19 (6)	PNS-3	Vao pigsty	Vao field tests	RC foundation blocks uniformly, soil	1975	11	J. Miljan
T-20 … T-23 (4)	PKZH-2	Torma cowshed	Torma field tests	RC curbstones uniformly, soil	1978	15	J. Miljan
L1 … L10 (10)	PNS-12 PNS-14	Luha cowshed	Tartu, EMU lab.	Hydrocylinder, 4-point bending, RC force floor	2000-2001	26	E. Laiakask
R1 … R8 (8)	PNS-12	Raadi garage	Tartu, EMU lab.	Hydrocylinder, 4-point bending, RC force floor	2002	Un-known	M. Kiviste, H. Tomann, M. Tarto
V8 … V12 (5)	PNS-12 PNS-14	Corridor of Vara pigsty	Tartu, EMÜ lab.	Hydrocylinder, 4-point bending, RC force floor	2005	32	R. Halgma, L. Linnus, T. Salu

As shown in Table 2, all tested panels had been in service for at least 10 years. The panels were demounted and singly loaded. The panels were tested in laboratory (K-8…K-10, P11…P13, L1…L10, R1…R8, V8…V12) as well as on the object (K-1…K-7, VA14…VA19, T-20…T-23). The structural tests with pre-stressed ribbed panels of mark PNS-12 and PNS-14 are discussed in more detail in another paper.

The panels were lifted to RC blocks, which acted as sub supports. Singly tested panels were simply supported on a steel pin and roller support. All tested panels were loaded in increments of 10 % of the control load (q_c) which was kept constant for at least ten minutes on each stage [4].

The control load was set to test new panels issued from factory. A few randomly chosen new panels were tested in the factory to check their crack resistance, rigidity and load capacity up to one increment higher than the control load. Repetition tests were due if the ultimate load of a panel issued from the factory was less than the control load but not less than 85 % of the control load. Panels did not meet the strength requirements if a single ultimate load in primary or repetition tests was less then 85 % of the control load [3]. The design load (q_d) was implemented by the structural engineering design of a building.

In all test series, uniformly distributed loads were imitated to compare the results with the control and design load. The panels were tested to failure or limit state whereby deflections of a panel increased without additional load [4]. The maximum load a panel could carry was recorded as the ultimate load (q_u). Existing cracks and cracks developing during the test were carefully recorded with a marker on the panel surface.

Vertical displacements were measured at the four corners (on supports) and on both longitudinal ribs at mid-span of a panel. Generally, dial gauges of precision 0.01 mm were applied at the corners and compliant measuring gauges (type Maksimov) of precision 0.1 mm and 0.01 mm at mid-span of a rib. The mid-span deflection of a panel was calculated as a difference of the mean mid-span deflection of both longitudinal ribs and of the mean displacement at supports of the panel [4].

Results and discussion

To compare the residual strength of panels of 4 different marks, the ratio (q_u/q_c) of ultimate load and control load was calculated. The *one-way analysis of variance* (*ANOVA*) did not reveal significant difference in the average ratio of the ultimate load and control load by the panel marks (PKZH-2, PNS-3, PNS-12, PNS-14) at the confidence level α=0.05. Also, in purpose of comparison the ultimate load (q_u) of the test panels was divided to design load (q_d).

The control loads of panels PKZH-2, PNS-3 (later PNS-12) and PNS-14 are 387 [2], 750 [3] and 1440 kgf·m^{-2} [3], transformed to kN·m^{-2}, respectively. The design loads of panels PKZH-2, PNS-3 (later PNS-12) and PNS-14 are 270 [2], 460 [3] and 950 kgf·m^{-2} [3], transformed to kN·m^{-2}, respectively. The results of visual assessment and flexural test of ribbed panels are presented in Table 3. The influence of visual condition (grade) on the load capacity (q_u/q_c) of 46 singly tested panels is presented in Figure 2. The box plot in Figure 2 was generated with statistical software R.

Figure 2 shows non-linear decreasing trend of q_u/q_c ratio with decreasing grade of panel. Only a few samples of high grades exist in the current data set. Neither statistical nor substantial reasons exist to assume a trend in q_u/q_c ratio at grade 2 or higher. However, box plots from grade 2 to 0 demonstrate evident decrease of q_u/q_c ratio. The one-way *ANOVA* revealed a significant effect for grades, $F(5,40)=5.35$; $p=0.0007$. The magnitude of the grade to q_u/q_c ratio was computed as $R^2=0.40$. *Tukey's HSD test for multiple comparisons of means* proved the significant difference of q_u/q_c ratio between grade 0 and higher grades.

The ultimate load of only five of the 46 singly tested panels was less than the control load. All of these five panels received grade 0 on the visual rating scale. Consequently, attention should be paid to panels where the concrete cover of longitudinal reinforcement has spalled (grade 0) which could be a sign of decreased load capacity. The visual scale proposed in the paper has the potential to serve as a rational tool for practitioners, operators and asset managers to make decisions about the optimal timing for repairs, strengthening, and/or rehabilitation of corrosion-affected concrete infrastructure. Scale-acquainted engineers can rate reinforced concrete structures relatively quickly and simply to fetch out ribbed ceiling panels (if any) of spalled concrete cover. Later on the residual flexural

capacity of panels with grade 0 needs structural expert judgment. It is also worth mentioning that no panels with a corrosion-induced crack in the longitudinal rib (grade 1) were dangerous from the aspect of ultimate residual load capacity. All studied panels (irrespective of their grade) were able to carry the design load (q_u/q_d.>1.01).

Table 3

Results of visual assessment and flexural test of ribbed panels

Panel	Mark	Grade	q_u, kN·m^{-2}	q_u/q_c	q_u/q_d	Panel	Mark	Grade	q_u, kN·m^{-2}	q_u/q_c	q_u/q_d
K-1	PKZH-2	0	4.52	1.19	1.71	L1	PNS-12	0	9.00	1.23	2.00
K-2	PKZH-2	1	5.18	1.36	1.96	L2	PNS-12	4	9.20	1.25	2.04
K-3	PKZH-2	0	3.97	1.05	1.50	L3	PNS-12	1	9.25	1.26	2.05
K-4	PKZH-2	1	4.79	1.26	1.81	L4	PNS-12	3	9.70	1.30	2.15
K-5	PKZH-2	1	5.16	1.36	1.95	L5	PNS-12	1	9.75	1.33	2.16
K-6	PKZH-2	0	4.31	1.14	1.63	L9	PNS-12	3	9.04	1.23	2.00
K-7	PKZH-2	1	4.54	1.20	1.71	L6	PNS-14	5	16.95	1.20	1.82
K-8	PKZH-2	0	4.10	1.08	1.55	L7	PNS-14	0	13.56	0.96	1.46
K-9	PKZH-2	0	2.67	0.70	1.01	L8	PNS-14	0	10.17	0.72	1.09
K-10	PKZH-2	0	2.67	0.70	1.01	L10	PNS-14	0	15.82	1.12	1.70
P11	PNS-3	2	11.01	1.50	2.44	R1	PNS-12	0	8.35	1.14	1.85
P12	PNS-3	1	8.07	1.10	1.79	R2	PNS-12	0	7.26	0.99	1.61
P13	PNS-3	2	9.56	1.30	2.12	R3	PNS-12	1	9.12	1.24	2.02
VA14	PNS-3	1	8.79	1.19	1.95	R4	PNS-12	1	9.64	1.31	2.14
VA15	PNS-3	1	8.79	1.19	1.95	R5	PNS-12	1	9.86	1.34	2.19
VA16	PNS-3	2	9.90	1.35	2.20	R6	PNS-12	0	8.59	1.17	1.90
VA17	PNS-3	2	9.90	1.35	2.20	R7	PNS-12	1	7.91	1.08	1.75
VA18	PNS-3	2	9.90	1.35	2.20	R8	PNS-12	0	8.28	1.13	1.84
VA19	PNS-3	2	9.90	1.35	2.20	V8	PNS-12	0	9.00	1.22	2.00
T-20	PKZ-2	1	5.64	1.49	2.13	V9	PNS-12	0	10.53	1.43	2.33
T-21	PKZ-2	2	5.94	1.57	2.24	V10	PNS-12	1	8.80	1.20	1.95
T-22	PKZ-2	1	5.64	1.49	2.13	V11	PNS-12	2	9.30	1.26	2.06
T-23	PKZ-2	1	5.43	1.43	2.05	V12	PNS-14	1	15.28	1.08	1.64

Figure 2 demonstrates that q_u/q_c ratio varies the most in panels with spalled concrete cover (grade 0). This means that panels, which may have just reached grade 0 as well as panels in critical state in terms of their load capacity are both rated as grade 0. Consequently, panels with spalled concrete cover should be differentiated to specify their different residual load capacity. Deterioration states employed for panel classification in the current study (in Table 1) were developed already in 1974 and could be updated. Durham et al. [5]; Heymsfield et al. [6] had tested 33 existing precast non-prestressed channel ribbed panels, which were used in short multi-span bridges in Arkansas in the 1950s through the early 1970s. The panels, constructed without shear reinforcement, were categorized as “good”, “average” or “poor” as a function of percentage and location of exposed longitudinal reinforcing steel. All these three classifications correspond to grade 0 on the visual rating scale of the current study.

The original objective of the study of Heymsfield et al. [6] was to establish a correlation for inspection purposes between the beam’s visual deteriorated state and its corresponding approximate structural capacity. 5.79 m channel ribbed panels with similar cross section were tested also on a four-point loading frame. It was found that the strength of beams was more a function of a concrete compressive strength rather than deterioration state.

Torres-Acosta et al. [7] had proposed a durability model based on experimental load capacity values from various investigations, where results of different structural members (beams, slabs) under accelerated corrosion were presented. Figure 3 represents an illustrative load-capacity model for a reinforced concrete flexural member referred in Torres-Acosta et al. [7] and the current study with the addition of research results by Heymsfield et al. [6] and Li et al. [8].

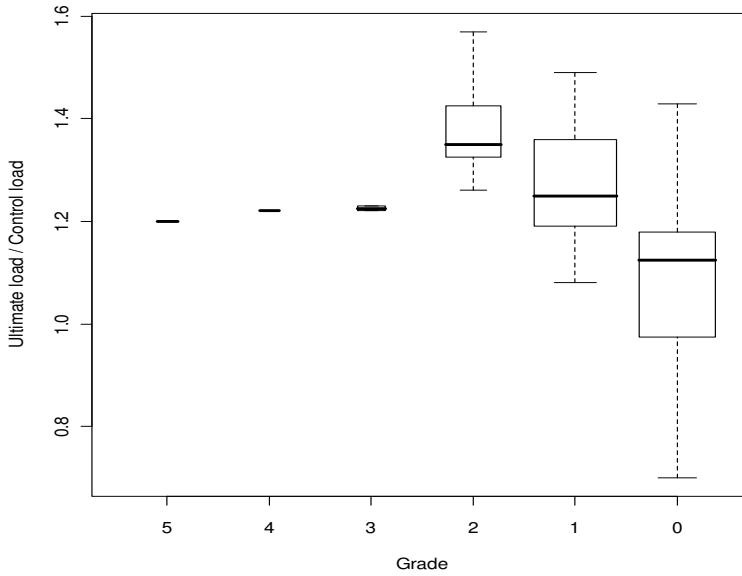

Fig. 2. **Box plot of q_u/q_c ratio for panels of different visual grades**
(The box plots show distribution characteristics: the median (thick horizontal line), upper and lower quartiles (horizontal edges of the box), minimum and maximum values (ends of vertical bar) of the q_u/q_c ratio by different grades)

The model presents the structural load capacity of a flexural member as a function of its lifetime. The lifetime T of the flexural member is defined as:

$$T = T_I + T_P + T_{RL}, \quad (1)$$

where T_I – corrosion initiation stage from the time of construction to the time of corrosion initiation;
T_P – corrosion propagation stage during which the steel corrodes until an unacceptable level of corrosion is reached and;
T_{RL} – residual life stage from serviceability to the ultimate limit state.

As corrosion progresses, there will be an increasing build-up of corrosion products and associated increased radial stresses, causing longitudinal cracking and, eventually, concrete spalling. In this study, the unacceptable level is defined as a corrosion-induced crack in the longitudinal rib of a panel more than 0.3 mm wide (grade 1). This also might be implied as serviceability limit state of a ribbed panel. Li et al. [8] stated that once the structure is considered to be unserviceable due to corrosion-induced cracking, there is considerable remaining lifetime before the structure can be considered to have become unsafe. Residual life stage T_{RL} starts from the time the structure becomes unserviceable until the ultimate limit state is reached, before structural collapse.

The categorization of "good", "average" and "poor" by Heymsfield et al. [6] is also included in Figure 3. An attempt has to be made to add the six detailed phases of the phenomenological model [8] for steel corrosion in concrete. However, the model by Li et al. [8] has a different approach. The latter differentiates six phases (D1, D2, C0, C1, C2, C3) from the mechanics of corrosion applied to the steel bar at a generic cross section of a reinforced concrete member. In addition, the initiation period of the model was based on corrosion induced by chloride attack. It was found that, for practical flexural members subject to chloride attacks, corrosion initiation may start quite early in their service life [8].

As mentioned before, all panels with visual grade 1 or higher overreached the control load, which explains the location of the control load on the time axis. Since the structural engineering designers

based their calculations on the design load, the latter is employed as an equivalent of the ultimate limit state in Figure 3. The thick load capacity line in Figure 3 represents the period for the reinforced concrete member covered by current structural tests. As observed from Figure 2 and Figure 3 the structural load capacity remains almost the same during the initiation and propagation period until reaching grade 0 (in residual life period), where the capacity decrease rate is accelerated.

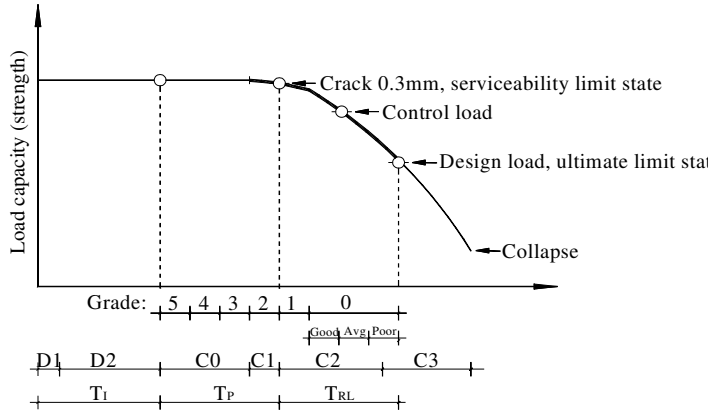

Fig. 3. **Load-bearing capacity model for a reinforced concrete member.**
Based on Torres-Acosta et al. [7] and the current study with the addition of the research results by Heymsfield et al. [6]; Li et al. [8]

Conclusions

Based on the results of the current experimental investigation of the existing precast concrete ribbed panels, the following conclusions are drawn:

1. All panels, the ultimate load of which was lower than the control load, received grade 0 on the visual rating scale. Consequently, attention should be paid to panels where the concrete cover of longitudinal reinforcement has spalled (grade 0) which could be a sign of decreasing load capacity.
2. No panels with a corrosion-induced crack in the longitudinal rib (grade 1) were dangerous from the aspect of the ultimate residual load capacity.
3. All studied panels (irrespective of their grade) were able to carry the design load. Since the structural engineering designers based their calculations on the design load, the latter is employed as an equivalent of the ultimate limit state

References

1. Miljan R. Lehmalautade uuenduse mõju piimatootjate majanduslikule suutlikkusele Eestis (The impact of cowshed modernisation on the economic capability of milk producers in Estonia). PhD thesis. Estonian Agricultural University, Tartu, 2005. 195 p. (In Estonian).
2. ГОСТ 7740-55. Плиты крупнопанельные железобетонные с армированными полями для покрытий производственных зданий (Reinforced concrete ribbed slabs of industrial building). Москва: Гос. комитет Совета Министров Союза ССР по делам строительства, 1955, 16 p. (In Russian).
3. Серия ПК-01-111. Крупнопанельные железобетонные предварительно напряженные плиты покрытий размером 1,5х6 м. Рабочие чертежи. (Prestressed concrete ceiling panels of dimensions 1.5 by 6m. Working drawings). Москва: Центральный институт типовых проектов, 1961. 20 p. (In Russian).
4. ГОСТ 8829-85. Конструкции и изделия бетонные и железобетонные сборные. Методы испытаний нагружением и оценка прочности, жестокости и трещиностойкости. (Concrete and reinforced concrete prefabricated structures and products. Test methods for loading and

estimation of strength, cruelty and crack). Москва: Государственный комитет СССР по делам строительства, 1985. 24 p. (In Russian).
5. Durham S.A., Heymsfield E., Tencleve K.D. Cracking and reinforcement corrosion in short-span precast concrete bridges. Journal of Performance of Constructed Facilities, 2007, vol. 21, No 5, pp. 390-397.
6. Heymsfield E., Durham S.A., Jones J.X. Structural behaviour of short span precast channel beam bridges without shear reinforcement. Journal of Bridge Engineering, 2007, vol. 12, No 6, pp. 794-800.
7. Torres-Acosta A., Navarro-Gutierrez S., Teran-Guillen J. Residual flexure capacity of corroded reinforced concrete beams. Engineering Structures, 2007, vol. 29, No 6, pp. 1145-1152.
8. Li C-Q., Yang Y., Melchers R.E. Prediction of reinforcement corrosion in concrete and its effects on concrete cracking and strength reduction. ACI Materials Journal, 2008, vol. 105, No 1, pp. 3-10.

II

Kiviste, M., Miljan, J. 2010.
EVALUATION OF RESIDUAL FLEXURAL CAPACITY
OF EXISTING PRE-CAST PRE-STRESSED
CONCRETE PANELS-A CASE STUDY.

Engineering Structures 32(10): 3377-3383.

Engineering Structures 32 (2010) 3377–3383

Contents lists available at ScienceDirect

Engineering Structures

journal homepage: www.elsevier.com/locate/engstruct

Evaluation of residual flexural capacity of existing pre-cast pre-stressed concrete panels—A case study

Mihkel Kiviste *, Jaan Miljan

Estonian University of Life Sciences, Institute of Forestry and Rural Engineering, Department of Rural Building, Tartu, 51014, Estonia

ARTICLE INFO

Article history:
Received 26 March 2010
Received in revised form
22 June 2010
Accepted 1 July 2010
Available online 7 August 2010

Keywords:
Flexural capacity
Corrosion
Pre-stressed panelspanel
Chloride
Carbonation

ABSTRACT

The residual flexural capacity of 28 existing pre-cast, pre-stressed, ribbed concrete ribbed panels was studied. Four-point bending was applied into the middle third of the panel. Fifteen panels of the 28 conformed to the strength and rigidity requirements of new factory-issued panels. In the study, all of the studied existing panels have retained sufficient residual flexural capacity to carry the design loads applied in service. Probably, it is likely that pre-stressing steel of an inferior strength mark was applied onto five of the panels studied. This, which could explain the poor flexural capacity of those panels of in good visual condition and the insignificant corrosion level on the pre-stressing bars. Twenty-two out of 28 panels exhibited flexural ductile failure. Three panels failed as a result of an anchorage (weld) rupture and three panels failed in shear. It is likely that the corrosion deterioration of the panels were probably neither carbonation nor chloride induced.

1. Introduction

Reinforcement corrosion is the most widespread cause of premature deterioration in reinforced concrete structures. Corrosion is a concern because of the associated cracking and spalling of concrete cover, reduction in steel cross-sectional area and loss of bond, which over time will decrease the strength and serviceability of concrete structures. Considerable resources are spent on repair and to rehabilitate deteriorating concrete structures. The degree of reinforcement corrosion, and the resulting decrease in the load-carrying capacity of the structural component, needs to be evaluated to develop effective repair strategies.

Most of the studies reporting structural tests on corroded reinforced concrete structures have been conducted under laboratory conditions. However, laboratory studies cannot fully represent all the aspects of the on-site behaviour of concrete structures. Although field studies can help us account for the reduction in strength and serviceability of concrete structures over time, investigations on the strength and condition of the existing reinforced and pre-stressed concrete structures, after long-term exposure to the on-site environment, are scarce in the literature.

Flexural capacity tests have been performed with beams in harbour docks [1] which had been in an aggressive environment for more than 10 years [2]. Wipf et al. [3] conducted an extensive field testing of pre-cast channel bridges as well as laboratory testing of their pre-cast panels. An experimental study was conducted on two 28-year-old reinforced concrete bridge arch ribs to explore the residual load carrying capacity and failure pattern [4]. In the study by Shdid et al. [5], 40-year-old pre-cast pre-stressed concrete bridge piles were rated visually and flexurally tested to failure. Heymsfield et al. [6] examined the flexural load capacity of 33 pre-cast channel beams, which were removed from existing bridges. These were 5.79 m long and 1.07 m wide channel beams and were used in a large number of bridges in Arkansas (USA) from the mid-1950s to the mid-1970s. The length and the loading arrangement of the beams in the study of Heymsfield et al. are similar to these employed in the present study.

In Estonia, the bearing structures of many agricultural and industrial buildings constitute a pre-cast concrete skeletal frame. Intensive construction, based on industrially produced elements, started in the 1960s when standardized design solutions and reinforced concrete structure designs were employed. After a relatively short period of service, the initial signs of corrosion of steel reinforcement became evident in agricultural buildings.

In Estonia today, there are about 4000 agricultural buildings with an average floor space of 1800 m^2. Many of their pre-cast concrete bearing structures (columns, beams and ribbed panels) have reached an undefined state. The pre-stressed ribbed panels examined in this study are very common in Estonian agricultural buildings. There is an increasing demand for informed decisions about the structures' capability to serve their intended function or, otherwise, the need for repair or demolition.

* Corresponding author.
E-mail address: mihkel.kiviste@emu.ee (M. Kiviste).

0141-0296/$ – see front matter © 2010 Elsevier Ltd. All rights reserved.
doi:10.1016/j.engstruct.2010.07.011

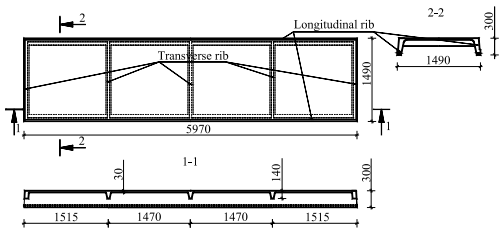

Fig. 1. Top view, longitudinal and transverse section of a ribbed panel [7]. Dimensions are in millimeter.

2. Experimental procedure

2.1. Test panels

The flexural capacity of 28 existing pre-cast, pre-stressed, ribbed concrete panels of mark PNS-12 and PNS-14 were studied experimentally. These panels, 1490 by 5970 mm (Fig. 1), were mass-produced in concrete factories of the former Soviet Union from the mid-1960-ies until at least 1990. The abbreviation PNS denote that the panels are pre-stressed and the numbers refer to panels of different capacities [7].

In general, the diameter of the pre-stressing bar was used to distinguish between the different marks of panels although on a few panels the factory-painted mark was still readable. Pre-stressed concrete panels PNS-10 …14 employed two hot-rolled low-alloyed pre-stressing bars of mark 35 GS (C = 0.3 … 0.37%, Mn = 0.8% … 1.2%, Si = 0.6% … 0.9%, Cr = 0.3%, Ni = 0.3, Cu = 0.3) [8]. The diameter (and pre-stress) of pre-stressing bars of panels PNS-12 and PNS-14 were 16 mm (343 N/mm^2) and 20 mm (481 N/mm^2), respectively [7]. The ultimate strength of pre-stressing steel (of both PNS-12 and PNS-14) should be at least 5500 kg f/cm^2 (539 MPa) to correspond to its mark [7]. Pre-stressing bars are welded to the details at the support ends of a panel [7]. Reinforcing and anchorage of panels PNS-12 and PNS-14 are shown in Fig. 2.

The strength of concrete of panels PNS-12 and PNS-14 should correspond to concrete strength mark M200 = 200 kg f/cm^2 and M300 = 300 kg f/cm^2, respectively [7]. Hence, the concrete strength of panels PNS-12 and PNS-14 should be at least 19.6 MPa and 29.4 MPa [7], respectively.

This study is a follow-up for the series of tests on the ribbed panels of type PKZH-2 and PNS-3 performed by J. Miljan since 1973 [9]. The panels, transported to the structural laboratory of the Eesti Maaülikool (EMÜ), the Estonian University of Life Sciences, were demounted from the following four different existing and abandoned structures.

1. Ceiling panels from cowshed No. 2, constructed in 1975 according to the design of type TP 891–254 at Luha farm I in the Vara district of Tartu county. Flexural tests on six panels PNS-12 and four panels PNS-14 (panels L1 … L10) from this cowshed were performed by Laiakask in 2000–2001 [10].
2. Roof-ceiling panels from the truck garage of the former Raadi military airfield the construction time of which is unknown due to their military origin. Flexural tests with eight panels PNS-12 (panels R1 … R8) from this garage were performed by Kiviste et al. in 2002 [11].
3. Ceiling panels from Vara pigsty, constructed in 1973 and abandoned in 1993, in the Vara district of Tartu county. Flexural tests with six panels PNS-14 (panels V1 … V6) from the pigsty were performed by Patrael et al. in 2005. Test results of panel V3 are omitted.
4. Roof-ceiling panels from the corridor of Vara pigsty in the Vara district of Tartu county. Flexural tests with four panels PNS-12 and one panel PNS-14 (panels V8.…V12) were performed by Halgma et al. in 2005–2006.

2.2. Requirements for a panel

According to former Soviet standard GOST 8829 [12], a randomly chosen pre-cast concrete element from each production batch from the factory must be tested to assess its conformity to strength, rigidity and crack resistance requirements. In this study only the requirements for strength and rigidity were considered. Due to corrosion deteriorations (cracked or spalled cover) most of the studied panels could not meet crack resistance requirements prior to loading.

The control load [12] (q_c) was set to check the strength requirements of a panel. A panel meets the strength requirements of its mark if the ultimate load of the tested panel exceeds the control load. Repetition tests were made if the ultimate load of a panel was less than the control load but not less than 85% of the control load. A panel does not meet the strength requirements if a single ultimate load in primary or repetition tests is less than 85% of the control load [7]. The control load (q_c) for panels PNS-12 and PNS-14 was set to 7.35 kN/m^2 and 14.12 kN/m^2, respectively [7].

The control load (q_c) was calculated with the following formula [7]:

$$q_c \geq \frac{s}{t} \cdot (q_d + q_{dead}) - q_{dead}, \tag{1}$$

where

s is the coefficient of overload, 1.4;
t is the coefficient of working conditions, 1.0;
q_d is the design load, kN/m^2; and
q_{dead} is the dead load of panel, kN/m^2.

The value of design load (q_d) was derived from catalogues and design drawings [7] of pre-cast concrete elements. The design load was implemented by the structural engineering design of a building.

A panel, including initial deflection, should be rigid enough not to exceed a deflection of 20 mm under a load of 3.73 kN/m^2 and 7.75 kN/m^2 for panels PNS-12 and PNS-14, respectively [7].

2.3. Test setup and loading

For the flexural test, a four-point bending test arrangement was set up whereby two loads, acting as an equivalent for the uniformly distributed load, were applied to the middle third of the panel (Fig. 3). The loads were applied by means of a hydraulic cylinder of a nominal maximum capacity of 250 kN. A steel main beam divided the total applied load from the cylinder into two loads. The distributing beams further divided it across the width of the panel, resulting in a total of four concentrated loads on the panel. The main and distributing beams acted as a simple beam with a pin and roller support. The application of load was controlled by a manually activated hydraulic pump. Panels were simply supported with a pin and roller support [12].

Before loading, a stressed wire was held on the supports to measure the initial deflection of each longitudinal rib in the mid-span of the panel, using a ruler with an accuracy of 1 mm. A mean initial deflection of both ribs was calculated as an initial mid-span deflection of a panel [12]. As a general rule, a negative initial deflection of a ribbed panel had been provided by pre-stressing it in the factory.

Panels were loaded in increments of 10% of the control load (q_c) which was kept constant for at least 10 min at each stage [12]. Panels were tested to failure or limit state whereby deflections of

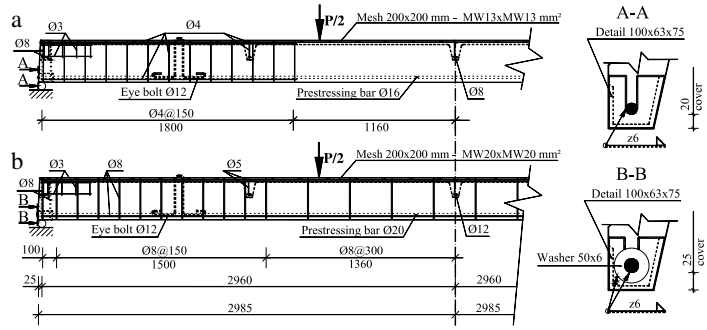

Fig. 2. Reinforcement and anchorage of the panels (a) PNS-12 and (b) PNS-14 [7]. Dimensions are in millimeter.

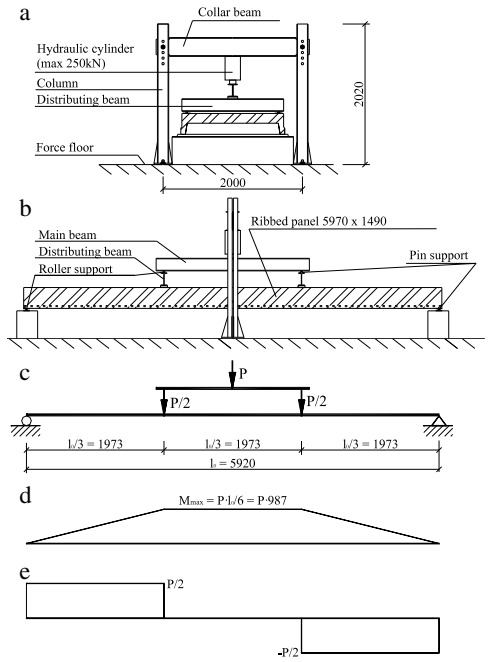

Fig. 3. (a) End and (b) side view of the test device with (c) load, (d) bending moment and (e) shear diagram. Dimensions are in millimeter.

a panel increased without adding further load [12]. The maximum load a panel could carry was recorded as the ultimate load (q_u). Then, according to the loading test arrangement, the applied force (kN) from the hydraulic cylinder was converted to bending moment (kN m) and the latter to the uniformly distributed surface load (kN/m^2).

Existing cracks and cracks developing during the test were carefully recorded with a marker on the panel surface.

Vertical displacements were measured at the four corners (on supports) and on both longitudinal ribs at mid-span of each panel. Dial gauges with a precision of 0.01 mm were applied at the corners and compliant measuring gauges with a precision of 0.1 mm and 0.01 mm at mid-span of a rib. The mid-span deflection of a panel was calculated as the difference of the mean mid-span deflection of both longitudinal ribs and of the mean displacement at the supports of the panel [12].

2.4. Cores, carbonation, cover and chloride content of concrete

The concrete core test was based on Estonian National Standard EVS-EN 12504–1:2003 [13]. Ten cores with a diameter of 54 mm were drilled from the longitudinal rib of each panel. Cores were cut by means of a rotary cutting drill with diamond bits. The ends of the cores were ground or capped with rapid hardening cement. Each core was measured in accordance with EVS-EN 12504–1:2003 [13]. The mean cross-sectional area was calculated from five diameter measurements and the mean height of each core was calculated from five height measurements. The estimated cube strength ($f_{est.cube}$) was calculated by applying the following Eq. (2) in BS 6089:1981 [14]:

$$f_{est.cube} = \frac{D}{1.5 + 1/\lambda} \cdot f_{core}, \tag{2}$$

where D is 2.5 for cores drilled horizontally (perpendicular to the cast direction for pre-cast units), or $D = 2.3$ for cores drilled vertically (parallel to the cast direction for pre-cast units),

λ is the height/diameter ratio, and

f_{core} is found by dividing the maximum load sustained by the core with its average cross-sectional area.

Cores with a height/diameter ratio 1 were tested, because cylinders with this ratio have very nearly the same strength as standard cubes [13]. The estimated cube strength was compared to the concrete mark from design drawings [7] to verify if the panels were cast in accordance with the drawings. The concrete mark (operative until 1984) was calculated as a mean compressive strength of standard cube specimens of sides 150 mm in kgf/cm^2 (e.g. concrete of mark M200).

Carbonation depth was measured by the conventional phenolphthalein test according to EVS-EN 14630:2006 [15]. Testing was undertaken by applying a phenolphthalein solution to a freshly opened surface of non-cracked concrete cover of pre-stressing bars after the flexural test. Carbonation depth was measured by means of a ruler at 10 different locations (at least five readings for each location) on the longitudinal rib of a panel. A mean value of carbonation depth ($D_{carb,m}$) of a panel was calculated.

A cover of pre-stressing bars was also measured by means of a ruler at the same location where the carbonation test was performed (at least five readings at each location). A mean value of cover (c_m) of pre-stressing bars of a panel was calculated.

Chloride content was determined on 20 samples taken from the concrete cover of pre-stressing bars of nearby panels of R1…R8 at the research object Raadi. Chloride content was determined by applying Quantab chloride titrator stripes.

2.5. Yield, ultimate strength and corrosion of steel

Six pre-stressing steel specimens of visually larger corrosion damage were cut from each panel. Specimens were cut to a length of 450 mm, cleaned and weighed. A percentage gravimetric mass loss of each pre-stressing steel sample was calculated. A mean gravimetric mass loss ($\Delta m_{gr,m}$) of six samples was found to show the mean corrosion penetration of pre-stressing bars of a panel. After mass loss determination, each pre-stressing bar was further inspected for evidence of pitting. However, no pits were found on the pre-stressing bars. At least 10 calliper gauge measurements were performed and a minimal diameter of each pre-stressing bar was recorded. A maximum diameter loss (Δd_{max}) out of six bars was calculated to represent the maximum corrosion penetration of pre-stressing bars of a panel.

All pre-stressing steel specimens were subjected to tensile testing. A universal testing machine R-20 (maximum capacity 200 kN) with the software for test data recording was applied. A mean yield ($f_{y,m}$) and ultimate strength ($f_{u,m}$) of six pre-stressing bars was calculated from test data.

3. Experimental results and discussion

3.1. Panels PNS-12

Results of flexural and material tests of 18 pre-stressed concrete ribbed panels PNS-12 are presented in Table 1. The control load (q_c) and the design load (q_d) for panels PNS-12 were set to 7.35 kN/m^2 and 4.51 kN/m^2, respectively [7].

Except for panel R2, the ultimate load (q_u) of all the panels PNS-12 were higher than control load and even for the R2 the capacity constituted 0.98 of the control load. The ultimate load of the studied panels PNS-12 constituted at least 1.60 of the design load. Table 1 shows that panel R2, with the largest initial mid-span deflection (Δ_{in}) of 53 mm, also had the lowest flexural capacity. Thus, visually detectable initial mid-span deflections of a panel could be a sign of decreasing flexural capacity. The mean yield strength of pre-stressing steel specimens of panel R2 was at least 53 MPa lower than that of other panels PNS-12. This could also have reduced the flexural capacity of R2, because most of the panels (including R2) were tested until deflections increased without further load, meaning that the pre-stressing steel of a panel had begun to yield.

A pre-stressing steel specimen no 3, cut from the mid-span of panel R1, was significantly more corroded (m_{red} = 19.6%, $d_{red,max}$ = 10.3%) and weaker (f_y = 458 MPa, f_u = 531 MPa) than any other specimen cut from panels PNS-12 (Table 1). The ultimate strength of pre-stressing steel of PNS-12 should be at least 539 MPa to correspond to its strength mark 35GS [7]. Except for specimen no. 3 from R1, the ultimate strength of all pre-stressing steel specimens from panels PNS-12 considerably exceeded their corresponding strength mark. However, the characteristics of that sample have not significantly reduced the flexural capacity (q_u/q_c = 1.14) of panel R1.

Sixteen panels PNS-12 had a flexural ductile failure, panel R7 had an anchorage failure and V8 failed in shear. The pre-stressing bars of PNS-12 are welded to the details at the supports of a panel (Section A–A in Fig. 2(a) [7]. During the failure of panel R7, the weld ruptured and the longitudinal pre-stressing bar slipped inwards at the support (Fig. 4). Panel R7 also showed a relatively low flexural capacity in comparison with the other panels. The ultimate load of R7 was registered shortly before weld rupture.

The critical shear crack of V8 started from the point of load application and ended at the lower end of the last stirrup (Fig. 5). No stirrups were in the critical shear crack, because the last stirrups ended at 1800 mm, and the point of load application was

Fig. 4. The support of panel R7 after anchorage failure.

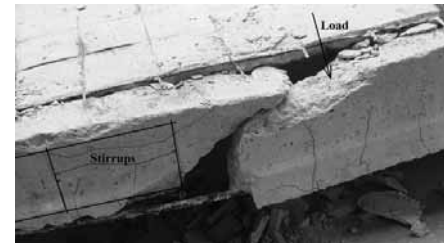

Fig. 5. Shear failure of panel V8.

1973 mm from the support (Fig. 2(a) and Fig. 5). Therefore, the shear resistance of V8 in the critical section depended only on concrete strength. Table 1 shows that the concrete strength of panel V8 ($f_{est,cube,m}$ = 18.4 MPa) was considerably lower than that of other panels of PNS-12. As mentioned earlier, the concrete strength of panels PNS-12 should be at least 19.6 MPa to be in accord with their strength mark [7]. Except for panel V8, the concrete strength of all panels PNS-12 substantially exceeded its strength mark (Table 1). Low concrete strength was probably the main reason for the shear failure of panel V8. This also explains why the cover of only V8 was fully carbonated ($D_{carb,m}$ = 24.7 mm > c_m = 24 mm). About one-third of the cover was carbonated on the other panels PNS-12.

The load–deflection curves of panels PNS-12, excluding and including initial deflection, are presented in Figs. 6 and 7, respectively. Curves with dashed lines indicate panels of spalled cover in the longitudinal rib. The authors managed to acquire several test documents of new panels (tested in the 1970s) from concrete factories in Estonia. The load–deflection curves of eight new panels, which conformed to the requirements [12] for PNS-12, are plotted with thick solid lines (Fig. 7). It should be noted that new panels were tested only up to the control load, i.e. until the strength requirement was met.

Fig. 7 shows that panels R2, R8 and V9 failed to meet the rigidity requirements, caused by their initial deflection of 18 mm or more. These panels also had a spalled cover. However, other panels with a spalled cover (e.g. panels V8, R1 and R6 in Figs. 6 and 7) met both strength and rigidity requirements. Fig. 7 also shows that the flexural behaviour of the analysed existing panels (which have been in service for at least 25 years) was not substantially different from the new panels PNS-12.

3.2. Panels PNS-14

Results of flexural and material tests of 10 pre-stressed concrete ribbed panels PNS-14 are presented in Table 2. The control load and

Table 1
Results of flexural and material tests of panels PNS-12.

Panel	Δ_{in} (mm)	q_u (kN/m^2)	q_u/q_c	Failure	$f_{est,cube,m}$ (MPa)	$D_{carb,m}$ (mm)	c_m (mm)	$f_{y,m}$ [*Min^n] (MPa)	$f_{u,m}$ [*Min^n] (MPa)	$\Delta m_{G,m}$ [*Max^n] (%)	Δd_{max} (%)
L1	NA	9.00	1.22	FD	37.6	NA	NA	605	652	8.7 [17.6^1]	6.3
L2	−15	9.20	1.25	FD	NA	NA	NA	NA	NA	NA	NA
L3	−19	9.25	1.26	FD	32.6	NA	NA	599	658	6.6	4.8
L4	−14	9.70	1.32	FD	NA	NA	NA	NA	NA	NA	NA
L5	−12	9.75	1.33	FD	30.6	NA	NA	624	674	7.3	5.1
L9	−21.5	9.04	1.23	FD	32.5	NA	NA	591	639	9.4	5.3
R1	−4	8.36	1.14	FD	45.4	11.8	32	537 [458^3]	646 [531^3]	9.7 [19.6^3]	10.3^3
R2	53	7.24	0.98	FD	47.1	NA	31	484	663	8.4	2.0
R3	−19	9.12	1.24	FD	41.6	10.1	30	605	723	5.9	0
R4	8	9.64	1.31	FD	34.7	9.9	24	539 [418^4]	681	8.4	2.0
R5	−10	9.86	1.34	FD	40.2	NA	33	582	702	7.1	1.0
R6	5	8.59	1.17	FD	41.7	8.8	31	547	695	5.1	0.7
R7	−1	7.91	1.08	WR	NA	NA	30	569	701	4.9	3.7
R8	34	8.28	1.13	FD	32.2	7.4	22	506	696	5.8	2.7
V8	−12	9.04	1.23	SH	18.4	24.7	24	620	699	NA	7.9^6
V9	18	10.53	1.43	FD	56.4	8.4	25	576	649	NA	3.4
V10	0.5	8.81	1.20	FD	43.7	9.7	27	576	636	NA	5.1
V11	−11	9.26	1.26	FD	45.8	8.6	24	566	661	NA	2.3

Note: NA = Result not available; Failure: FD = Flexural ductile, WR = Weld rupture at supports, SH = Shear; [*Min/Max] = shown if different from mean; []^n = no. of pre-stressing bar.

Table 2
Results of flexural and material tests of panels PNS-14.

Panel	Δ_{in} (mm)	q_u (kN/m^2)	q_u/q_c	Failure	$f_{est,cube,m}$ (MPa)	$D_{carb,m}$ (mm)	c_m (mm)	$f_{y,m}$[*Min^n] (MPa)	$f_{u,m}$[*Min^n] (MPa)	$\Delta m_{gr,m}$(%)	Δd_{max} (%)
L6	−18.5	16.95	1.20	FD	48.4	NA	NA	598	649	6.8	2.6
L7	0	13.56	0.96	WR	38.1	NA	NA	588	640	5.6	2.5
L8	7.5	10.17	0.72	WR	27.1	NA	NA	606	652	4.4	2.4
L10	−3	15.82	1.12	SH	35.3	NA	NA	585	642	7.2	3.6
V1	−4	15.2	1.08	FD	48.6	10.5	27	442 [302^6]	540 [369^6]	NA	1.6
V2	−5.5	14.82	1.05	FD	45.3	10.3	26	283	417	NA	1.6
V4	−3	11.36	0.80	FD	49.1	8.0	32	345 [267^1]	520 [401^1]	NA	2.1
V5	−5.5	13.80	0.98	FD	38.5	8.8	28	360	525	NA	2.6
V6	−8	12.17	0.86	FD	45.8	10.0	31	362 [255^3]	521 [427^3]	NA	0.5
V12	0	14.81	1.05	SH	42.7	11.7	20	552	616	NA	3.8

Note: NA = Result not available. Failure: FD = Flexural ductile, WR = Weld rupture at supports, SH = Shear; [*Min/Max] = shown if significantly different from mean; []^n = no. of pre-stressing bar.

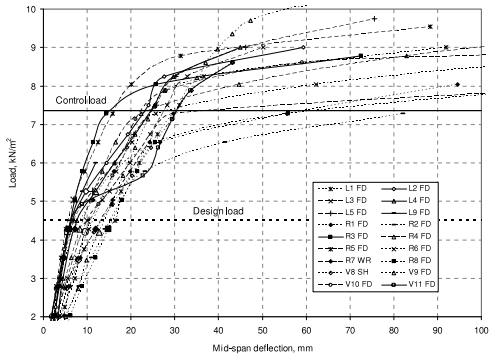

Fig. 6. Load–deflection curves of 18 panels PNS-12 excluding initial deflection. Large markers indicate load increment at which first flexural crack appeared. Failure: FD = Flexural ductile, WR = Weld rupture at supports, SH = Shear.

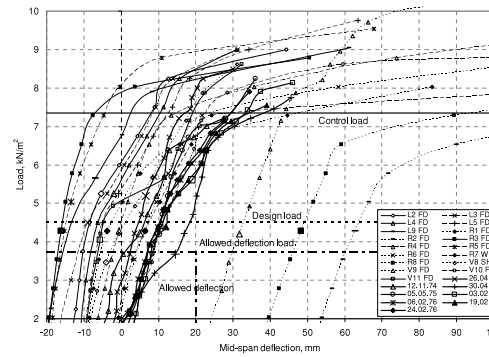

Fig. 7. Load–deflection curves of 17 panels PNS-12 including initial deflection. Thick solid curves denote new panels. Large markers indicate load increment at which first flexural crack appeared. Failure: FD = Flexural ductile, WR = Weld rupture at supports, SH = Shear.

the design load of panels PNS-14 was set to 14.12 kN/m^2 and 9.32 kN/m^2, respectively [7].

The ultimate load of five panels PNS-14 was less than the control load. The ultimate load of L7, V5 and V6 consisted of more than 0.85 of the control load, which would mean repetition tests for new panels issued from the factory. The strength of L8 and V4 was less than 0.85 of the control load. Hence, these panels failed to meet the strength requirements for new panels.

Nevertheless, the lowest ultimate load of panel L8 constituted 109% of the design load. That means that all analysed panels (both PNS-12 and PNS-14) have retained sufficient residual flexural capacity for design loads applied in service.

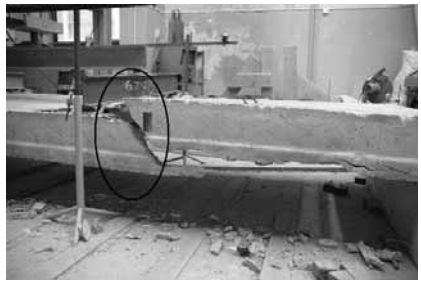

Fig. 8a. Shear failure of panel V12.

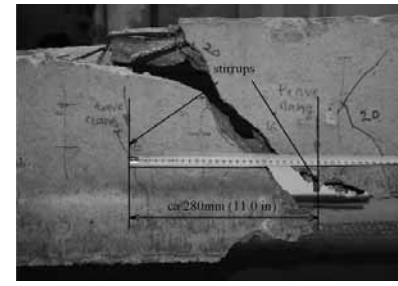

Fig. 8b. (b) Closer view of the shear crack in the longitudinal rib of panel V12.

Both yield and ultimate strength of pre-stressing steel specimens from panels V1 … V6 (test series 3) were low in comparison with other samples from panels PNS-14 (Table 2). The ultimate strength of pre-stressing steel 35GS (applied in PNS-14) should be at least 539 MPa [7]. The mean ultimate strength of pre-stressing bars from panels of test series 3 was on the verge (panel V1) or lower (panels V2, V4, V5, V6) than steel mark 35GS. The mean yield strength of pre-stressing bars from panels V1 … V6 was 442 MPa or less. Therefore, these pre-stressing bars would have started to yield under the pre-stress of 481 N/mm^2 for panels PNS-14 [7]. The visual condition of these panels was good and the corrosion level on the pre-stressing bars was insignificant ($d_{red,max} \leq 2.6\%$). Hence, probably the pre-stressing steel of an inferior strength mark was applied to the panels V1 … V6. This also explains the poor residual flexural capacity of those panels.

Seven panels PNS-14 had a flexural ductile failure. Panels L7 and L8 failed as a result of weld rupture at the support ends. As reported earlier, the ultimate load of both panels was less than the control load. The pre-stressing bar of panel PNS-14 was welded to the washer, which itself was welded to the detail at the support (Section B–B in Fig. 2(b) [7]. Therefore, the condition of anchorage (weld) should be checked at the support ends, because it could reduce the flexural capacity of a panel. The concrete strength mark of panels PNS-14 should be at least 29.4 MPa [7]. Except for panel L8 the concrete strength of all panels PNS-14 corresponded to (or exceeded) its strength mark (Table 2). Even the concrete strength of L8 ($f_{est,cube,m} = 27.1$ MPa) was not considerably lower than the strength mark for panels PNS-14. The mean gravimetric mass loss ($\Delta m_{gr,m} \leq 7.2\%$) and the maximum diameter loss ($\Delta d_{max} \leq 3.8\%$) of the pre-stressing bar sample cut from panels PNS-14 was not significant.

Both panels L10 and V12 failed in shear with a large inclined crack at the longitudinal rib starting from the point of load application (panel V12 in Figs. 8a and 8b). This type of failure can be accounted for by the loading arrangement involved. Former Soviet standard GOST-8829 [12] recommends a loading scheme of a concrete structure with a uniformly distributed load (Fig. 9(a)) and its equivalent load (Fig. 9(b)). An equivalent load with four equally concentrated loads can replace the uniformly distributed load if a total uniformly distributed control load exceeds 35 kN [12]. The bending moment (Fig. 9(b1)) and shear (Fig. 9(b2)) of equivalent load [12] (solid line) are compared to those of the current study (dashed line). Equivalent loading arrangement would result in half the shear stresses (P/4 in Fig. 9(b2)) as those (P/2 in Figs. 9(b2) and 3(e)) developed with the chosen loading arrangement at the section of load application.

The load–deflection curves of panels PNS-14, excluding and including initial deflection, are presented in Figs. 10 and 11, respectively. Fig. 11 shows that panels L8 and L10 just failed to meet the rigidity requirements set for the new panels of PNS-14 [7].

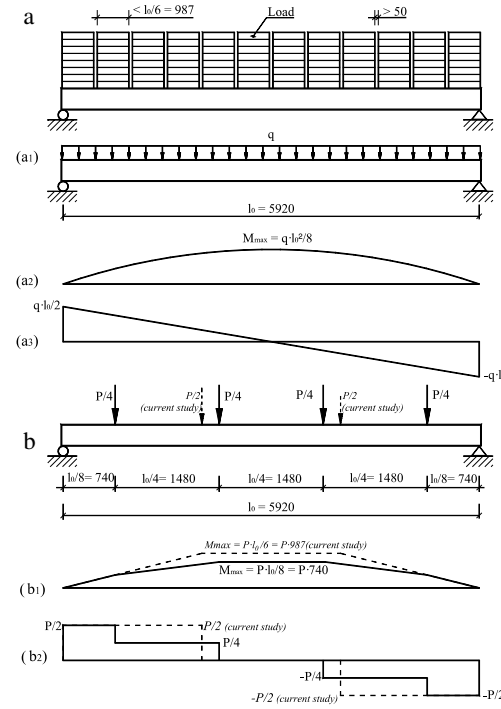

Fig. 9. Loading scheme of concrete structure [12] with (a) uniformly distributed load and (b) equivalent load with corresponding bending and shear diagrams. Dimensions are in mm.

3.3. Carbonation and chlorides

Except for panel V8, about one-third of the concrete cover of all studied panels was carbonated (Tables 1 and 2). The cover of the pre-stressing bar of V8 was fully carbonated because of its low concrete strength when compared to the other panels.

Chloride content was determined on 20 samples taken from the nearby panels of R1 … R8 at the research object Raadi. The mean chloride content was 0.20% with a minimum and maximum value of 0.15% and 0.22% by mass of cement, respectively. Chloride-induced corrosion can only take place once the chloride content in concrete in contact with the steel surface has reached a threshold value. The morphology of chloride attack is that typical of pitting

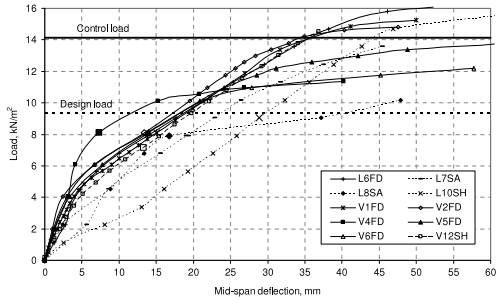

Fig. 10. Load–deflection curves of panels PNS-14 excluding initial deflection. Large markers indicate load increment at which first flexural crack appeared. Failure: FD = Flexural ductile, WR = Weld rupture at supports, SH = Shear.

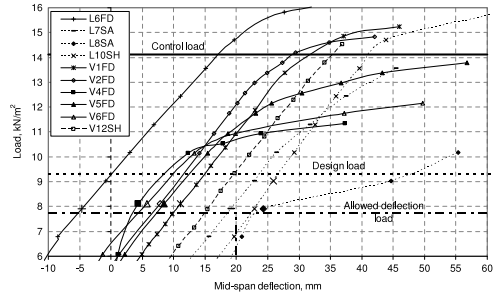

Fig. 11. Load–deflection curves of panels PNS-14 including initial deflection. Large markers indicate load increment at which first flexural crack appeared. Failure: FD = Flexural ductile, WR = Weld rupture at supports, SH = Shear.

or localised corrosion. However, no signs of pitting corrosion were found visually on any of the pre-stressing bars of panels studied. Tables 1 and 2 also show no serious local cross-section reduction ($d_{red,max} \leq 10.3\%$) of the studied pre-stressing bar samples. These results show that corrosion deteriorations in the studied panels were probably neither carbonation nor chloride induced.

4. Conclusions

This study presents the results of flexural and material tests of 28 existing pre-cast pre-stressed concrete ribbed panels, which have been in service for at least 25 years. Based on test results, the following conclusions were drawn.

1. Fifteen panels of the 28 conformed to the strength and rigidity requirements of new factory-issued panels. The flexural behaviour of the analysed existing panels was not significantly different from new panels.
2. The ultimate load of all studied panels constituted at least 109% of the design load. That means that all the analysed existing panels have retained sufficient residual flexural capacity to carry design loads applied in service.
3. It is likely that pre-stressing steel of an inferior strength mark was applied to panels V1 … V6 (PNS-14). Only this could explain the poor flexural capacity of those panels of good visual condition and insignificant corrosion level on pre-stressing bars.
4. Twenty-two of the 28 panels exhibited flexural ductile failure. Three panels failed as a result of an anchorage (weld) rupture and three panels failed in shear.
5. It is likely that the corrosion deterioration of the panels was neither carbonation nor chloride induced.

References

[1] Jin W-L, Chen J, Wu J-H, Zhang Y-Z, Tao Y-L, Wang H-W. Experimental study on flexural capacity of reinforced concrete beams in marine environment. J Zhejiang Univ (Eng Sci) 2004;38(5):603–9.
[2] Fan Y-F, Zhou J, Feng X. Prediction of load carrying capacity of corroded reinforced concrete beam. China Ocean Eng 2004;18(1):107–18.
[3] Wipf TJ, Klaiber FW, Ingersoll JS, Wood DL. Field and laboratory testing of precast concrete channel bridges. Transp Res Record 2006;1976:88–94.
[4] Zhang J-R, Li C-X, Wang L, Xu F-H, Yu X-M. Experiment and analysis on the ultimate strength of existing reinforced concrete arch rib. Eng Mech 2006; 23(12):136–42.
[5] Shdid CA, Ansley MH, Hamilton III HR. Visual rating and strength testing of 40-year-old precast prestressed concrete bridge piling. Transp Res Board 2006; 1975:3–9.
[6] Heymsfield E, Durham SA, Jones JX. Structural behaviour of short span precast channel beam bridges without shear reinforcement. J Bridge Eng 2007;12(6): 794–800.
[7] Series PK-01-111 Pre-stressed concrete ceiling panels of dimensions 1.5 by 6m. Construction drawings. Moscow: Central institute of typical design drawings; 1961. 20 p [in Russian].
[8] GOST 5058-65 Low-alloyed structural steel. Marks and general technical requirements. Moscow. 1965. 10 p [in Russian].
[9] Keskküla T, Miljan J. Bearing capacity of roofing slabs in cattle farm buildings after the end of service life Conc & Reinf Conc 1982;2:24–5 [in Russian].
[10] Laiakask E, Miljan J. Influence of steel reinforcement corrosion on the agricultural building reinforced concrete structure bearing capacity. In: Concrete for sustainable agriculture: agro-, aqua- and community applications. Ghent; 2002. p. 157–64.
[11] Miljan J, Keskküla T, Miljan R, Kiviste M, Laiakask E, Tomann H. Service life prediction of reinforced concrete structures damaged by deinforcement corrosion. In: CIB world building congress 2004 building for the future, 2004.
[12] GOST 8829-85 Concrete and reinforced concrete prefabricated constructions and products. Loading test methods and assessment of strength, rigidity and crack resistance, 1985 [in Russian].
[13] EVS-EN 12504-1:2003 Testing concrete in structures. Part 1: cored specimens. Taking, examining and testing in compression. Tallinn: Estonian Centre of Standardisation; 2003. 11 p [in Estonian].
[14] BS 6089:1981. Guide to assessment of concrete strength in existing structures. UK: British Standard Institution; 1981. 16 p.
[15] EVS-EN 14630:2006. Products and systems for the protection and repair of concrete structures. Test methods. Determination of carbonation depth in hardened concrete by the phenolphthalein method. Tallinn: Estonian Centre of Standardisation; 2006. 15 p.

III

Miljan, J., Keskküla, T., Miljan, R., **Kiviste, M.**,
Laiakask, E., Tomann, H. 2004.
SERVICE LIFE PREDICTION OF REINFORCED
CONCRETE STRUCTURES DAMAGED BY
REINFORCEMENT CORROSION.

CIB World Building Congress 2004.
Building for the Future, Toronto: 155-165.

SERVICE LIFE PREDICTION OF REINFORCED CONCRETE STRUCTURES DAMAGED BY REINFORCEMENT CORROSION

Jaan Miljan, Ph.D; Tõnu Keskküla, D.Sc.; Riina Miljan; Mihkel Kiviste; Erki Laiakask; Heiki Tomann[1]

Abstract

A structural assessment was performed on agricultural production buildings according to external (e.g. grade 5 means no visual deterioration and grade 0 shows that concrete cover has spalled) and internal (e.g. grade 20 means that concrete cover in not carbonized and grade 0 shows that concrete cover has spalled) characteristics. Based on latter data, a structural durability model was developed. This theoretical model describes structural serviceability from the point of construction (i.e. grade 20) until spalling of the concrete cover for reinforcement is evident (i.e. grade 0). Bearing capacity tests of prestressed ribbed panels having been assigned different grades were conducted to verify the reliability of the model. Highlighting on these grades is caused by change of appearance of structures in that stadium.

The focus of this paper is based on homogenous corrosion, which occurs after full carbonation of the concrete cover. There is no influence of chlorides in the structures investigated.

From the bending tests of corroded ribbed panels it was found that the corrosion-damaged structures met the requirement for the serviceability limit state i.e. they were strong enough not to exceed the maximum permissible deflection under test load. When the scale for characterising the degree of deterioration internally was compared to Tuuti's service life model (1982), it was shown that in terms of homogenous corrosion, a further use of these structures is still possible between grade 0 and an acceptable level of safety. Large deflections of reinforced concrete ceiling panels and beams inside agricultural buildings provide warning of potential safety concerns.

1. INTRODUCTION

In Estonia from the beginning of 1960s to the end of 1980s precast reinforced concrete structures (columns, beams, ribbed panels) were used in agricultural buildings. After a relatively short period of use, the initial signs of corrosion of steel reinforcement were evident. It was a common belief in the 1970s that reinforced concrete structures could endure until the concrete cover was fully carbonized. The level of knowledge at that time precluded taking into consideration corrosion of reinforcement in durability calculations (Alekseyev 1976). But there were structures, for example, in dairy-cattle farms, in which spalled concrete cover was evident but no significant reduction in bearing capacity was detected (Keskkula and Miljan 1982).

In Estonia, there are many similar agricultural buildings that have comparable structures and that are subjected to the same microclimatic conditions (about four thousand buildings each with a floor space of 2000 m^2 on average). If corrosion-damaged structures were considered to be unusable and needed repair or demolishing, then the potential economic damage could be significant. It was considered that provided the aesthetic appearance of the buildings allowed their continued use, the other limiting idea was to evaluate the structure's bearing capacity.

A method to assess the situation and predict the bearing capacity of existing structures was developed. If a corroded structure's actual bearing capacity is determined, essential conclusions can be made to predict the time until it reaches the limit for bearing capacity. This enables an owner to plan investments to either repair or demolish a building.

[1] J. Miljan is professor, Faculty of Rural Engineering, Estonian Agricultural University (EAU); T. Keskkula is professor, Faculty of Rural Engineering, EAU; R. Miljan is lecturer, Faculty of Economics and Social Sciences, EAU; E. Laiakask, M. Kiviste, and H. Tomann are Master students of EAU.

2. STRUCTURE'S SERVICE LIFE

2.1 Description of Typical Cowshed and Structures

Reinforced concrete cowsheds, of the type typically built in Estonia, have a partial or full reinforced concrete skeletal frame, a cross-section of which is presented in Figure 1. Usually the cowsheds have three naves and columns are erected using reinforced B20 and B25 class concrete columns with cross-section area of 240 by 240 or 300 by 300 mm^2. Precast B25 and B30 class reinforced concrete beams are used in the structures. The span of the beams ranges between 4 to 12 m. The ceilings are constructed using precast ribbed panels with the dimension of 1.5 by 6.0 or 3.0 by 6.0 m.

The Institute for Rural Building of Estonian Agricultural University (EAU) has gathered data describing the state of such agricultural buildings from 1974 to the present. There exist two sets of data: one the result of using a non-destructive method and essentially an survey of the exterior of the buildings, having a six-point estimation scale (ranging from 0 to 5), the other set containing data obtained using a destructive method on components of the structures, using a twenty-one-point estimation scale (ranging from 0 to 20).

The critical indicators of the structures observed by both methods are:

- Grade 1 –evidence of the occurrence of over 0.3 mm wide cracks in the reinforcement cover concrete, and
- Grade 0 – serviceability limit state– indicated by spalling of the reinforcement cover concrete.

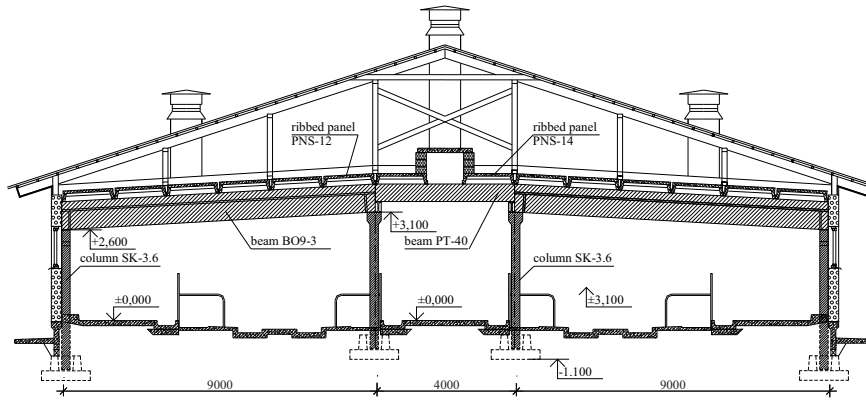

FIGURE 1. Cross-section of a reinforced concrete structure agricultural building

2.2 Methods and Predictions of Panel Visual Assessment

2.2.1 Scale for estimating degree of deterioration - The level of grade used to assess the degree of deterioration of the exterior of the buildings characterizes the changes in the functional state of the structure on basis of the state of all its steel reinforcement elements and their concrete cover established using a visual survey of the exterior elements of the building. The scale used in the survey for the different states of structural deterioration distinguishes six different states as shown in Table 1. The amount of stages of deterioration process on visual assessments was determined on special investigations. When demanding the probability 90% engineers can divide the deterioration process to 4 stages. Engineers with special experience may divide the deterioration process to 6 stages (Miljan 1977). The scale was set to indicate the linear decrease in residual service life.

TABLE 1.
Description of Deterioration States of the Ribbed Ceiling Panels

Grade	Description of state
5	No corrosion has been found
4	1) Less than 20% of the concrete cover of slab has spalled; 2) Noticeable longitudinal cracks (0.3-1.0 mm) in transverse ribs.
3	1) More than 20% of the concrete cover of slab reinforcement has spalled; 2) Less than 20% of the concrete cover of stirrups in the longitudinal ribs has spalled; 3) In transverse ribs wide (>1.0 mm) cracks have occurred; 4) Less than 20% of the concrete cover in transverse ribs has spalled.
2	1) More than 20% of the concrete cover of stirrups in longitudinal ribs has spalled; 2) More than 20% of the concrete cover of reinforcement in transverse ribs has spalled; 3) Longitudinal micro cracks (0-0.3 mm) due to corrosion in longitudinal ribs.
1	1) Longitudinal cracks (width > 0.3 mm) in longitudinal ribs;
0	1) Concrete cover of the reinforcement in longitudinal rib has spalled; 2) Serviceability limit state.

If only one characteristic of a lower grade can be determined during the inspection process, then this grade is assigned to the component. For example: there is no visual deterioration in the slab or longitudinal rib (may be nominally characterised Grade 3), but most of the concrete cover reinforcement in transverse rib has spalled. Since this latter characteristic is associated with Grade 2 (i.e. more than 20% of the concrete cover of reinforcement in transverse ribs has spalled), then Grade 2 is assigned.

Using this method, reinforced concrete structures were investigated in 258 different buildings over three different periods (i.e. 1974-75, 1978-79, 1995-97), giving values for 19486 ribbed ceiling panels. The in-service age of the structures investigated in this survey ranged from 1 to 32 years.

Changes in the condition of structures estimated by visual inspection are best described by the assessment of the different deterioration states of ribbed ceiling panels. This is caused by different thickness of concrete cover and diameter of reinforcement in slabs, transversal and longitudinal ribs. Statistical information was also gathered and used to determine key factors influencing the prediction results.

2.2.2 Lifetime Prediction - Regression Analysis - A general prognosis of the situation can be obtained by regression analysis using the mean data values of ceiling panels. The grade y of the ribbed ceiling panel corrosion is expressed in the equation of linear regression, where x is time

$$y = \alpha_1 x + \alpha_0 , \quad (1)$$

On average for ribbed ceiling panels and columns, the serviceability limit state (Grade 0) occurs in the sixty-second (62) year of exploitation and for beams in the one hundred and third (103). For the data set on ribbed ceiling panel, the regression line describes 30.6% of the coefficient of determination is approximately the same for columns and beams.

2.2.3 Lifetime Prediction - Generalised Linear Model (GENMOD) - The second lifetime prediction on the same data set was developed using the generalized linear model theory and completed using the SAS/STAT statistical software package. An attempt was made to predict the duration of the serviceability period for farm building structures before the structure weakens to a dangerous state. During the investigation of the reinforced concrete panels, several factors were taken into account. These factors include:

1. Type of building (on three levels: 1– usable high loft; 2– unusable low loft; 3– flat roof),
2. Type of enterprise (LL – dairy cattle stable; NK– young stock stable; S– pigsty),
3. Type of farm (79 different farms),
4. Region,
5. Size of the building, and
6. Type of panels.

Using the GENMOD Model (Miljan 1999) it is possible to establish the probability and time dependence of each grade for every different farm. "Critical" is the probability (summarized) of Grade 0 and Grade 1 forming a hazardous criterion for operation. For example, in Figure 2, 88% of ceiling panels of the Karstna farm are in the hazardous state (Grade 1 or 0) in its forty-seventh (47) year of exploitation. Whereas when the state of ceiling panels does not noticeably influence the bearing potential and stability of buildings, 20% probability is recommended. The 20% probability of a "critical" state for the Karstna farm is achieved at age 25-years.

The type of building, farm, and the location of the farm significantly influenced the condition of the reinforced concrete structures but that influence was much smaller than that due to the exploitation of age. The method developed to predict the condition state in structures allows a reasonable evaluation to be given for the critical state of cowsheds built of reinforced concrete in all 10 counties investigated.

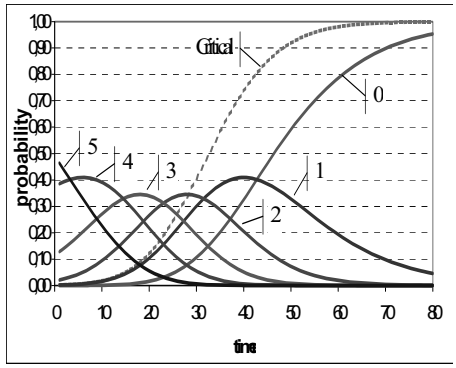

FIGURE. 2. Dependence of the probability of occurrence of different deterioration grades on the lifetime of ceiling panels at the Karstna farm.

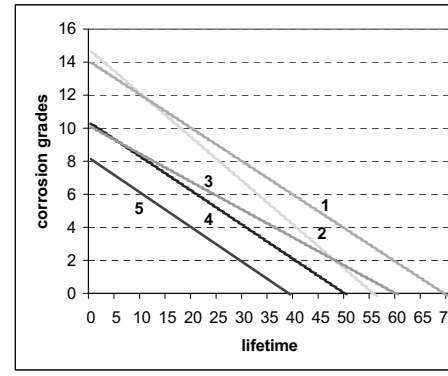

FIGURE 3. Deterioration of different structures on the basis of data obtained inside the buildings: 1 – beam, 2 – longitudinal rib, 3 – column upper end, 4 – column lower end, 5 – transversal rib

2.3 Assessment of Panels by Internal Grades

2.3.1 Complex Estimation Scale - In some sheds inspected using the external survey the reinforced concrete structures have been assessed using destructive methods. The data acquired using the destructive method gives more detailed information on the state of the structures.

Determining the carbonation depth of concrete and the thickness of concrete reinforcement cover in the same place we give the assessment to the state of reinforced concrete structures that will show us the relative carbonation on a 11-point scale (second column in Table 2). Grade 10 denotes uncarbonized concrete; Grade 0, completely carbonized concrete cover. Working steel reinforcement bars were exposed and assessed by an 11-point scale that is given in the third column of Table 2.

Summing up the grade of carbonation of cover and the grade of corrosion of steel bars we obtain a complex assessment of the state of corrosion in the structure (first column in Table 2) that, in turn, determines the state of the structure from its intact state to a state in which spalling of the cover is evident.

Of the 'livestock' farm buildings having different ages there were estimated 624 ribbed ceiling panels, 592 beams and 585 columns.

2.3.2 Lifetime Prediction with Regression Analysis - On the basis of data obtained inside the structures, predictions will be made to establish the occurrence of the pre-serviceability and serviceability limit states (Grades 1 and 0 respectively). Here regression analysis has been used with values of average structure grades and dispersion analysis that in addition to service life takes into consideration several other factors as well.

TABLE 2.
Grades of deterioration due to corrosion of Reinforcement Concrete Structures

Complex Corrosion Grades by Keskkula and Miljan (1977)	Relative Carbonation	Steel Grades (Oit and Ojamaa 1974)	Description of the State	Corrosion Stages (Tuuti 1982)
20	10	10	Cover is not carbonized	Initiation
19	9	10	Cover is 10% carbonized	
18	8	10	Cover is 20% carbonized	
17	7	10	Cover is 30% carbonized	
16	6	10	Cover is 40% carbonized	
15	5	10	Cover is 50% carbonized	
14	4	10	Cover is 60% carbonized	
13	3	10	Cover is 70% carbonized	
12	2	10	Cover is 80% carbonized	
11	1	10	Cover is 90% carbonized	
10	0	10	Cover is 100% carbonised, no corrosion	Depassivation
9	0	9	<20% dots of corrosion, < 3 mm;	Propagation
8	0	8	>20% dots of corrosion;	
7	0	7	<20% stains of corrosion, > 5 mm;	
6	0	6	>20% stains of corrosion;	
5	0	5	>80% corrosion;	
4	0	4	Full corrosion;	
3	0	3	Full corrosion, signs of the growing volume of corrosion products;	
2	0	2	Full corrosion, the corrosion products press into concrete;	
1	0	1	Cracks in the concrete cover in result of growing volume of corrosion products;	
0	0	0	Spalling of the concrete cover of reinforcement in result of reinforcement	

The dependence of the complex deterioration grade of structural corrosion *y* on exploitation time *x* is expressed as linear regression equation (1). As shown in Figure 3, as a result of regression analysis the prediction of the serviceability limit state for different types of structural components is different and ranges, for example, from 38.7 years, for a transversal rib, to 69.2 years for a beam. Although the prediction of the serviceability limit state of a transversal rib is chronologically closest to that of older farm buildings, its influence upon the serviceability limit state of the whole building cannot be taken into consideration because the load bearing capacity of the ribbed ceiling panel depends on the state of the longitudinal rib. We could consider that presently, the whole farm building reaches a serviceability limit state on average after 49.7 years (column lower end).

2.3.3 Lifetime Prediction - General Linear Model (GLM) - The SAS/STAT statistical software program was used to carry out a multivariate analysis using the procedure for general linear models GLM. In that analysis (Miljan 1999) the following factors were taken into consideration:

- Category of roof of the farm building,
- Category of farm,
- Measurement site inside the building
  - 1 and 3 – in the end of the building in the outer row,
  - 2 – in the center of the building in the outer row,
  - 4 and 6 – in the end of the building in the middle row,
  - 5 – in the center of the building in the middle row
- Thickness of concrete cover (as constant factor), and
- Exploitation age.

Different factors turned out to be significant to different structures. In its generalized form the corrosion grade can be calculated using the following equation:

$$y = \beta_0 + \beta_2 + \beta_3 + \beta_4 x_1 + \beta_5 x_2 + \beta_6 \qquad (2)$$

The corrosion assessment of all structures depends on their service life. In addition, the assessment of the lower column ends depends on the farm-building category - the corrosion assessment for byres is noticeably higher than for pigsties or sheds that house young cattle. The corrosion assessment of beams and the upper ends of columns in addition to the exploitation time depends on the thickness of the protective layer. But the corrosion assessment of longitudinal ribs depends on the location where measurements are taken, i.e. near the walls the corrosion process is slower than in the middle of the building. The measurement site 1 differs significantly from sites 4 and 5 (in the middle and at the end of the central row). Measurement site 2 also differs from site 5 and site 3 differs from all the measurement sites in the central row (4, 5, 6). In all cases there was no clear connection between assessment of construction and building roof type.

2.4 Theoretical Model of Bearing Capacity Reduction of Columns, Beams and Ribbed Panels

Considering that the corrosion rate can reach up to 120 to 150 μm per year (Ostrovsky, 1984) and using the values for predicting a serviceability limit state, based on regression analysis, we can present the time dependence of the bearing capacity of reinforced concrete structure as shown in Figure 4. This gives a working hypothesis for further experimental studies. We can see that the axial bearing capacity of a column after reaching the serviceability limit state is about 0.25-1% per year and reaches the residual value of 55% i.e. the load is carried by the concrete alone. The column's bending capacity decreases about 0.25-2% per year. After a serviceability limit state is reached, the decrease in bending capacity is about 2-2.5% for ribbed panels, and about 2% for beams. We can add new points to the graph by testing the bearing capacity of reinforced concrete structures at different corrosion levels.

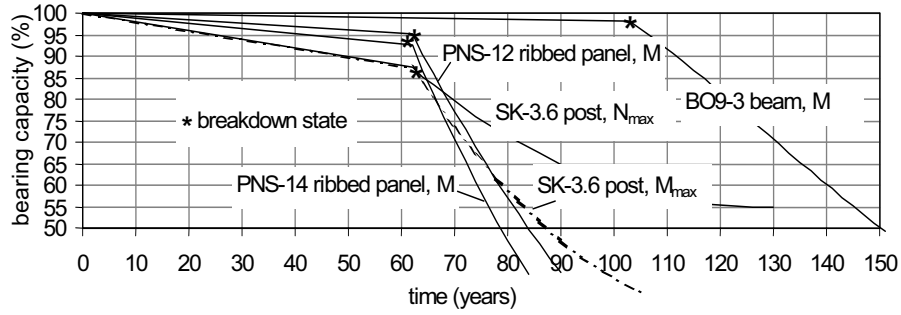

FIGURE 4. A theoretical model describing the decrease in bearing capacity of the most common reinforced concrete structures used in agricultural buildings (Laiakask and Miljan 2002). After serviceability limit state a corrosion rate of 125μm per year is assumed (Ostrovsky, 1984).

2.5. Determination of the Bearing Capacity of Panels

2.5.1 Methods. During the bending test we followed the method worked out at the Institute for Rural Buildings; the equipment was designed and constructed specifically to perform this testing. While executing the bending test we measured vertical displacements of a ribbed panel. For this purpose we used compliant measuring gauges (precision 0.1 mm) in the middle of ribbed panels and indicator gauges (precision 0.01 mm) at the corners. To measure displacements it is necessary, first, to fix the deflection of a ribbed panel. The pre-stressed ribbed panel is loaded step by step.

The compressive strength of the concrete was determined by universal testing machine type P-20. From each panel, 6 test specimens from the main reinforcement were tested. The same testing machine

(P-20) was used to measure the breaking force of the reinforcement. From this, the characteristic yield strength was calculated.

2.5.2 Results - Visually, all prestressed ribbed panels (PNS-12) were in poor condition. According to the visual assessment scale, most panels scored either 1 or 0 points. This meant that the longitudinal rib of the ribbed panel had noticeable cracks, of widths >0.3mm (estimation point 1). Estimation point 0 meant that in many places, the main reinforcement of the ribbed panel had not any remaining concrete cover. The purpose of the bending test was to find out if the panels were capable of sustaining the design load.

As a result we concluded that the panels graded with 1 estimation point exceeded their designed bending strength by 20% and the panels graded with 0 estimation point by 10% (Figure 5).

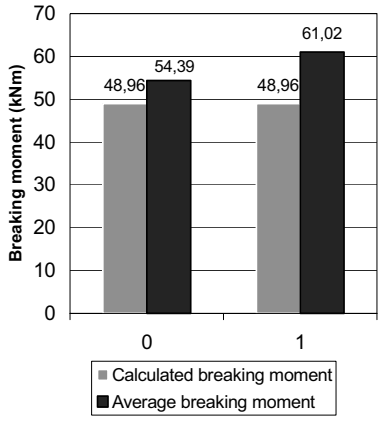

FIGURE 5. Average breaking force (kN m) Depending on grade of estimation points

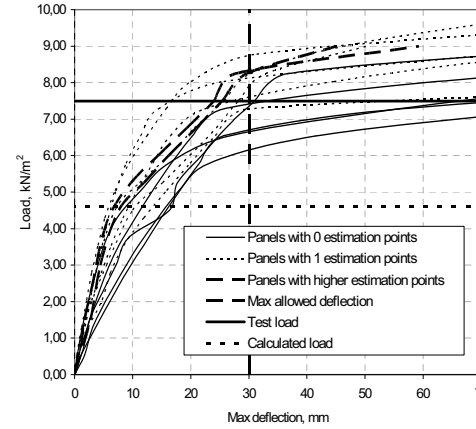

FIGURE 6. Dependence of deflection of PNS-12 panels with different estimation points on magnitude of load

Thus all the panels were in accordance to the ultimate limit state. At the same time they must meet the requirements of the serviceability limit state. According to the limit state for deflection, the vertical displacements should not exceed 1/200 of the span (i.e. 30 mm in our case) on the calculated load.

As we can see from the Figure 6 (so-called panel stress-strain diagram) all panels meet the requirement of serviceability limit state. Most of the panels (except with 0 estimation points) were strong enough not to exceed the maximum allowed deflection in a test load. As well, on average, the panels visually graded with 1 estimation point or higher were more persistent than panels graded with 0 estimation points. The test results also showed that the bearing capacity of the panels graded with 2 to 5 estimation points was sometimes equal with that of the panels graded with 1 estimation point. This phenomenon can be accounted for by the fact that the bearing capacity of a ribbed panel starts to decrease significantly when there are big cracks in the protecting concrete cover and the cover starts to fall off (i.e. between 1 and 0 estimation points).

2.5.3 Strength characteristics of concrete and steel - As shown in Figure 7, the strength of concrete, measured in tests, is significantly higher than the one prescribed in the design of the structure. Thus, we can assume that the compressive strength of the concrete situated in chemically aggressive surroundings has not decreased. The designed yield strength of the main reinforcement of a PNS-12 panel is 550 MPa (Figure 8).

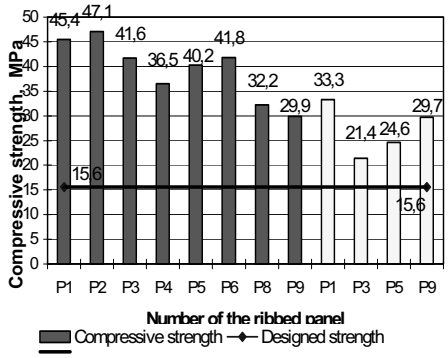

FIGURE 7. Mean compressive strength of concrete test samples (dark columns 2002 test results; light columns previous results of 1999)

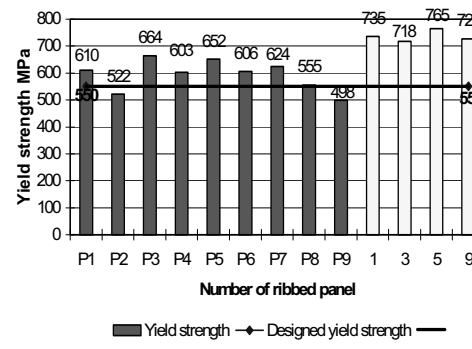

FIGURE 8. Mean yield strength of the main reinforcement (dark columns test results for 2002, light columns previous results for 1999)

The results of the tensile tests show that the yield strength of nearly all the tested reinforcements is higher than is assumed in the design of the agricultural buildings. However, the steel reinforcement for panels P2 and P9 are still under the designed yield strength. When comparing our test results to those obtained previously in 1999 it seems that tests of reinforcement steel undertaken in 2002 were lower. This trend, however, was not evident from the results of bending tests.

2.6 Service Life Prediction of a Structure

2.6.1 Service Life Determined by Corrosion Stages. The most well-known service life model for concrete reinforcements is that Tuuti published in 1982. From this work it is understood that service life may be divided into stages: an initiation period and propagation period. The initiation period comprises the time taken by aggressives (chlorides or carbonation) to reach the reinforcement and depassivate the steel. The propagation stage is when steel starts to corrode and corrosion products cause cracking and spalling. Eventually a situation is reached, defined as the end of service life, when either repair or demolition must take place. Alekseyev (1976) has indicated that there is a depassivation period that exists between the initiation and propagation phases. Broomfield (1997), likewise includes an additional period but refers to it as an 'activation' stage.

Since there is no evidence of chloride attack in the agricultural buildings we investigated, carbonation in concrete is then the rate-determining parameter during the initiation period. The initiation period is comprised in our internal assessment scale by grades from 20 to 11, as shown in Figure 9. Grade 10 is equal to depassivation period and Grades from 9 to 0 are a part of the propagation period. Grade 1 is when cracks occur in the concrete cover of the main reinforcement. Grade 0 is a situation, when spalling of the concrete cover is evident. Further investigations are required to show the length of period r (Figures 9 and 10) from Grade 0 to the end of the service life. Period r depends on the reduction in cross-section of the steel reinforcement.

2.6.2 Service Life Determined by Bearing Capacity - The deterioration of reinforced concrete structures in agricultural buildings starts with concrete carbonation. Tests have shown that carbonated concrete is not weaker than normal concrete. It could be even stronger and therefore could theoretically increase the structure's bearing capacity. When the concrete cover is fully carbonized the steel reinforcement starts to corrode. Even if a crack occurs in the concrete cover (Grade 1) or the concrete cover has spalled (Grade 0), the bearing capacity of a structure is not reduced to a limit state (acceptable level) (Figure 10).

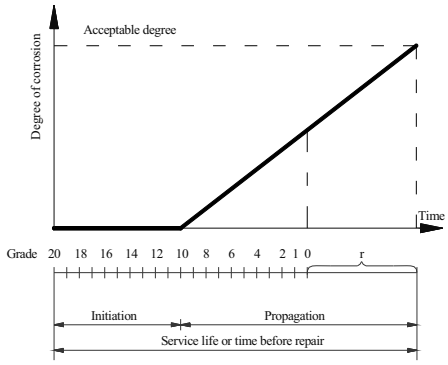

FIGURE. 9. Service Life Model for Reinforcement Corrosion (Tuuti 1982; Miljan 1977)

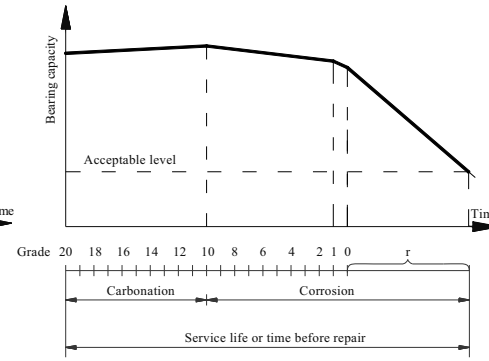

FIGURE 10. Service Life Model for Bearing Capacity

3. DISCUSSION

3.1. Different grade systems and their comparison

There are quite similar problems caused by corrosion in Japan (Yoshifumi et al. 2002). Some of the reinforced concrete structures built for the railway in the 1970s began to show signs of early deterioration in less than 30 years from the time the structures were built. In June and October 1999, there were two cases of accidents caused by concrete pieces falling from tunnel lining surfaces. Results from a report presented by an Investigation Committee showed that, amongst other measurements, the degree of corrosion in the reinforcing steel, evaluated by observing the embedded reinforcement after removing the cover concrete, could be evaluated on a 6-level scale (see Table 3).

TABLE 3
Degree of Corrosion in the Reinforcing Steel

Corrosion level	Evaluation standard
0	Conditions at time of construction maintained and no subsequent corrosion seen
1	Light corrosion seen over the partly of the surface
2a	Corrosion seen over the majority of the surface
2b	Loss of cross-section seen over the partial surface
3	Loss of cross-section seen over the entire surface
4	Loss of cross-section is 1/6 or more

If this evaluation standard is compared to the Steel Grades (Oit and Ojamaa 1974) it is evident that the corrosion level given in Table 3 equals Grade 10. The corresponding grade for corrosion level 1 is 7 or 8 and for 2a is Grade 5. Further comparison is disputable, since different factors are used as an indicator: loss of cross section and corrosion products (and their results). From an empirical point of view, corrosion level 2b could be equivalent to Grade 2, corrosion level 3 to Grade 0 and corrosion level 4 would be out of scale and somewhere in the negative values. This indicates that corrosion grades need further development. The addition of new grades describing the loss of cross-section of reinforcement could be a solution.

3.2 Corrosion rate

According to Alekseyev (1976), the corrosion rate in all metals is approximately 50 μm per year. The rate depends on the acidity, temperature and humidity of the environment. If the decrease in bearing capacity of reinforced concrete structures is to be estimated, it is reasonable to investigate its time

dependence. In instances where the surroundings are sufficiently humid, the corrosion rate of the reinforcement in carbonated concrete ranges between 20 to 25 μm per year (the reinforcement diameter loss per year is 0.04 to 0.05 mm; Ostrovsky 1984). The corrosion rate of such order results in a relatively rapid formation of longitudinal cracks in the concrete cover. The increase in volume of corrosion products causes further widening of cracks. In the region of a crack, the corrosion rate reaches up to 120 to 150 μm per year (Ostrovsky 1984). So it is reasonable to suggest that that in case of a deteriorated concrete layer, an estimate of the decreases in diameter of reinforcement could be 1 mm in 7 to 8 years.

Rodriguez et al. 2002 have developed an equation to find the loss of reinforcement radius caused by corrosion:

$$P_x = 0.0116 \cdot \alpha \cdot I_{corr} \cdot t \qquad (3)$$

Where P_x is the loss of reinforcement radius,

α is the pitting factor, which takes into account the type of corrosion, if it is homogeneous $\alpha = 2$ and localized (usually chloride induced) $\alpha = 10$,

I_{corr} in measured corrosion current, and

t is time since the corrosion started.

4. CONCLUSIONS

Our tests have shown that a ribbed concrete panel (which has greatest degree of deterioration due to its' thin concrete cover), even after having attained a deterioration level of Grade 0, has nonetheless retained sufficient bearing capacity. This means that is still possible to obtain further use (and longer service life) of agricultural buildings that have reached a deterioration level of Grade 0 possibly for many years. However, establishing the length of this period will (Figure 10) require additional research.

The reduction of bearing capacity of reinforced concrete structures is mainly caused by a loss of reinforcement cross-section albeit the loss in reinforcement cross-section is difficult to observe and assess visually. Bending elements indicate insufficient bearing capacity at large deflections (and therefore a safety concern), which further clearly indicates that the structure needs to be repaired or demolished.

5. REFERENCES

Alekseyev, S. N., and N. K. Rozental 1976. Corrosion durability of reinforced concrete structures in industrial environment (in Russian)., p. 205 Moscow: Stroiizdat.

Broomfield, J. P. 1997. Corrosion of Steel in Concrete: Understanding, Investigation and Repair, p. 264 Routledge.

Keskkula, T.E., and J.A. Miljan 1982. A bearing capacity of roofing slabs in cattle farm building after the end of service life (in Russian). Concrete and reinforced concrete. No 2. pp. 24-25.

Laiakask, E., and J. Miljan 2002. Influence of steel reinforcement corrosion on the agricultural building reinforced concrete structure bearing capacity. Concrete for Sustainable Agriculture. Agro-, Aqua- and Community Applications, Belgium: Ghent. pp.157-164.

Miljan, J. 1977. Full scale examination of the condition of reinforcrd concrete constructions in livestock buildings. Reports of Estonian Agricultural Academy. pp 26-32.

Miljan, R. 1999. The Economical Efficiency of Reproduction of Cowsheds. Master's Thesis (in Estonian). Tartu, 92 pp.

Oit, I., and E. Ojamaa 1974. Is steel in concrete always protected from corrosion? (in Estonian) Technics and Production. No. 7, pp. 358-360.

Ostrovsky, A. B. 1984. The durability of concrete and reinforced concrete structures in agricultural buildings (in Russian) p. 45 Moskow.

Rodriguez, J., L. Ortega, and D. Izquierdo 2002, Detailed assessment of concrete structures affected by reinforcement corrosion, Proceedings of the First FIB Congress 2002, Andrade, C. Ed., Osaka, Japan, pp. 57-64.

Tuuti, K. 1982. Corrosion of steel in concrete. CBI Research. Stockholm.

Yoshifumi, M., A. Satoshi, and K. Yukio 2002, Evaluation of strength and maintenance methods for railway reinforced concrete structures with aged deterioration. Proceedings of the First FIB congress, Osaka, Japan, 20 pages.

IV

Kiviste, M., Miljan, J., Miljan, R., Kiprušenkov, M.† 2009.
CONDITION OF STRUCTURES AND
PROPERTIES OF CONCRETE OF AN
EXISTING OIL SHALE CHEMICAL PLANT.

Oil Shale 26(4): 513-529.

Oil Shale, 2009, Vol. 26, No. 4, pp. 513–529
doi: 10.3176/oil.2009.4.07
ISSN 0208-189X

CONDITON OF STRUCTURES AND PROPERTIES OF CONCRETE OF AN EXISTING OIL SHALE CHEMICAL PLANT

M. KIVISTE[(a)*], J. MILJAN[(a)], R. MILJAN[(b)], M. KIPRUSHENKOV[(a)]

[(a)] Institute of Forestry and Rural Engineering, Estonian University of Life Sciences, Kreutzwaldi 1, Tartu 51014, Estonia
[(b)] Institute of Economics and Social Sciences, Estonian University of Life Sciences, Kreutzwaldi 1, Tartu 51014, Estonia

A case study for investigating the condition of concrete structures and properties of concrete of an existing oil-shale chemical plant is presented. The condition of concrete structures in the plant (constructed in 1951) was assessed visually on a six-point scale. It was found on visual inspection that concrete structures with cracked or spalled concrete cover need extensive repairs. Compressive strength of cores, carbonation depth, cover, water absorption as well as sulphate, chloride and nitrate content in concrete were determined. According to the results suggestions were proposed to repair deteriorated concrete structures in the plant.

Introduction

The production of oils alternative to petroleum has received worldwide attention in regards to increasing prices of fuel. One of these alternatives is producing oil from oil shale. The production of oil shale oil is successfully competing with oil products and is gaining growing significance [1]. The production of oil from oil shale is now developed in China [2], Bulgaria [3], Brazil, Jordan, Australia, etc.

The effects of pulverized-fired oil shale on the technological equipment in Estonian power stations have been studied in companies involved in production of oil shale. High-temperature corrosion resistance of a number of boiler steels was tested experimentally in laboratory and industrial conditions in the presence of chlorine-containing external deposits [4-6].

However, the deterioration of concrete structures and infrastructures is also a widespread problem in many countries. In order to assess such structures for

* Corresponding author: e-mail *mihkel.kiviste@emu.ee*

continued future service, simple and practical tools need to be developed for evaluating their reliability and performance. Several studies have been dealing with condition and reliability assessment of concrete structures in nuclear power plants [7–9] or bridges [10–12]. However, no attention has been given to the effects of the gases and phenols that arise from oil shale retorting on the load-bearing concrete structures of a chemical plant. The aggressive environment inside the plants, which manufacture shale oil could affect adversely to the material properties and structural capacity inside the building. The residual flexural and shear capacity of the concrete load-bearing structures in the studied plant was determined analytically earlier [13]. This paper presents a case study for investigating the condition of concrete structures and properties of concrete of an existing oil-shale chemical plant.

In order that structural condition be predictable the defining attributes and properties must be quantifiable [14]. For that reason visual inspection of load-bearing concrete structures in the plant was performed. Also, on the basis of visual assessment concrete structures with most severe deterioration were located for subsequent investigation. The deterioration mechanism is analytically divisible into two factors that combine to produce a specific mechanism: 1) the inherent properties of the specific material or system and 2) the atmosphere or environment in which those properties are operating [14].

Compressive strength as the most important property of concrete has been studied in most detail. With respect to durability, carbonation depth, cover, chloride, sulphate and nitrate content and water absorption of concrete were determined in order to have an overview of the inherent properties of concrete.

A brief description of the present and past situation of the indoor environment near generators of the plant is provided. It was found that serious deterioration of load-bearing concrete structures in the studied oil plant building may originate already from the 1950-ies. At that time due to different production technology slag was removed from all generators each day. The columns and beams were exposed to a large concentration of gases exiting through the hatches of a generator during slag removal.

According to the results suggestions are proposed to repair deteriorated concrete structures in the plant.

General description of the generator building

The studied generator building is located in North-Eastern Estonia. The seven-storied building measuring 64 × 15 m has been almost constantly in service since the construction in 1951. The generator processes 1.4 million tonnes of oil shale every year. Oil shale is processed in the plant's generators to produce shale oils, fuel oils and resins. There are 12 generators in the plant. The flow sheet of generator involves transportation of oil shale to the bunkers located in the upper part of the building from where it is led to the

generator. In the generator shale oil is separated by the process of retorting. The generators are continuously filled and emptied. The vertical position of the generators allows them to empty by gravity pull. The conveyor under the generator leads semicoke out of the building. The structures carrying generator are located on the 1st and 2nd floors. As semicoke exits the generator immediately after burning, it is quenched with water which produces a lot of gases (Fig. 1).

The mixture of gases contains carbon dioxide (CO_2), sulphur dioxide (SO_2), hydrogen sulphide acid (H_2S), phenols, aliphatic hydrocarbons, methane, ethane, propane, butane, etc. According to classification [15] these gases are of type I and II, which react with $Ca(OH)_2$ to neutralize concrete or produce salts. These salts generate III type of corrosion, which damage the structure of concrete [16].

The conveyor is located on 1st floor extending across the full length of the building. The columns and beams on the 1st and 2nd floors are directly exposed to the gases from the conveyor since the 1st floor is only partially separated from the 2nd floor by a concrete ceiling. The condition of several columns and beams on the 1st and 2nd floor has raised a concern on the durability of those structures.

The cooling of the processed oil shale takes place on the 3rd floor. There is no leakage of gases on the 4th, 5th, 6th and 7th floors. Oil shale is loaded from the bunker onto the generator on the 6th floor. On the 7th floor oil shale is loaded onto the bunker.

The bearing structures of the generator building perform as a monolithic concrete frame the columns of which are made of concrete mark M110 (10.8 N/mm^2) and beams are made of concrete mark M140 (13.7 N/mm^2). Steel reinforcement of class A-I (smooth, yield strength 210 N/mm^2) has been applied both in the beams and columns.

Fig. 1. Concrete structures exposed to the gases generated in water quenching of semicoke.

Experimental and analytical methods

Visual inspection, concrete tests and chemical analysis were performed from February to December 2006. Additional cores were drilled and tested in April 2009.

Visual inspection

The purpose of visual inspection was to: 1) classify the structures according to visually discernible corrosion damage and 2) point out the structures with most severe deteriorations. The elements of the monolithic concrete frame were assessed as individual structures. All concrete columns and beams in the plant were assessed visually on a six-grade scale (Table 1) developed at the department of Rural Building of Estonian University of Life Sciences in the 1970-ies. Grades reflect visually discernible changes in the functional state of the structures on the basis of the condition of steel reinforcement and concrete cover. If even one feature of a lower grade can be determined during the inspection process, this lower grade is assigned to the structure.

Table 1. **Classification of deterioration states of concrete beams and columns [17]**

Grade	Description of condition
5	No corrosion detected
4	Less than 20% of stirrups are corroded (cracks or spalled concrete cover)
3	More than 20% of stirrups are corroded
2	Micro-cracks (width 0-0.3 mm) in the concrete cover of the main reinforcement
1	Cracks (width >0.3 mm) in the concrete cover of the main reinforcement
0	Concrete cover of the main reinforcement has spalled

Compressive strength of concrete cores

The concrete core test was based on Estonian National Standard EVS-EN 12504-1:2003 [18]. In order to determine the compressive strength of concrete 55 cores with diameter of 75 mm were drilled from columns and beams. 36 cores were acquired from the 1st floor (columns) or the 2nd floor (beams) where highest structural loads and most deteriorated structures were present. Cover meter was applied to locate the reinforcement in the structure before drilling. This generally enabled extraction of cores from a such location that they contain no reinforcement.

After that the non-destructive rebound hammer test was conducted. However, the methods and results of the rebound hammer test in this study are omitted. The reasons are briefly stated in discussion.

Cores were cut by means of a rotary cutting drill with diamond bits. The device was properly attached to the beams and columns to prevent shaking during drilling. In this manner, cylindrical specimens were obtained which were marked, brushed with phenolphthalein solution for carbonation depth measurements and transported to testing laboratory. The authors managed to

acquire 29 cores from columns and 26 cores from beams. The ends of cores were ground or capped with rapid-hardening cement. Each core was measured in accordance with EVS-EN 12504-1:2003 [18]. Mean cross-sectional area was calculated from five diameter measurements, and the mean height of core was calculated from five height measurements. The core was tested according to EVS-EN 12390-3:2002 [19]. The estimated cube strength ($f_{est.cube}$) was calculated by applying the following equation (1) in BS 6089:1981 [20]:

$$f_{est.cube} = \frac{D}{1.5 + 1/\lambda} \cdot f_{core}, \quad (1)$$

where

D is 2.5 for cores drilled horizontally (perpendicular to cast direction), or D is 2.3 for cores drilled vertically (parallel to cast direction),

λ is the height/diameter ratio, and

f_{core} is found by dividing the maximum load sustained by the core to its average cross-sectional area.

Cores with height/diameter ratio 1 were tested, because cylinders with this ratio have very nearly the same strength as standard cubes [18]. The estimated cube strength was compared to concrete mark from design drawings to verify if the columns and beams were built in accordance with the drawings. Concrete mark (operative until 1984) was calculated as a mean compressive strength of standard cube specimens of side 150 mm in kg/cm^2.

Carbonation depth and cover of concrete cores

Carbonation depth test by the phenolphthalein method was based on EVS-EN 14630:2006 [21]. Phenolphthalein, when applied to the freshly opened surface of concrete turns non-carbonated concrete red, and remains colourless in carbonated concrete. Testing was undertaken by applying a phenolphthalein solution to a freshly drilled surface of concrete cores *in situ*. Carbonation depth was measured by means of a ruler on 10 locations of the core. Carbonation depth measurements should be taken only on the hardened cement paste (not on a place of large piece of aggregate) of the core.

Concrete cover was also measured by means of a ruler on 10 locations in core hole. In most cases the core hole had to be widened to find the nearest reinforcement. Carbonation depth and concrete cover were measured on 19 randomly chosen cores and core holes, respectively.

Chemical analysis of concrete cores

In order to have an overview of deleterious salts in concrete an chemical analysis was performed. After compression test three cores extracted from the beams carrying generator (on the 2nd floor) were sent to the Remmers chemical laboratory by the company REV Special OÜ. From these cores samples were obtained for quantitative analysis of water soluble salts. With respect to durability sulphate, chloride and nitrate content were determined as

a percentage of mass of concrete samples. The analysis was performed following German standard DIN 51100 [22].

Water absorption of concrete

In order to determine the water absorption of concrete ten samples were extracted from the columns on the 1st floor. Soviet standard water absorption measuring method [23] was applied since the building was constructed in 1951. Samples were immersed in 20 °C water and weighed every 24 hours until a constant value was reached. After that, samples were oven-dried until reaching a constant dry mass. Water absorption was found with the formula (2):

$$W = \frac{m_H - m_0}{m_0}, \tag{2}$$

where W is the water absorption (%),
m_H is the mass of a water-saturated sample (g), and
m_0 is the mass of a dried sample (g).

Results and discussion

Visual inspection

The condition of each column and beam in the plant was carefully assessed visually. The summary of visual assessment of beams and columns on different floors is presented Table 2.

Table 2 shows that the condition of beams is somewhat worse than that of the columns – the beams on floors 2–4 operate with spalled concrete cover. However, columns with spalled concrete cover are located on floors 1–3. Probably, the condition of beams is worse because they are more exposed to aggressive gases and nearer to the generator. On the upper floors of the generator building the concentration of gases is less intense and the temperature is lower. On the basis of visual assessment concrete structures with most severe deterioration were located for subsequent investigation.

Table 2. **Visual assessment grades of reinforced concrete members**

Floor no.	Mean grade of beams	Mean grade of columns
1	–*	0
2	0	0
3	0	0
4	0	3
5	3	3
6	4	4
7	5	5

* There are no beams on the 1st floor

From the structures to which grade 0 was assigned the beams carrying generator on the 2nd floor were in the worst condition. Numerous visually discernible structural deteriorations occurred on those girders and joists. For example, the concrete cover of tensile (but sometimes also neutral or compressive) reinforcing bars has spalled (Fig. 2–3), many stirrups are loose or broken (Fig. 2–3), concrete is delaminated (Fig. 3) or containing incompatible aggregates such as brick pieces etc. (Fig. 2). Due to uniform corrosion the cross-section of longitudinal rebars was not reduced considerably.

Fig. 2. Bottom view of a girder fragment carrying generator on the 2nd floor.

Fig. 3. Bottom view of a joist fragment carrying generator on the 2nd floor.

The columns on floors 1–3 and beams on floors 3–4 received also grade 0 i.e. operate with spalled concrete cover. Their condition was slightly better in comparison with beams carrying generator on the 2nd floor.

In general, concrete structures with cracked or spalled cover (grade 1 and 0) need extensive repairs from the owner of the building. Cracked or spalled concrete cover does not serve its function of providing fire and corrosion protection as well as bond to the reinforcement. Loose stirrups have to be reattached or replaced during repairs to restore the initial shear capacity of beams on the 2nd floor.

Compressive strength of concrete

The results of compressive strength of 55 cores acquired from columns and beams are presented in Fig. 4 and Fig. 5, respectively.

The mean core strength (derived to the mean estimated cube strength) drilled from columns (in Fig. 4) was 15.8 N/mm^2 with the standard deviation of 6.9 N/mm^2.The mean core strength drilled from beams (in Fig. 5) was

18.3 N/mm^2 with the standard deviation of 4.4 N/mm^2. The mean core strength of cores drilled both from columns and beams exceed the Soviet compressive strength marks M110 (10.8 N/mm^2) and M140 (13.7 N/mm^2), respectively. It should be mentioned that Fig. 4 and Fig. 5 present the compressive strength of unbroken cores only. Eight cores broke during drilling as a result of cracks or large voids (e.g. core 13* in Fig. 6) and could not be repaired for compressive test.

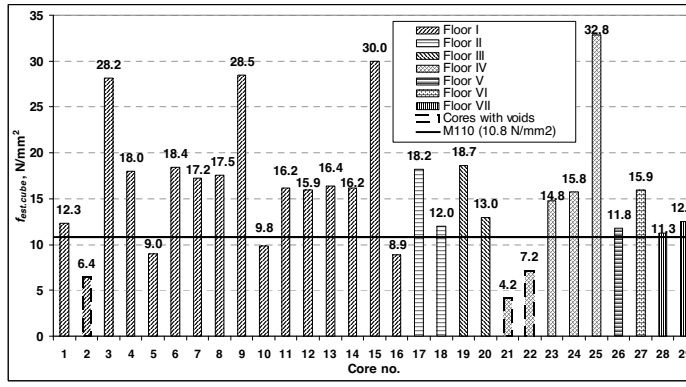

Fig. 4. Compressive strength of 29 cores drilled from columns.

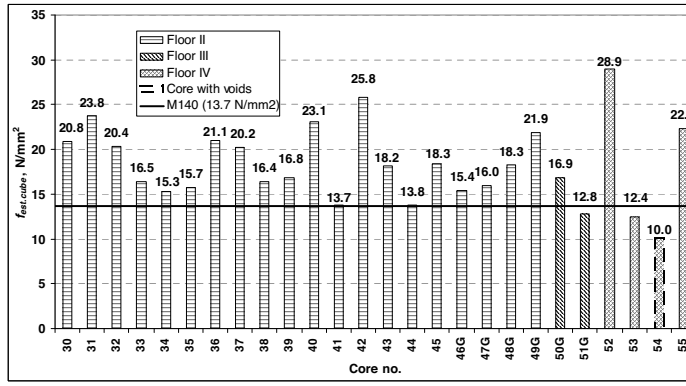

Fig. 5. Compressive strength of 26 cores drilled from beams. *Note: G behind core number denotes cores drilled from beam carrying generator*.

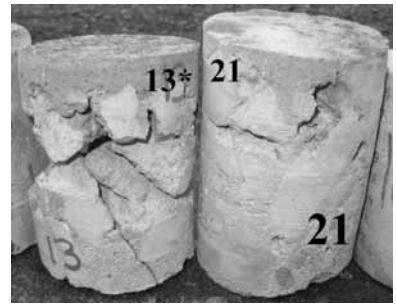

Fig. 6. Concrete cores 13* and 21 after drilling from columns.

Assessment of *in-situ* compressive strength directly from core tests is based on the reference method described in EVS-EN 13791:2007 [24], which enables to compare the results to concrete strength classes applied today [25]. The lower value of the estimated *in-situ* characteristic strength (according to Approach A in [24]) of cores drilled from columns and beams was 5.6 N/mm^2 and 11.8 N/mm^2, respectively. Therefore, the strength of cores drilled from beams corresponds to the lowest strength class - C8/10. The strength of cores drilled from columns was lower than any strength class applied today.

The strength of concrete should be taken into account when considering the bond between repair mixture (or concrete) and original concrete in the repairs of concrete structures of the plant.

Compressive test revealed some cores with questionably low compressive strength (eg. cores 2, 21, 22 in Fig. 4 and core 54 in Fig. 5). In engineering practice, the strength of concrete at a given age and cured in same conditions at a prescribed temperature is assumed to depend primarily on two factors only: the water/cement ratio and the degree of compaction [26]. According to construction drawings of the building the water/cement ratio of concrete is the same on different floors of the given structure (beam or column). However, the actual water/cement ratio may vary a little in monolithic concrete structures as a result of segregation and bleeding. Segregation involves larger aggregate particles falling towards the lower parts of the freshly placed concrete. Bleeding is the process of the upward migration or upward displacement of water. They often occur simultaneously. The other factor affecting the strength of concrete is the degree of compaction. As a result of insufficient compaction air voids may occur in concrete. The presence of voids in concrete greatly reduces its strength: Approximately 1% voidage decreases the strength by 5-8% [26]. Also in this study, voids of cores 2, 21 (in Fig. 6), 22 and 54 reduced significantly their strength in comparison with others. Voids in columns and beams were a result of insufficient compaction of concrete during the construction of the plant in 1951.

The mean estimated cube strength ($\overline{f}_{est.cube}$) as well as standard deviation of cores drilled from columns and beams on different floors are presented in Table 3.

Table 3 shows no trend in core strengths drilled from columns or beams on different floors. These results contrast with the results of visual inspection, where clear trend of grades on different floors was observable. On the basis of Table 2 and Table 3, the visual condition and the strength of the material (concrete) of the structure are not related. However, since the majority of cores were drilled from either the 1st floor (columns) or the 2nd floor (beams) no detailed comparison of strength can be performed on cores drilled from different floors in Table 3.

In this study also non-destructive rebound hammer test was conducted. However, rebound hammer test reflects only the surface of concrete. The measured rebound number is an indication of about the first 30 mm depth of concrete. Changes affecting only the surface of the concrete such as degree of saturation, carbonation, temperature, surface preparation, etc., have little influence on the properties of concrete at depth of a structure. That also explains why statistically insignificant (p-value = 0.11) and very weak (R^2 = 0.089) relationship was found between core strength and rebound number. More detailed information about the results of rebound hammer test can be found in a separate paper of the authors [27].

The rebound hammer test is largely comparative in nature. It was found on each floor that rebound hammer values *i.e.* surface strength for the beams carrying generator, thus, close to generator (*ca.* 0.4 m) were lower than for those located at some distance (*ca.* 1.5 m) [13].

The mean strength of six cores drilled from beams carrying generator (*i.e.* cores 46G-51G in Fig. 5) was 16.9 N/mm^2 with the standard deviation of 3.0 N/mm^2. The mean strength of 20 cores drilled from other beams was 18.7 N/mm^2 with the standard deviation of 4.7 N/mm^2. The mean strength of cores drilled from beams carrying generator was slightly lower (by 1.8 N/mm^2) that of the cores drilled from other beams. However, due to small difference in mean strength and high standard deviation no clear trend can be found in the results.

Table 3. **Concrete strength of columns and beams on different floors**

Floor no.	$\overline{f}_{est.cube} \pm s$ from columns, N/mm^2 (no. of cores)	$\overline{f}_{est.cube} \pm s$ from beams, N/mm^2 (no. of cores)
1	16.8 ± 7.1 (16)	–[a]
2	15.1 ± 4.4 (2)	18.6 ± 3.4 (20)
3	15.8 ± 4.0 (2)	14.9 ± 2.9 (2)
4	14.9 ± 11.1 (5)	18.4 ± 8.8 (4)
5	11.8 (1)	–[b]
6	15.9 (1)	–[b]
7	11.9 ± 0.9 (7)	-[b]

[a] – There are no beams on the 1st floor
[b] – No cores were drilled from beams on floors 5-7

Estonian Standard EVS-EN 12504-1:2003 [18] specifies that concrete strength is influenced when the core diameter is less than three times the maximum size of aggregate. In such cases the drilling operation can affect the bond between the aggregate and the surrounding hardened cement paste. As the maximum size of aggregate increases, the strength of the core decreases. The effect is more pronounced for small diameter cores [28].

In this study cores with diameter 75 mm were drilled. The maximum size of aggregate was not known. It is possible that 75 mm diameter cores violated the requirement of a minimum ratio of core diameter to aggregate size. However, cores of larger diameters were not drilled because of the risk of structural damage and congestion of the reinforcement. Overall, in view of the numerous factors influencing the strength of cores, the effect of core size can be considered to be unimportant. However, small cores have a higher variability than standard-size cores [24, 26]. Thus, an increased number of cores has to be tested. Therefore, in this study additional 35 cores were drilled besides the initial 20 cores.

Carbonation depth and cover of concrete

The results of carbonation depth as well as concrete cover measurements are presented in Fig. 7.

Figure 7. shows that mean carbonation depth of cores is considerably lower than the corresponding concrete cover. Thus, in general carbonation front has not reached the vicinity of the surface of the rebar. Only one core exists in Fig. 7 where mean carbonation depth (core 19) was nearly the same

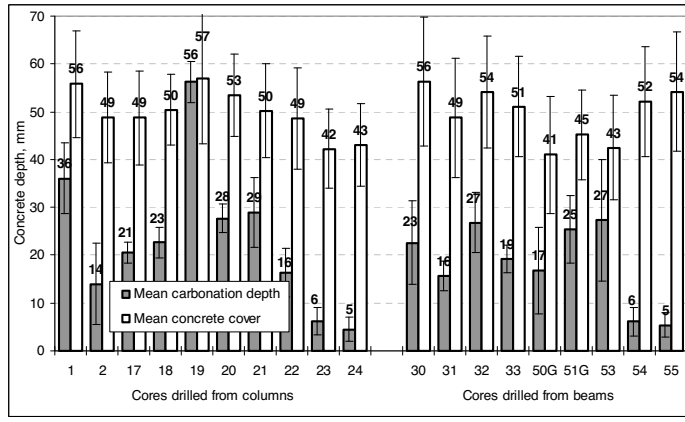

Fig. 7. Carbonation depth and concrete cover on cores drilled from columns and beams. "Whiskers" on bars denote standard deviation of the measurements. *Note: G behind core number denotes cores drilled from beam near generator.*

as concrete cover. Also, a single carbonation depth measurement on core 53 could overreach the cover (shown as an overlap of standard deviations of cover and carbonation depth on core 53). Still, according to the data sample presented in Fig. 7, the corrosion of steel reinforcement in the studied generator building was not carbonation-induced.

A photograph of the most representative cores is presented in Fig. 8. Because of the presence of coarse aggregate, carbonation depth may vary considerably on the same core e.g. core 50G in Fig. 8.

It might also be noted that, if cracks are present, CO_2 can ingress through them so that carbonation "front" advances locally from the penetrated cracks. In many cases, corrosion can take even when the full carbonation front is still a few millimetres away from the surface of the steel if partial carbonation has taken place [29].

Phenolphthalein test is easy to perform and is rapid but it should be remembered that the pink colour indicates the presence of $Ca(OH)_2$ but not necessarily a total absence of carbonation. Indeed, the phenolphthalein test gives a measure of the pH but does not distinguish between a low pH caused by carbonation and by other acidic gases.

The authors found statistically insignificant (p-value = 0.48) relationship between carbonation depth and the strength of cores. Figure 7 shows that carbonation depth and concrete cover do not differ substantially between the cores drilled from columns or beams. Also, carbonation depth and concrete cover were not differing on different floors.

According to the design drawings the cover to longitudinal reinforcement of both columns and beams was 50 mm. The actual concrete cover depends on the quality of casting of monolithic concrete. The mean cover on different columns and beams in Fig. 7 varied from 41 to 57 mm. Also, relatively high standard deviation of concrete cover was measured on the same column or beam. As an extreme example a cover from 38 to 65 mm was measured on the same column on the 3rd floor. The variable results of cover measurements in this study characterize the quality of concrete placing in the 1950ies.

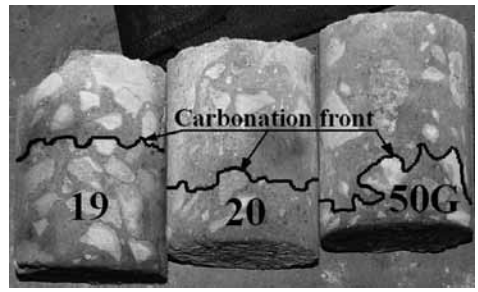

Fig. 8. Carbonation front estimated by phenolphthalein method on cores 19, 20 and 50G.

Chemical analysis of concrete

The results of chemical analysis of water-soluble deleterious salts in concrete cores are presented in Table 4. The content of water soluble salts in concrete was interpreted following WTA guidelines 4-5-99 [30] in Table 5.

Table 4 and Table 5 show that the sulphate content near the surface of concrete beams carrying generator on the 2nd floor was from middle (in samples 46G and 48G) to very high (in sample 46G). In depth of a concrete beam carrying generator on the 2nd floor the sulphate content was low.

Generally, the chloride content in surface as well as in depth of concrete was medium. Nitrate content was found to be low in all samples presented in Table 4.

Only four samples are not enough for thorough conclusions. However, it is evident that the content of deleterious salts in concrete beams carrying generators is too high. Solid salts do not attack concrete but, when present in solution, they can react with hydrated cement paste. The effect of sulphate and chloride ions to concrete is presented as follows.

Sulphate ions can penetrate the concrete and react with components of the cement matrix to cause expansive chemical reactions. Swelling may occur that, starting from the corners of a concrete structure gives rise to cracking and disintegration. Sulphate attack can also manifest itself as a progressive loss of strength of the cement paste due to loss of cohesion between the hydration products. In this study the strength of concrete cores 46G-48G (in Fig 5.) was not substantially lower than that of cores drilled from other beams. Therefore, a sulphate content ranging from middle to very high had not reduced the strength of cores.

Chloride contamination of concrete is a frequent cause of corrosion of reinforcing steel. Chloride-induced corrosion can only take place once the

Table 4. **Results of chemical analysis of deleterious salts in concrete**
Note: G behind core number denotes cores drilled from beam near generator

Core no.	Sample location in core	Content of water soluble salts in concrete, percentage of mass			
		Sulphate $(SO_4)^{2-}$	Chloride Cl^-	Nitrate NO_3^-	Total
46G	Surface	3.817	0.214	0.045	4.075
46G	Middle	0.173	0.654	0.012	0.839
47G	Surface	0.738	0.421	0.044	1.202
48G	Surface	0.751	0.236	0.021	1.009

Table 5. **Classification of the content of water soluble salts in concrete [30]**

	Content of water soluble salts in concrete, percentage of mass		
	Low	Middle	High
Sulphate	< 0.5	0.5–1.5	> 1.5
Chloride	< 0.2	0.2–0.5	> 0.5
Nitrate	< 0.1	0.1–0.3	> 0.3

chloride content of concrete in contact with the steel surface has reached a threshold value. Chlorides lead to a local breakdown of the protective oxide film on the reinforcement in alkaline concrete, so that a subsequent localized corrosion takes place. The morphology of the attack is that typical of pitting corrosion. However, no pitting was found on the exposed reinforcement of columns and beams (Fig. 2 and 3) as a result of visual inspection.

At least the beams carrying generator on the 2nd floor should be treated with steam to reduce the concentration of sulphates and chlorides in concrete. The mortar applied during repairs has to protect the steel by both physical means (i.e. preventing the ingress of deleterious substances) and by chemical means (providing repassivation).

Water absorption of concrete

Water absorption was determined on ten concrete samples, which were extracted from the columns on the 1st floor. The mean water absorption was 5.2% with the standard deviation 1.1%. It should be noted that two pitchy concrete samples had also the lowest water absorption values. Therefore, the mean water absorption could have been higher if clean concrete samples would have acquired.

The Soviet Building Code [31] distinguishes between three different concrete types: normal permeability (N), lowered permeability (P) and particularly low permeability (O) with water absorption values of 4.8-5.7%, 4.3-4.7%, 4.2% and under, respectively.

According to the mean water absorption value concrete of normal permeability (N) was applied on the columns on the 1st floor.

As mentioned before the columns on the 1st floor should be treated with steam to reduce the concentration of pitch from concrete during repairs. Considering the aggressive indoor environment in generator building the repair mixture has to be of low permeability.

Aggressive indoor environment in the plant in the 1950-ies

As mentioned in introduction, the studied oil plant was launched in 1951. At that time besides oil production these generators supplied the nearby gas plant with heating gas. The gas plant was supplying former Leningrad (St. Petersburg) with domestic gas through more than 200 km long gas pipeline (under a banner “Gas for Leningrad”).

The middle part of the 125-tonne generator designed by Lengiprogaz was more constricted when compared to preceding generators. This caused an unequal temperature distribution in those generators. As a result uncomposed oil-shale pieces fell together with semicoke into the gasification chamber at the lower part of generators. Oil shale pieces ignited with air contact and raised the temperature in the gasification chamber whereby oil-shale ash melted to become slag. Slag had to be removed (by raking) from the generator since it constrained the outlet of semicoke. Slag was raked through all four

hatches of the generator manually. Hot slag was broken more efficiently by spraying water into the generator. Therefore, ash dust and harmful gases in large concentration left through hatches of the generator during slag removal. Air addition into the generator was suspended during raking. Slag raking was performed in all generators more than once a day by a schedule. Slag was removed more rarely after reconstruction of generators from the end of the 1950-ies to the beginning of the 1960-ies. Later the amount of air added to the generator was reduced. From the start of the 1980-ies the gasification process of generators was discarded and hatches were opened only for repairs [32].

Employees of the plant had noticed exposed reinforcement *i.e.* spalled concrete cover of load-bearing concrete structures near gas generators already at the beginning of the 1960-ies. Therefore, the deterioration of load-bearing concrete structures in the studied gas-generator building originates probably from the 1950-ies.

Conclusions and suggestions

A case study for investigating the condition of concrete structures and properties of concrete of an existing oil-shale chemical plant is presented. The studied seven-storied plant, located in North-Eastern Estonia, was constructed in 1951.

It is found that the deteriorations of load-bearing concrete structures in the studied oil plant building may originate already from the 1950-ies. At that time, due to a different technology, slag was removed from all generators each day. The columns and beams were exposed to a large concentration of aggressive gases exiting through the hatches of the generator during slag removal. These gases were the most probable cause of deterioration of concrete structures.

The following steps of repair based on the results of the current study are suggested:

- Removal of cracked and delaminated concrete to expose the surface of the damaged steel.
- Steaming of structures to reduce the concentration of chlorides, sulphates as well as pitch from concrete.
- Treatment of the steel rebars to remove rusting layers. Application of protective coating to the steel. Reattachment or replacement of loose stirrups. Placement of additional steel bars if necessary.
- Application of bond coat on substrate concrete to provide bond with repair mortar.
- Application of cement-based and low-permeability repair mortar to replace the damaged concrete that was removed. The repair mixture has to protect the steel by both physical means (*i.e.* preventing the ingress of deleterious substances) and by chemical means (providing repassivation of steel).

Deteriorated concrete structures on the 1st and 2nd floor of the studied generator building were repaired quite similarly to the above steps by the company REV Special OÜ. The authors recommend repairing also deteriorated concrete structures on the floors 3–7.

REFERENCES

1. *Raukas, A.* Oil shale industry and sustainability – governance through dialogue // Oil Shale. 2005. Vol. 22, No. 1. P. 3–4.
2. *Jiang, X. M., Han, X. X., Cui, Z. G.* New technology for the comprehensive utilization of Chinese oil shale resources // Energy. 2007. Vol. 32, No 5. P. 772–777.
3. *Razvigorova, M., Budinova, T., Petrova, B., Tsyntsarski, B., Ekinci, E., Ferhat, M. F.* Steam pyrolysis of Bulgarian oil shale kerogen // Oil Shale. 2008. Vol. 25, No 1. P. 27–36.
4. *Klevtsov I., Tallermo, H., Bojarinova, T., Dedov, A.* Assessment of remaining life of superheater austenitic steel tubes in oil shale PF boilers // Oil Shale. 2006. Vol. 23, No. 3. P. 267–274.
5. *Tallermo, H., Klevtsov, I.* High-temperature corrosion of martensitic and austenitic steels under on-tube oil shale ash deposits // Oil Shale. 2002. Vol. 19, No. 1. P. 19–33.
6. *Ots, A., Paist, A.* Laboratory investigations of high temperature corrosion of boiler alloys under the impact of Estonian oil shale ash // Oil Shale. 1997. Vol. 14, No. 3 Special. P. 236–245.
7. *Ellingwood, B. R., Mori, Y.* Reliability-based service life assessment of concrete structures in nuclear power plants: optimum inspection and repair // Nucl. Eng. Des. 1997. Vol. 175, No. 3. P. 247–258.
8. *Braverman, J. I., Miller, C. A., Hofmayer, C. H., Ellingwood, B. R., Naus, D. J., Chang, T. Y.* Degradation assessment of structures and passive components at nuclear power plants // Nucl. Eng. Des. 2004. Vol. 228, No. 1–3. P. 283–304.
9. *Naus, D. J., Oland, C. B., Ellingwood, B. R., Hookham, C. J., Graves III, H. L.* Summary and conclusions of a program addressing aging of nuclear power plant concrete structures // Nucl. Eng. Des. 1999. Vol. 194, No. 1. P. 73–96.
10. *Sasmal, S., Ramanjaneyulu, K.* Condition evaluation of existing reinforced concrete bridges using fuzzy based analytic hierarchy approach // Expert Syst. Appl. 2008. Vol. 35, No. 3. P. 1430–1443.
11. *Stewart, M. G.* Reliability-based assessment of ageing bridges using risk ranking and life cycle cost decision analyses // Reliab. Eng. Syst. Saf. 2001. Vol. 74, No. 3. P. 263–273.
12. *Enright, M. P., Frangopol, D. M.* Reliability-based condition assessment of deteriorating concrete bridges considering load redistribution // Struct. Saf. 1999. Vol. 21, No. 2. P. 159–195.
13. *Kiprushenkov, M., Miljan, J., Kiviste, M., Miljan, R.* Condition assessment of concrete structures in chemical plants gas generator building // Proc. 5th Int. Conf. Concrete Under Severe Conditions Environment and Loading, Tours-France, LCPC, France, 2007. P. 223–230.
14. *Harris, S. Y.* Building Pathology: Deterioration, Diagnostics, and Intervention. – New York: John Wiley & Sons, Inc., 2001. 654 p.
15. *Alekseyev, S. N., Rozental, N. K.* Corrosion Durability of Reinforced Concrete

Structures in Industrial Environment. – Moscow: Stroiizdat, 1976. 205 p. [in Russian].
16. *Alekseyev, S. N., Ivanov, F. M., Modrõ, C., Schiessel, P.*. Durability of Reinforced Concrete in Aggressive Environment. – Moscow: Stroiizdat, 1990. 314 p. [in Russian].
17. *Miljan, J., Keskküla, T.* Durability prediction of reinforced concrete structures in cattle-breeding buildings. In: Questions about the Reliability of Reinforced Concrete Structures. – Kuiboshev, 1975. P. 120–122 [in Russian].
18. EVS-EN 12504-1:2003 Testing concrete in structures. Part 1: Cored specimens. Taking, examining and testing in compression. – Tallinn: Estonian Centre of Standardisation, 2003. 11 p. [in Estonian].
19. EVS-EN 12390-3:2002 Testing hardened concrete. Part 3: Compressive strength of test specimens. – Tallinn: Estonian Centre of Standardisation, 2002. 18 p. [in Estonian].
20. BS 6089:1981 Guide to Assessment of Concrete Strength in Existing Structures. – UK: British Standard Institution, 1981. 16 p.
21. EVS-EN 14630:2006 Products and systems for the protection and repair of concrete structures. Test methods. Determination of carbonation depth in hardened concrete by the phenolphthalein method. – Tallinn: Estonian Centre of Standardisation, 2006. 15 p.
22. DIN 51100 Testing of ceramic raw materials and materials; determination of the soluble salts (percolator method). – Berlin: German Institute for Standardization, 1957. 30 p. [in German].
23. GOST 12730-67 Heavy concrete. Methods for determination density, porosity and water absorption. Concrete and reinforced concrete products. Methods of testing. – Moscow: Standards Publishing, 1974. P. 115–122 [in Russian].
24. EVS-EN 13791:2007 Assessment of in-situ compressive strength in structures and precast concrete components. – Tallinn: Estonian Centre of Standardisation, 2007. 28 p.
25. EVS-EN 206-1:2007 Concrete Part 1: Specification, performance, production and conformity. – Tallinn: Estonian Centre of Standardisation, 2007. 82 p. [in Estonian].
26. *Neville, A. M.* Properties of Concrete. – London, etc.: John Wiley & Sons, Inc., 1995. 844 p.
27. *Kiviste, M., Miljan, J.* Structural concrete compressive strength determination with rebound hammer // Vagos. 2007. No. 74 (27). P. 15–20.
28. *Arioz, O., Ramyar, K., Tuncan, M., Tuncan, A., Cil, I.* Some factors influencing effect of core diameter on measured concrete compressive strength // ACI Materials J. 2007. Vol. 104, No. 3. P. 291–296.
29. *Parrot, L. J., Killoch, D. C.* Carbonation in a 36 year old, in-situ concrete // Cement Concrete Res. 1989. Vol. 19, No. 4. P. 649–656.
30. WTA Guidelines 4-5-99/D: Evaluation of Masonry. – Munich: WTA Publications, 1999. 16 p. [in German].
31. SNIP 2.03.11-85 Corrosion Protection of Building Structures. – Moscow, 1985. 45 p. [in Russian].
32. *Rooks, I.* From the First Oil Shale Industry to Kiviter: 1938–1998 Memories and Facts. – Kohtla-Järve, 2004. 132 p. [in Estonian].

Presented by I. Valgma
Received June 3, 2009

Kiprušenkov, M†., Miljan, J., **Kiviste, M.**, Miljan. R. 2007.
CONDITION ASSESSMENT OF CONCRETE STRUCTURES IN CHEMICAL PLANT'S GAS GENERATOR BUILDING.

5th International Conference on Concrete under Severe Conditions of Environment and Loading (CONSEC), Tours: 223-230.

CONSEC'07 Tours, France *Concrete under Severe Conditions : Environment & Loading*
F. Toutlemonde et al. (eds)

CONDITION ASSESSMENT OF CONCRETE STRUCTURES IN CHEMICAL PLANTS GAS GENERATOR BUILDING

EVALUATION DE L'ETAT DES STRUCTURES EN BETON D'UN BATIMENT DE GENERATEUR DE GAZ DANS UNE USINE CHIMIQUE

Mihhail KIPRUSHENKOV[1], Jaan MILJAN[1], Mihkel KIVISTE[1], Riina MILJAN[1]
[1] *Estonian University of Life Sciences, Tartu, Estonia*

ABSTRACT – In this paper reinforced concrete structures of an oil-shale chemical plant are investigated**.** The study included visual assessment of all structures, measurements of surface concrete compressive strength with rebound hammer and acquisition of some concrete samples for the determination of water absorption values. In order to verify whether the bearing structures were built according to the construction drawings, the cross section concrete and reinforcement diameter of different columns and beams were measured. The residual bearing capacity of the reinforced concrete bearing structures was calculated according to the measured data. The results show that in some places concrete beams are in critical condition. The owner of the building should immediately halt production and employ specialists to rehabilitate reinforced concrete structures in the building.

RÉSUMÉ **–** Dans cet article on s'intéresse aux structures en béton armé d'une usine pétrochimique. L'étude comprend l'inspection visuelle de toutes les structures, l'évaluation non-destructive de la résistance en compression du béton et le prélèvement de quelques échantillons pour détermination du coefficient d'absorption d'eau. Afin de vérifier si les structures porteuses ont été construites conformément aux plans, la section de béton et le diamètre des armatures a été mesuré pour plusieurs poteaux et poutres. La capacité portante résiduelle des structures porteuses en béton armé a été recalculée grâce aux valeurs mesurées. Le résultat montre qu'à certains endroits les poutres en béton sont en situation critique. Le maître de l'ouvrage devrait arrêter immédiatement la production et confier à des spécialistes la réhabilitation des structures en béton armé des bâtiments.

1. Introduction

This paper presents a study of the reinforced concrete structures of an oil-shale chemical plant. The studied chemical plant's gas generator building is located in North-Eastern Estonia. The 6-storey building measuring 64m × 15m has been constantly in service since its construction in the 1953. The generator processes 1.4 million tons of oil shale every year. Oil-shale is processed in the plant's gas generators to produce shale oils, fuel oils and resins. There are 12 gas generators in the plant. The gas generator technology scheme involves the transportation of oil-shale to the bunkers located in the upper part of building from where it is led to the gas generator. In the generator shale oil is separated by the process of retorting. The gas generator is being constantly filled and emptied. The vertical position of the generators allows them to

empty by gravity pull. The conveyor under the generator leads the remains of oil-shale (semi-coke) out of the building. The bearing structures of the gas generator building are located on the first and second floor. As oil-shale exits the generator immediately after burning, it is quenched with water which produces a lot of gases (fig. 1).

Figure 1. Mixture of gases produced with oil-shale water quenching

Figure 2. Condition of some concrete beams on the first floor

The mixture contains carbon dioxide (CO_2), sulfur dioxide (SO_2), hydrogen sulphide acid (H_2S), phenols, aliphines, methane, ethane, propane, butane, etc. According to classification (Alekseyev and Rozental, 1976) these gases are of type I and II, which react with $Ca(OH)_2$ and neutralize concrete or produce salts. These salts generate III type of corrosion, which damage the structure of concrete (Alekseyev et al., 1990).

The conveyor is located on the ground floor extending across the full length of the building. The columns and beams on the first floor (fig. 2) are directly exposed to the gases from the conveyor since the ground floor is only partially separated from the first floor by a concrete ceiling.

The cooling of the processed oil shale takes place on the second floor. There is no separation of gases on the third, fourth, fifth or sixth floor - on the fifth floor the oil shale is loaded from the bunker onto the generator. On the sixth floor the oil shale is loaded onto the bunker.

The bearing structures of the gas generator building perform as a monolithic concrete frame the columns of which are made of concrete mark M110 (~11 N/mm^2) and beams are made of concrete mark M140 (~14 N/mm^2). Steel reinforcement of class A-I (smooth, yield strength ... N/mm^2) has been used both in the beams and columns.

2. Materials and methods

2.1 Visual inspection

All columns and beams in the plant were assessed visually on a 6-grade scale developed at the Estonian University of Life Sciences department of Rural Building (Table 1). The condition indicator of the lowest grade determines the grade assigned to the element.

Table 1. Classification of deterioration states of reinforced concrete beams and columns (Miljan and Keskküla, 1975; Miljan et al., 2004)

Grade	Description of state
5	No corrosion detected
4	Less than 20% of stirrups are corroded (cracks or spalled concrete cover)
3	More than 20% of stirrups are corroded
2	Micro-cracks (width 0-0.3mm) in the concrete cover of main reinforcement
1	Cracks (width >0.3mm) in the concrete cover of main reinforcement
0	1) Concrete cover of the main reinforcement has spalled; 2) Serviceability limit state

2.2 Concrete compressive strength non-destructively

Concrete rebound hammer Digi-Schmidt 2000 ND was used to determine the surface hardness of the concrete non-destructively. The visual inspection suggested that the condition of the concrete structures in the gas generator building depends on the distance between the generator and the coke unloading site. We determined the surface hardness of concrete beams at a distance of 0.4m and 1.5m from the generator on each floor. Ten rebound values were gathered at each measuring spot the mean value of which was converted to surface compressive strength of concrete applying the curve *B-Proceq* Conversion (Digi-Schmidt …, 2001).

2.3 Water absorption of concrete

To determine water absorption of concrete the Soviet standard water absorption measuring method (GOST 1974) was applied. The samples were immersed in 20°C water and weighed every 24 hours until a constant value was reached. Then, the samples were oven-dried until a constant weight was reached. Water absorption was found with the formula:

$$W = \frac{m_H - m_O}{m_O}, \qquad (1)$$

where W – water absorption (%), m_{H} – weight of a water-saturated sample (g), m_{O} – weight of a dried sample (g). The Russian Building Code (SNiP, 1985) distinguishes between three different concrete types: normal permeability (N), lowered permeability (P) and particularly low permeability (O) with water absorption values of 4.8-5.7%, 4.3-4.7%, 4.2% and under, respectively.

2.4. Reduction in the load-bearing capacity of the structure

We measured the dimensions of the concrete beams and columns with a tape measure and the diameter of the reinforcement with a calliper gauge. The results were used to calculate the load-bearing capacity of the existing concrete structures. To calculate the flexural capacity of continuous beams two different methods have to be applied.

In the mid-span of the beam the compressive zone is in the upper part of a section and the concrete cover has spalled in the tension zone. In flexural capacity calculations the cross-section height is to be reduced when compared to the design height of the beam.

Over the support of the beam the compressive zone is in the lower part of a section and the concrete cover has spalled in the compressive zone.

Cross-section height and reinforcement diameter were reduced in our flexural capacity calculations.

Because of loose stirrups the *shear capacity* of the critical state concrete structures was calculated in the way it is calculated for a cross section with no stirrups. Shear calculation results are compared with those of attached stirrups.

The load-bearing capacity calculations are performed in accordance with the Estonian Standard (EVS 1992-1-1:2003) which is based on Eurocode 2 (BS EN 1992-1-1).

3. Results and discussion

3.1 Visual inspection

The grades attached to the columns and beams were calculated as the mean of the four assessments performed (Table 2).

Table 2. Visual assessment grades of reinforced concrete elements

Floor no.	Mean grade of beams	Mean grade of columns
1	-*	0
2	0	0
3	0	0
4	0	3
5	3	3
6	4	4
7	5	5

* There are no beams on the ground floor.

Table 2 suggests that the condition of beams is worse than that of the columns - the beams on floors 2…4 are in a serviceability limit state. However, columns are in a serviceability limit state on floors 1…3. The condition of beams is worse because they are more exposed to the aggressive gases and nearer to the generator, ie the temperature is high. On the upper floors of the gas generator building the concentration of gases is less intense and the temperature is lower.

3.2 Concrete compressive strength non-destructively

The results of the concrete rebound hammer Digi-Schmidt non-destructive test mean values converted to the compressive strength of concrete are shown in Table 3.

Table 3. Mean compressive strength of concrete beams and columns

Floor no.	Mean compressive strength of beams, N/mm^2		Mean compressive strength of columns, N/mm^2
	Distance from generator ~ 0.4m	Distance from generator ~ 1.5m	
1	-*	-*	19.6
2	18.8	21.1	26.9
3	12.8	18.1	27.9
4	18.4	42.5	27.6
5	23.9	28.1	35.1
6	26.2	29.2	24.9

* There are no beams on the ground floor.

The concrete strength values (Table 3) are comparable to the results obtained by the visual inspection (Table 2). All the values for the beams located close to the gas generator are lower than for those located at some distance. The strength of the concrete in semi-coke unloading area (floor 1) is lower than that registered in the upper floors. In beams the actual compressive strength of concrete mostly exceeds the design value of ~ 14 N/mm^2.

In columns the compressive strength is the lowest in the semi-coke unloading zone on the ground floor. These values exceed the design value of 11 N/mm^2 in all measured spots.

The above distribution of concrete compressive strength can be accounted for by the different movement patterns of gases of low water content and gases of high water content.

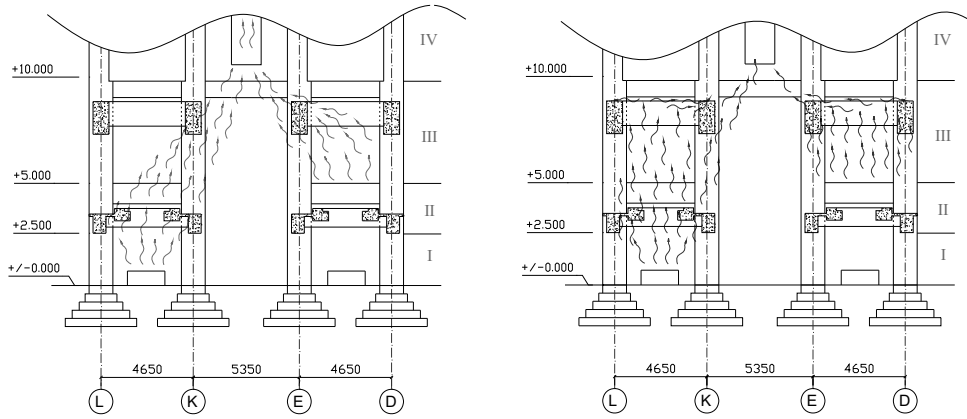

Figure 3. Movement of gases of different water content in the gas generator building: a) gases of low water content – lower temperature; b) gases of high water content – higher temperature 0…IV – floor numbers

On the second floor the semi-coke is exiting the generator to enter the tank filled with cooling water. The cooling process yields anorganic gases (CO_2, H_2S, SO_2, etc.) and the vapour

of high temperature (~ 150˚C). The drop in the vapour temperature initiates condensation and the mist occurs.

The inorganic gases (mainly H_2S and SO_2) are dissolved in the drops of water and the reaction results in an acid environment (eg H_2SO_3). The temperature of the gases of higher water content is higher and these rise vertically and condense on the structures (Fig 3b). The temperature of the gases of lower water content is lower and these move from the surface of semi-coke towards the ventilation vent (Fig 3a). The gases reacting with concrete produce a mixture of salts like $CaCO_3$, $CaSO_3$, CaS, $CaSO_4 \cdot 2H_2O$ and $CaSiO_3$. The salts enter the pores and cracks of concrete that extend and widen to enhance the destruction of concrete. The layer of salts formed is irregular, hygroscopic and amorphous.

Similar reactions occur in those parts of the structure which are reached by the mixture of the gases of low water content. However, as SO_2 does not to react with water, the layer of salt mixture is denser and more compact than the one formed with the mixture of gases of higher water content.

Thus, the strength of concrete is reduced and if the actual stress is greater than the strength of concrete cover and salt layer, the corroded layer of concrete cover is spalling.

3.3 Water absorption of concrete

To determine the water absorption of concrete 10 samples were extracted from the columns in the second floor. The mean absorption value read 5.3%, standard deviation 0.8%.

The Russian Building Code (SNiP, 1973) assigns the water absorption concrete as of normal permeability (N).

3.4. Reduction of the load bearing capacity of the structure

To determine the bearing capacity the steel reinforcement diameters and the cross-sections of the deteriorated structures were measured on all the floors. Table 5 presents the reduction in cross-section area (%) of steel reinforcement and concrete in comparison with the respective design values.

The calculated bearing capacity was computed on the basis of the actual dimensions of the structures. The compressive strength of concrete was determined by the rebound hammer Digi-Schmidt. The data about the strength of reinforcement are those found in the design data. The reduction in bearing capacity (%) was calculated in comparison with the bearing capacity of the structure of design dimensions (Table 5).

Table 5 shows that reduced cross-section area of the steel reinforcement and reduced concrete cross-section area results in the reduction of flexural capacity of beams on floors no. 2…4. To keep the structures in service actual loads on beams need to be clarified and beams of the first 4 floors rehabilitated immediately. The bearing capacity of the columns was slightly reduced on floor no. 1…4. There is no reduction in structural bearing capacity on floor no. 5 or higher.

As the bearing capacity of the beams on floors 2…4 was significantly reduced, the reductions in the flexural and shear capacity were calculated for different sections (Fig. 4).

Table 5. Reduction in steel reinforcement and cross-section of concrete structure and calculated bearing capacity, % out of the design capacity

Floor no.	Beams			Columns		
	Reduction in steel reinforce-ment area, %	Reduction in concrete cross-section area, %	Reduction in structural bearing capacity, %	Reduction in steel reinforce-ment area, %	Reduction in concrete cross-section area, %	Reduction in structural bearing capacity, %
1	-	-	-	8	4	5
2	20	12	22.5	8	4	5
3	20	7	16.5	6	3	4
4	17	17	17	4	2	2
5	0	0	0	0	0	0
6	0	0	0	0	0	0
7	0	0	0	0	0	0

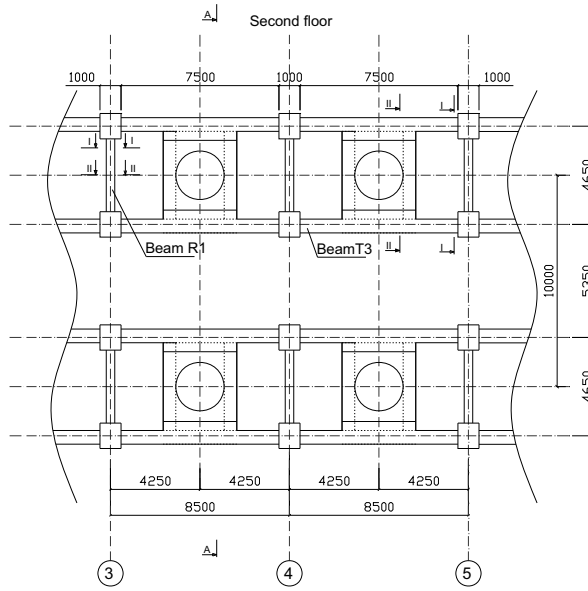

Figure 4. Fragment of the second floor plan with beams R1 and T3, for the sections I – I and II – II of which the reduction in flexural capacity and shear capacity was calculated

The flexural capacity is reduced in both beams while the reduction is of similar size in different sections.
Reduction in shear capacity is substantially greater in the mid-span than at the edge.

The owner of the building should immediately take measures to avoid the collapse of the structures.

Table 6. Reduction in flexural capacity and shear capacity for different sections of beams on the second floor, compared to the initial design data

Structure name	Reduction in flexural (M) capacity, %		Reduction in shear (V) capacity, %	
	Section I – I	Section II - II	Section I - I	Section II - II
T3	18.0	19.5	6.7	40
R1	15.3	16.7	3	50

4. Conclusions

The shale oil production in the gas generator buildings results in an extremely aggressive environment for both the concrete and the reinforced concrete.

The design of such structures should consider the data about the movement of harmful gases, their alleged reaction with water vapour and the high temperature of technology devices and by-products.

The owner of the building should immediately halt production and employ specialists to rehabilitate reinforced concrete structures in the building.

5. References

Alekseyev S. N. and Rozental N. K. (1976). Corrosion Durability of Reinforced Concrete Structures in Industrial Environment (in Russian)., Moscow: Stroiizdat, p. 205.

Alekseyev S. N., Ivanov F. M., Modrõ C., Schiessel P. (1990). Durability of Reinforced Concrete in Aggressive Environment (in Russian), Moscow: Stroiizdat, 314 pages.

BS EN 1992-1-1 (1992) Common rules for buildings and civil engineering structures

Digi-Schmidt 2000 model ND operating instructions (2001) Proceq SA, Zurich, 21 pages.

EVS 1992-1-1:2003. (2003) Concrete structures - Part 1-1: General rules and rules for design of buildings

GOST 12 730-67 (1974). Heavy concrete. Methods for determination density, porosity and water absorption (in Russian) Concrete and reinforced concrete products. Methods of testing. Standards publishing. Moscow, p. 115-122

Miljan J., Keskküla T., Miljan R., Kiviste M., Laiakask E., Tomann H. (2004). Service Life Prediction of Reinforced Concrete Structures Damaged by Reinforcement Corrosion. CIB World Building Congress 2004. Building for the Future. Toronto, Canada.

Miljan, J., Keskküla, T., (1975). Durability Prediction of Reinforced Concrete Structures in Cattle-breeding Buildings (in Russian). In: Questions About the Reliability of Reinforced Concrete Structures. Kuiboshev, pp. 120 – 122.

SNIP 2.03.11-85 (1985) Protection of structures from corrosion. (in Russian), Moscow, 45 pages.

ACKNOWLEDGEMENTS

This study was carried out at the Department of Rural Building of the Estonian University of Life Sciences. Research was financed by the Department (former Institute) of Rural Building, base-funding No 8-2/T8003MIMI and Estonian University of Life Sciences. I am grateful to my supervisor Prof. Jaan Miljan for sharing his research results as well as supplying me with the literature and measuring equipment.

I would like to thank:

Prof. Emer. Egil A. Berge from Agricultural University of Norway for his advice and valuable comments to the manuscripts submitted to ACI Structural Journal and Engineering Structures.

Prof. Andres Kiviste for his comprehensive support and encouragement through my bachelor, master and doctoral studies. Also, his contribution at the statistical analysis of test results should be pointed out.

PhD Olav Sammal from ETUI BetonTEST OÜ for supplying me with information and measuring equipment as well as for the comments to the manuscript submitted to Oil shale.

Erki Laiakask for sharing his research results as well as the design and construction of 4-point bending device for the testing of ribbed panels.

Co-testers Heiki Tomann and Meelis Tarto as well as Regina Patrael, Jane Hinto-Kivimaa, Janar Toper, Lauri Linnus, Riho Halgma and Taivo Salu for performing structural and material tests with ribbed panels.

All my colleagues from the Department of Rural Building, who have contributed in one way or another to the tests, manuscripts and preparation or defence of the thesis.

Last but not least I am indebted to my family, especially to my wife, Helen, for her support, understanding and patience.

CURRICULUM VITAE

Personal data

Name: Mihkel Kiviste
Date of birth: 6. April 1980
Address: Estonian University of Life Sciences, Kreutzwaldi 5, Tartu
Contact: *phone* +372 7313178, *e-mail* mihkel.kiviste@emu.ee
Family: Married, 3 children

Career

Institution and position held:

2004-…	Estonian University of Life Sciences, Institute of Forestry and Rural Engineering, Department of Rural Building; lecturer.
2002-2004	Scanhouse OÜ; project manager.

Education:

2005-…	Estonian University of Life Sciences, Institute of Forestry and Rural Engineering, Engineering Sciences, PhD study.
2004-2005	Estonian University of Life Sciences, Institute of Forestry and Rural Engineering, Rural Building, PhD study.
2002-2004	Estonian Agricultural University, Faculty of Rural Engineering, Institute of Rural Building, Rural building, MSc study.
1998-2002	Estonian Agricultural University, Faculty of Rural Engineering, Institute of Rural Building, Rural building, Bachelor study.
1987-1998	Tartu Mart Reiniku Gymnasium (Tartu 10. Secondary School).

Administrative responsibilities:

2007-2010	Member of defence board of Rural Building master curriculum.
2009	Chairman of the 16th Baltic Building Symposium.
2007-…	Delagate of Estonian University of Life Sciences Sports Club representative council.
2006-2007	Member of Institute of Forestry and Rural Engineering board.

2005-2006 Member of defence board of Rural Building bachelor curriculum.

Case studies and tests:

- Aug.-Sept. 2005. J. Miljan, **M. Kiviste**. Existing Kungla cowshed at Kambja municipality at Tartu County. Condition assessment and residual bearing capacity calculations of reinforced concrete bearing structures. Reconstruction drawings of a cowshed. Customer: FIE Lembit Räisa.
- Aug.-Sept. 2006. **M. Kiviste**, M.-J. Miljan, J. Miljan. Extension of Centre of Vocational Education at Tartu (Kopli 1). Testing of joint between reinforced concrete column and beam. Customer: AS Ehitusfirma Rand ja Tuulberg.
- Oct.-Dec. 2006. **M. Kiviste**, J. Miljan. Reconstruction of an office building at Tartu (Vasara 50). Evaluation of concrete strength of reinforced concrete bearing structures of a building by rebound hammer and concrete cores. Customer: Snorge Ehitus OÜ.
- Sept.- Oct. 2008. K. Sahk, **M. Kiviste**. Existing fuel filling station at Külitse at Tartu County. Condition and residual bearing capacity assessment of the bearing structures (incl. ribbed ceiling panels PNS-12) of a building. Customer: AS PK Oliver.
- Feb. 2010. **M. Kiviste**. Reinforced concrete tribune of Tehvandi ski stadium at Otepää. Evaluation of concrete strength of reinforced concrete bearing structures by rebound hammer. Customer: AS Sa.Met Ehitus.
- Apr. 2010. **M. Kiviste**. Extension of Palamuse gymnasium at Jõgeva county. Comparative evaluation of concrete strength of reinforced concrete columns by rebound hammer. Customer: Agretten OÜ.

Research activity

Degree information:

2004 Master of Engineering sciences in Rural Building (Estonian Agricultural University) The influence of corrosion of steel reinforcement on the bearing capacity of ribbed reinforced concrete panels (in Estonian), (sup.) Jaan Miljan.

Honours and awards:

2008 Supervisor of master thesis, which was awarded by Estonian Concrete Society.

2008 Estonian University of Life Sciences Raefond scholarship laureate.

Field of research:

Natural Sciences and Engineering, Construction and Municipal Engineering (Durability of reinforced concrete structures, corrosion).

Current projects:

2008-2011 Base-funded research project: 8-2/T8003MIMI Assessment, analysis and modelling of environmental sustainability of buildings life cycle. Researcher. (Researcher in charge: Jaan Miljan).

Dissertations supervised:

2010 Taavi Ojaste, Master's degree, (sup) **Mihkel Kiviste**, Development of concrete strength transformation diagrams by combined non-destructive methods for Estonian conditions (in Estonian).

2010 Rainer Põvvat, Master's degree, (sup) Jaan Miljan, **Mihkel Kiviste**, Investigation of the causes of deterioration of reinforced concrete structures of bridges. Example of Tartu Sõpruse bridge (in Estonian).

2009 Valentina Pure, Master's degree, (sup) **Mihkel Kiviste**, Energy efficiency and cost of buildings: a case study of primary health care centre (in Estonian).

2008 Jegor Tšumakov, Master's degree, (juh) **Mihkel Kiviste**, Design of extra floor for block of flats (in Estonian).

2008 Vahur Schmidt, Master's degree, (sup) **Mihkel Kiviste**, Estimating concrete strength non-destructively with rebound hammer and ultrasonic method (in Estonian).

2007 Marju Laurits, Master's degree, (sup) **Mihkel Kiviste**, Trevor Sadd (UK), Specialist estimating services and their potential benefit to construction companies.

2007 Riho Halgma, Lauri Linnus, Master's degree, (sup) **Mihkel Kiviste**, Determination of some properties of concrete and reinforcement of prestressed concrete ribbed panels.

Publications:

1.1. **Kiviste, Mihkel**; Miljan, Jaan (2010). Evaluation of residual flexural capacity of existing pre-cast pre-stressed concrete panels - A case study. *Engineering structures*, **32** (10), 3377 - 3383.

1.2. Miljan, Jaan; **Kiviste, Mihkel** (2010). Estimation of residual flexural capacity of existing precast concrete panels by visual inspection. *Agronomy Research*, **8** (Special Issue 1), 177 - 191.

3.1. Miljan, Jaan; **Kiviste, Mihkel** (2010). Influence of visual condition on residual flexural capacity of existing precast concrete panels. 9th International Scientific Conference Engineering For Rural Development (260 - 266). Jelgava: Latvia University of Agriculture, Faculty of Engineering.

1.1. **Kiviste, Mihkel**; Miljan, Jaan; Miljan, Riina; Kiprušenkov, Mihhail † (2009). Condition of ctructures and properties of concrete of an existing oil shale chemical plant. *Oil Shale*, **26** (4), 513 - 529.

3.2. **Kiviste, Mihkel** (2009). Residual flexural strength of existing pre-stressed concrete panels. Proceedings of the 16th Baltic Building Symposium (77 - 82). Tartu: Department of Rural Building, Estonian University of Life Sciences.

3.2. **Kiviste, Mihkel** (2008). Residual flexural capacity of existing pre-stressed concrete panels. J. Rikala, M. Sipi (Toim.). Wood engineering - products and their utilization (5 - 10). University of Helsinki, Department of Forest Resource Management: Helsinki University.

6.3. **Kiviste, Mihkel** (2008). Concrete strength estimation with rebound hammer and ultrasonic pulse velocity (in Estonian). *Ehitaja*, **10**, 64 - 67.

1.2. **Kiviste, Mihkel**; Miljan, Jaan (2007). Structural concrete compressive strength determination with rebound hammer. *Vagos*. Research papers, **74(27)** (1), 15 - 20.

3.4. **Kiviste, Mihkel**; Miljan, Jaan. (2007). Determination of flexural strength of precast prestressed ribbed panels. Asst Prof. Murude Celikag (Ed.). Proceedings of the 11th International Conference on Inspection Appraisal Repairs & Maintenance of Structures (263 - 268). North Cyprus: Eastern Mediterranean University.

3.4. Kiprushenkov, Mihhail; Miljan, Jaan; **Kiviste, Mihkel**; Miljan, Riina (2007). Condition assessment of concrete structures in chemical plants gas generator building. Francois Toutlemonde

(Ed.). Proceedings of the 5th International Conference on Concrete under Severe Conditions of Environment and Loading (223 - 230). Paris: Laboratoire central des ponts et chaussees.

3.2. Tomann, Heiki; **Kiviste, Mihkel**; Miljan, Jaan; Miljan, Riina. (2005). Strength testing of concrete and corroded steel reinforcement in precast concrete panels. Elvira Sanchez Espinosa, Miguel Angel Garcimartin Molina (Eds). Proceedings of the V International Symposium on Concrete for a sustainable agriculture Agro-, Aqua- and Community Applications (363 - 371). Universidad Politecnica de Madrid.

2.3. **Kiviste, Mihkel**. (2004) The influence of corrosion of steel reinforcement on the bearing capacity of ribbed reinforced concrete panels (in Estonian). MSc thesis. Tartu: Estonian Agricultural University

3.2. Miljan, Jaan; Keskküla, Tõnu; Miljan, Riina; **Kiviste, Mihkel**; Laiakask, Erki; Tomann, Heiki. (2004). Service life prediction of reinforced concrete structures damaged by reinforcement corrosion. The 16th CIB World Building Congress 2004. Building for the Future. (155 - 165). Institute for Research in Construction, National Research Council, Canada.

3.2. **Kiviste, Mihkel**; Tomann, Heiki; Miljan, Jaan. (2003). The determination of residual bearing capacity of reinforced concrete panels. Proceeding of the 2-nd International Symposium ILCDES 2003 (343 - 348). Association of Finnish Civil Engineers RIL.

3.4. Miljan, Jaan; **Kiviste, Mihkel**; Tomann, Heiki. (2003). The accordance of corrosion damaged ribbed panels to limit state. Civil Engineering ’03. International Scientific Conference Proceedings (45 - 50). Jelgava: Latvia University of Agriculture.

3.2. Miljan, Jaan; **Kiviste, Mihkel**; Tomann, Heiki (2002). The influence of concrete carbonization and corrosion of steel reinforcement on the bearing capacity of ribbed reinforced concrete panels. Agricultural machinery, buildings, energy and hydraulic engineering, 215, 135 - 139. Tartu: Estonian Agricultural University

ELULOOKIRJELDUS

Isiku andmed

Nimi: Mihkel Kiviste
Sünniaeg: 6. aprill 1980
Aadress: Eesti Maaülikool, Kreutzwaldi 5, Tartu
Kontakt: *telefon* +372 7313178, *e-post* mihkel.kiviste@emu.ee
Perekond: Abielus, 3 last

Teenistuskäik

Töökoht ja amet:

2004-…	Eesti Maaülikool, metsandus- ja maaehitusinstituut, maaehituse osakond; lektor
2002-2004	Scanhouse OÜ; projektijuht

Haridustee:

2005-…	Eesti Maaülikool, Metsandus- ja maaehitusinstituut, Tehnikateaduse õppekava, doktoriõpe
2004-2005	Eesti Maaülikool, Metsandus- ja maaehitusinstituut, Maaehituse õppekava, doktoriõpe
2002-2004	Eesti Põllumajandusülikool, Maainseneriteaduskond, Maaehituse instituut, Maaehituse õppekava, magistriõpe
1998-2002	Eesti Põllumajandusülikool, Maainseneriteaduskond, Maaehituse instituut, Maaehituse eriala, bakalaureuseõpe
1987-1998	Tartu Mart Reiniku Gümnaasium (Tartu 10. Keskkool)

Teadusorganisatsiooniline ja -administratiivne tegevus:

2007-2010	Eesti Maaülikooli Maaehituse eriala 5-aastase ehitusinseneriõppe magistritööde kaitsmiskomisjoni liige
2009	16. Balti Ehitussümpoosioni eesistuja
2007-…	Eesti Maaülikooli Spordiklubi esindajatekogu liige
2006-2007	Eesti Maaülikooli Metsandus- ja maaehitusinstituudi nõukogu liige üliõpilasena
2005-2006	Eesti Maaülikooli Maaehituse eriala bakalaureuseõppe kaitsmiskomisjoni liige

Eksperthinnangud ja katsed:

- 2005 august-september. J. Miljan, **M. Kiviste**. Olemasolev Kungla lüpsilaut Kambja vallas Tartumaal. Lauda raudbetoonist kandetarindite seisundi hinnang, jääkkandevõime arvutused ning rekonstrueerimisprojekt. Tellija: FIE Lembit Räisa.
- 2006 august-september. **M. Kiviste**, M.-J. Miljan, J. Miljan. Tartu Kutsehariduskeskuse juurdeehitus (Kopli 1). Raudbetoonist posti ja tala ühendussõlme kandevõime katseline kontroll. Tellija: AS Ehitusfirma Rand ja Tuulberg.
- 2006 oktoober-detsember. **M. Kiviste**, J. Miljan. Büroohoone rekonstueerimine Tartus (Vasara 50). Hoone raudbetoonist kandetarindite betooni survetugevuse hindamine põrkevasara ja kärnidega. Tellija: Snorge Ehitus OÜ.
- 2008 september-oktoober. K. Sahk, **M. Kiviste**. Olemasolev mootorikütuse tanklahoone Tartumaal Külitses. Hoone kandetarindite (sh. ribipaneelide PNS-12) seisundi hinnang. Tellija: AS PK Oliver.
- 2010 veebruar. **M. Kiviste**. Tehvandi suusastaadioni raudbetoonist tribüün Otepääl. Raudbetoonist kandetarindite betooni survetugevuse hindamine põrkevasaraga. Tellija: AS Sa.Met ehitus.
- 2010 aprill. **M. Kiviste**. Palamuse gümnaasiumi juurdeehitus Jõgevamaal. Valatud raudbetoonpostide betooni survetugevuse võrdlev hindamine põrkevasaraga. Tellija: Agretten OÜ.

Teadustegevus

Teaduskraadi info:

2004 Tehnikateaduste magister maaehituse erialal (Eesti Põllumajandusülikool) Armatuurterase korrosioon ja selle mõju ribipaneelide kandevõimele, (juh) Jaan Miljan

Teaduspreemiad ja –tunnustused:

2008 Eesti Betooniühingu kõrgkoolide preemia saanud magistritöö juhendaja

2008 Eesti Maaülikooli Raefondi stipendiumi laureaat

Teadustöö põhisuunad:

Loodusteadused ja tehnika, Ehitus- ja kommunaaltehnika (Raudbetoontarindite kestvus, korrosioon)

Jooksvad projektid:

2008-2011 Baasfinantseeritav teadusteema: 8-2/T8003MIMI Hoonete elutsükli keskkonnasäästlikkuse hindamine, analüüs ja modelleerimine. Põhitäitja. (Vastutav täitja: Jaan Miljan).

Juhendatud väitekirjad:

2010 Taavi Ojaste, magistrikraad, 2010, (juh) **Mihkel Kiviste**, Eesti tingimustesse sobivad teisendusgraafikud betooni tugevuse hindamiseks põrkevasara-ultraheli mittepurustaval meetodil

2010 Rainer Põvvat, magistrikraad, (juh) Jaan Miljan, **Mihkel Kiviste**, Raudbetoonsildade kandekonstruktsioonide kahjustuste uurimine Tartu Sõpruse silla näitel.

2009 Valentina Pure, magistrikraad, (juh) **Mihkel Kiviste**, Hoone energiavajaduse ja maksumuse analüüs perearstikeskuse projekteerimise näitel.

2008 Jegor Tšumakov, magistrikraad, (juh) **Mihkel Kiviste**, Korterelamule lisakorruse projekteerimine.

2008 Vahur Schmidt, magistrikraad, (juh) **Mihkel Kiviste**, Betooni survetugevuse hindamine põrkevasara ja ultraheli mittepurustaval meetodil.

2007 Marju Laurits, magistrikraad, (juh) **Mihkel Kiviste**, Trevor Sadd (UK), Specialist estimating services and their potential benefit to construction companies (Eelarvestamisele spetsialiseerunud ettevõtted ja nende teenuse kasutamise võimalikud eelised ehitusettevõtete jaoks).

2007 Riho Halgma, Lauri Linnus, magistrikraad, (juh) **Mihkel Kiviste**, Eelpingestatud ribipaneelide sarruse ja betooni mõningate omaduste määramine.

Publikatsioonid:

1.1. **Kiviste, Mihkel**; Miljan, Jaan. 2010. Evaluation of residual flexural capacity of existing pre-cast pre-stressed concrete panels - A case study. *Engineering structures*, **32** (10), 3377 - 3383.

1.2. Miljan, Jaan; **Kiviste, Mihkel**. 2010. Estimation of residual flexural capacity of existing precast concrete panels by visual inspection. *Agronomy Research*, **8** (Special Issue 1), 177 - 191.

3.1. Miljan, Jaan; **Kiviste, Mihkel** (2010). Influence of visual condition on residual flexural capacity of existing precast concrete panels. 9th International Scientific Conference Engineering For Rural Development (260 - 266). Jelgava: Latvia University of Agriculture, Faculty of Engineering.

1.1. **Kiviste, Mihkel**; Miljan, Jaan; Miljan, Riina; Kiprušenkov, Mihhail † (2009). Condition of structures and properties of concrete of an existing oil shale chemical plant. *Oil Shale*, **26** (4), 513 - 529.

3.2. **Kiviste, Mihkel** (2009). Residual flexural strength of existing pre-stressed concrete panels. Proceedings of the 16th Baltic Building Symposium (77 - 82). Tartu: Department of Rural Building, Estonian University of Life Sciences.

3.2. **Kiviste, Mihkel** (2008). Residual flexural capacity of existing pre-stressed concrete panels. J. Rikala, M. Sipi (Toim.). Wood engineering - products and their utilization (5 - 10). University of Helsinki, Department of Forest Resource Management: Helsinki University.

6.3. **Kiviste, Mihkel** (2008). Põrketugevuse ning ultraheli kaudu saab betooni hinnata. *Ehitaja*, **10**, 64 - 67.

1.2. **Kiviste, Mihkel**; Miljan, Jaan (2007). Structural concrete compressive strength determination with rebound hammer. *Vagos*. Research papers, **74(27)** (1), 15 - 20.

3.4. **Kiviste, Mihkel**; Miljan, Jaan. (2007). Determination of flexural strength of precast prestressed ribbed panels. Asst Prof. Murude Celikag (Toim.). Proceedings of the 11th International Conference on Inspection Appraisal Repairs & Maintenance of Structures (263 - 268). North Cyprus: Eastern Mediterranean University.

3.4. Kiprushenkov, Mihhail; Miljan, Jaan; **Kiviste, Mihkel**; Miljan, Riina (2007). Condition assessment of concrete structures in chemical plants gas generator building. Francois Toutlemonde (Toim.). Proceedings of the 5th International Conference on Concrete under Severe Conditions of Environment and Loading (223 - 230). Paris: Laboratoire central des ponts et chaussees.

3.2. Tomann, Heiki; **Kiviste, Mihkel**; Miljan, Jaan; Miljan, Riina. (2005). Strength testing of concrete and corroded steel reinforcement in precast concrete panels. Elvira Sanchez Espinosa, Miguel Angel Garcimartin Molina (Toim.). Proceedings of the V International

Symposium on Concrete for a sustainable agriculture: Agro-, Aqua- and Community Applications (363 - 371). Universidad Politecnica de Madrid.

2.3. **Kiviste, Mihkel** (2004). Armatuurterase korrosioon ja selle mõju ribipaneelide kandevõimele: magistritöö tehnikateaduste magistri kraadi taotlemiseks maaehituse erialal. Tartu: Eesti Põllumajandusülikool

3.2. Miljan, Jaan; Keskküla, Tõnu; Miljan, Riina; **Kiviste, Mihkel**; Laiakask, Erki; Tomann, Heiki. (2004). Service life prediction of reinforced concrete structures damaged by reinforcement corrosion. The 16th CIB World Building Congress 2004. Building for the Future. (155 - 165). Institute for Research in Construction, National Research Council, Canada.

3.2. **Kiviste, Mihkel**; Tomann, Heiki; Miljan, Jaan. (2003). The determination of residual bearing capacity of reinforced concrete panels. Proceeding of the 2-nd International Symposium ILCDES 2003 (343 - 348). Association of Finnish Civil Engineers RIL.

3.4. Miljan, Jaan; **Kiviste, Mihkel**; Tomann, Heiki. (2003). The accordance of corrosion damaged ribbed panels to limit state. Civil Engineering '03. International Scientific Conference Proceedings (45 - 50). Jelgava: Latvia University of Agriculture.

3.2. Miljan, Jaan; **Kiviste, Mihkel**; Tomann, Heiki (2002). The influence of concrete carbonization and corrosion of steel reinforcement on the bearing capacity of ribbed reinforced concrete panels. Agricultural machinery, buildings, energy and hydraulic engineering, 215, 135 - 139.